eman ta zabal zazu

Universidad del País Vasco
Euskal Herriko Unibertsitatea

FACULTY OF ENGINEERING BILBAO
UNIVERSITY OF THE BASQUE COUNTRY

Faculty of Engineering Bilbao (ESI)
Department of Automatic Control and Systems Engineering (DISA)

Ph.D. Thesis

Validation Of Trajectory Planning Strategies For Automated Driving Under Cooperative, Urban, And Interurban Scenarios

Author: Ray Alejandro Lattarulo Arias

Director: Dr. Vicente Gómez Garay
Director: Dr. Joshué Pérez Rastelli
October 2019


tecnalia
Inspiring
Business

Acknowledgement

Firstly, I would like to thank my parents, Mr. Pasquale Lattarulo and Mrs. Marleni Arias, and my sister, Miss Vanessa Lattarulo, due to encouraging me during difficult times throughout this work, and their wise counsel when I needed inspiring words to continue the Ph.D. process.

I would like to acknowledge my supervisor and friend, Dr. Joshué Pérez Rastelli, for supporting, guiding, and inspiring advice in this work, especially in situations of uncertainty. Also, I would like to acknowledge my friends and colleagues, of the Tecnalia's automated driving team, for their comprehension in moments of stress, and for helping, in a direct or indirect form, this work. I would like to acknowledge Mrs. Lucia Isasi for reviewing, totally, this dissertation.

Finally, I would like to thank my Ph.D. supervisor Dr. Vicente Gómez Garay for its help during this work.

Thank you,
Ray Alejandro Lattarulo Arias
Bilbao, October 2019

Contents

List of Figures

List of Tables

Abstract

Automated Driving (AD) is committed with passenger's and pedestrian's safety as well as the inclusion of people with reduced mobility, the increment of free time while driving, and the mitigation of traffic jams problems.

In the last two decades, the industry has created new mobility concepts and improved traditional vehicle technologies. Automated shuttles, buses, robotaxi, trucks, and vehicles are examples of the desired targets. Nonetheless, state of the art emphasized some AD issues, such as the increment of safety, reliability, and comfort on vehicles' trajectory generation.

Consequently, this work considers a modular architecture, divided into six modules, for the validation and verification of a novel automated vehicles' decision and control approach. Firstly, the proposed method generates a nominal trajectory based on Bézier curves, improving passengers' comfort and smoothness in trajectory changes. Next, a Model Predictive Control (MPC) strategy, merged with Bézier curves, permits a safe trajectory generation in case of unexpected situations. Lateral and longitudinal models evaluate the system and scenario constraints, and both models are decoupled to obtain computationally fast responses.

Finally, this Ph.D. thesis has proposed a cooperative maneuver method that improves the trajectory generation in terms of safety and traffic flow. The negotiation and coordination process among drivers have inspired this strategy.

Urban scenarios were used for the validation and verification of the algorithms due to their complex conditions, such as interactions among drivers on intersections, roundabouts, and obstacle avoidance when the road is blocked. Additionally, the overtaking was used for the validation and verification of the maneuver negotiation approach because it is a safety-critical scenario.

All the algorithms of this Ph.D. thesis were validated and verified in virtual and real (Renault Twizy) environments, under the framework of the EnableS3 EU project. Moreover, the cooperative maneuver approach was tested in multiple automated vehicles, under the scope of UnCoVerCPS EU project, verifying its reliability.

The achieved results coming from this Ph.D. thesis have brought significant contributions to Tecnalia's AD team, such as: (1) improvements in the vehicle trajectories resulting in an increment of the speed up to $60km/h$, (2) the addition of capacities to react in case of obstacles on the road, and (3) the validation and verification process of the algorithms based on the Dynacar simulator.

In spite of the contributions provided by this Ph.D. thesis, further work is demanded in areas such as terrain mapping, prediction of other vehicles' intention, and shared control strategies between the driver and the vehicle, in order to accomplish a total market deployment of automated vehicles.

"You cannot teach a man anything, you can only help him to find it within himself".

Galileo Galilei

1 Introduction

The improvement of road transportation has been a constant research field of engineering since the birth of the automobile back in 1886 (Carl Benz's prototype [4]). However, whereas the aim of these first pioneers was essentially focused on mechanics, the future of the industry is all about the development of automation systems. From maximum speeds to passengers' safety, as well as electronic devices installed in the vehicle, comfort, aerodynamic designs, and eco-friendly systems, great progress has been achieved with the introduction of Electronic Control Units (ECU). Definitely, "the velocity of technological change is only going to continue and will accelerate" as it is mentioned by Joseph Coughlin, director of the AgeLab, on the Chicago Tribune [5].

In this context, the interest shown by the European Union and leading automotive companies is a very important indicator of the revolution that these technologies will mean for the industry, the environment, and society in a foreseeable future. The Strategic Research Agenda (SRA) for the 9^{th} EU Framework Programme (FP9), established for the 2020 - 2030 timeframe, has as main topics for researching: ensuring mobility in urban areas, environmental sustainability, efficient and resilient road transport system, connectivity and automation for mobility, and safety [6]. In addition to development and research issues, the idea of the Original Equipment Manufacturers (OEM) is to introduce Automated

Driving (AD) systems in markets by 2030 with some basic functionalities, and becoming mass-market around 2050 with advanced functionalities, being used by more than 50% of the population (in some countries) [7].

Some research areas related to AD systems, such as communication Vehicle-to-Vehicle (V2V), Vehicle-to-Infrastructure (V2I), Vehicle-to-Pedestrian (V2P), and Vehicle-to-anything (V2X) have been well-studied in the past. Another well-studied subject in literature with proven results is the perception (vehicle and environment's information using onboard sensors). However, other research topics such as trajectory planning and control demand further research and improvement.

Therefore, this Ph.D. thesis contributes to the automated driving technologies regarding trajectory planning of automated vehicles and considering the demands of challenging scenarios such as cooperative driving, obstacle avoidance, and overtaking maneuvers in urban environments, always taking into consideration comfort and safety aspects.

The following work has been done in the Automated Driving group of the Automotive Area in Tecnalia Research and Innovation, located in the Basque Country, Spain. The current chapter will explain the thesis framework and the general explanation of the contributions done with this work.

1.1 Motivation

The recent development of automation technology and its application to the automotive industry has shown incredible results and promises bigger achievements. In these terms, AD is the main motivation of this Ph.D. thesis, where some of the AD's benefits are [8]:

- Increase of drivers' free time, delegating the driving task to the vehicle.
- Health improvement due to the reduction of stress during traffic situations.
- Establishment of new businesses related to the growing of "sharing economy" and the possibility of using a car among different travelers.
- Reduction of traffic problems, such as pollution and parking.
- Economic benefits due to the optimization of travel time and speed.
- Safety benefits thanks to cooperative vehicles that reduce the possibility of a collision and warn about future conditions.

"A Speed Planner Approach Based On Bézier Curves Using Vehicle Dynamic Constrains and Passengers Comfort", R. Lattarulo, E. Martí, M. Marcano, J. Matute and J. Pérez, in **IEEE International Symposium on Circuits and Systems (ISCAS) 2018**, pp. 1 - 5.

"Towards Improved Validation of Autonomous Systems for Smart Farming", M. Rooker, P. Horstrand, A. Rodriguez, S. Lopez, R. Sarmiento, J. Lopez, R. Lattarulo, J. Perez, Z. Slavik, D. Pereira, M. Pusenius and T. Leppälampi, in **Workshop on Smart Farming 2018**, pp. 1 - 7.

"Analisis de Riesgos de Ciberseguridad en Arquitectura de Vehiculos Automatizados", L. González, M. Vaca, R. Lattarulo, I. Calvo, J. Perez and A. Ruiz, in **Jornadas de automática 2018**, pp. 838 - 845.

"Fault Injection Method for Safety and Controllability Evaluation of Automated Driving", G. Uriagereka, R. Lattarulo, J. Rastelli, E. Calonge, A. Lopez and H. Ortiz, in **IEEE Intelligent Vehicles Symposium (IV) 2017**, pp. 1867 - 1872.

"Early Safety Assessment of Automotive Systems Using Sabotage Simulation-Based Fault Injection Framework", G. Juez, E. Amparan, R. Lattarulo, A. Ruíz, J. Pérez and H. Espinoza, in **International Conference on Computer Safety, Reliability, and Security 2017**, pp. 255 - 269.

"A Complete Framework for Developing and Testing Automated Driving Controllers", R. Lattarulo, J. Pérez and M. Dendaluce, in **IFAC World Congress 2017**, pp. 258 - 263.

"Safety Assessment of Automated Vehicle Functions by Simulation-Based Fault Injection", G. Juez, E. Amparan, R. Lattarulo, J. Rastelli, A. Ruiz and H. Espinoza, in **IEEE International Conference Vehicular Electronics and Safety (ICVES) 2017**, pp. 214 - 219.

"Overtaking Maneuver for Automated Driving Using Virtual Environments", R. Lattarulo, M. Marcano and J. Pérez, in **International Conference on Computer Aided Systems Theory 2017**, pp. 446 - 453.

"Citymobil2: San Sebastian ARTS demonstration", J. Murgoitio, M. Izaguirre, A. Inclan, J. Pérez and R. Lattarulo , in **ITS Europa 2017**.

"Study of the Lane Change Maneuver: Automated Driving Use Case" (Extended abstract), R. Lattarulo and J. Pérez, in **EUROCAST 2017**, pp. 298 - 300

"The secret to getting ahead is getting started".
Mark Twain

2
State of the art

A great amount of interest has been given to the Intelligent Transportation Systems (ITS) field, especially to Automated Driving (AD), in the last decades. This technology can be seen as a "tendency" in our days and, consequently, some important announcements were presented such as the automated Mercedes Benz Trucks by 2025. Those will have a great variety of sensors, high-quality maps, AD capacities, and communications V2X [23]. In 2015, Mary Barra, the CEO of General Motors Company (GM), has assured that: "...the industry will experience more change in the next 5-10 years than it has in the last 50 years" [24]. This statement was given in terms of moving the vehicular automation towards connected self-driving vehicles, and the electric vehicle as a replacement of fossil fuel [25]. In 2016, Ford announced some of their plans on car-sharing business using automated vehicles of their brand. Next, Elon Musk reacted with a similar option but using Tesla's vehicles. Another good example is the great number of trials conducted by Uber, in partnership with Volvo, in the city of Pittsburgh in the United States (US) [26].

On the other hand, pushing forward the technology so fast sometimes ends up with deadlines that cannot be fulfilled. A good example of this underachievement is Volvo in 2017: the company promised 100 automated vehicles to the city of Gothenburg in Sweden under the program DriveMe, but it was not accom-

plished in the foreseen dates [27]. This kind of misinformation generates distrust in the technology which is considered in the analysis developed by the American Automobile Association (AAA) from the same year. The study revealed that 78% of the US citizens thought automated vehicles were uncomfortable, or they have fear while the automated mode was activated [28]. In 2018, the AAA completed the work and found out that the number of people who felt uncomfortable about the technology had decreased to 63% [29].

Nevertheless, newer approaches have been done in 2019, for example:

- Volkswagen testing five automated vehicles in the city of Hamburg, Germany [1].
- The presentation of the concept Chevrolet Bolt with the technology of Cruise AV which has automated driving capacities removing the steering wheel and the pedals [2].
- The US postal service started to test autonomous trucks [3].
- Toyota is investing a total of $100 million in automated driving and mobile robotics technologies [4].
- Nissan will update the version of its ProPilot, and they will improve the current properties of Tesla's autopilot and the Cadillac's Super Cruise. Furthermore, the new ProPilot will include lane-change capacities [5].

In the automotive industry, there are two tendencies in the development of AD capacities: Semi-automated and automated vehicles [30]. Regarding this discussion, SAE has presented a table with the automation levels [31] (illustrated in Fig. 2.1), which are described as follows:

- SAE Level 0, no vehicle automation.
- SAE Level 1 - 2, Advanced Driver-Assistance Systems (ADAS).
- SAE Level 3, the first level of automated driving with total supervision of the driver.

[1] `https://www.greencarcongress.com/2019/04/20190403-v.html`

[2] `https://www.youtube.com/watch?v=WEHq2oUeD9c`

[3] `https://observer.com/2019/05/usps-driverless-delivery-vehicles/`

[4] `https://www.cnbc.com/2019/05/02/toyota-to-invest-100-million-in-autonomous-driving-and-robotic-startups.html`

[5] `https://edition.cnn.com/2019/05/25/success/nissan-propilot-hands-free-driving/index.html`

- SAE Level 4 and 5, total automated capacities in most of the scenarios and all scenarios, respectively.

After this brief presentation, the following sections expose a historical review from ADAS systems to AD, passing through highlighted events and recent achievements. It considers the current state of technology in Europe, and some of the most interesting projects. The projects EnableS3 and UnCoVerCPS are highlighted because they were the framework of this Ph.D. thesis. The chapter finishes with the explanation of the trajectory planning and control problem in automated vehicles and some of the approaches used in the past.

2.1 Evolution of Automated Driving Technology

2.1.1 First ADAS

Passenger car safety has improved considerably in the last decades, decreasing 90% fatal risks and in 50% major injuries in the period from the early 80s to late 2000s. During this period, ADAS was key for risk reduction [32]. These systems date back the 70s, with the first introduction on passenger cars, with the purpose of increasing safety while driving. However, characteristics more

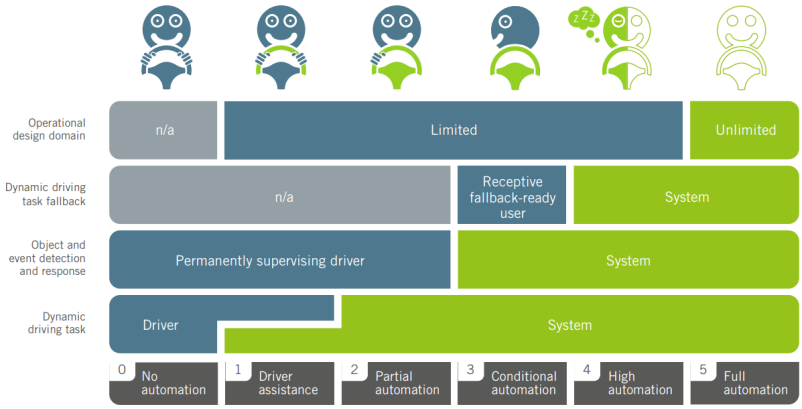

Figure 2.1: Representation of the SAE levels shown in [2]

related to the comfort were added years after [33]. Hence, this section has a brief historical review of the first and most common ADAS to better understand the evolution of the AD systems.

One of the oldest ADAS, still in use, is the Anti-lock Braking System (ABS). Its first design was shown in 1908 and the idea was to incorporate them on trains. Decades after, Bosch patent the system, and it was used in aircraft in 1936 [34]. In 1969, the ABS was introduced by Ford in their vehicles, and a short time after, the system was retired from the market due to the system's reliability and costs. After, in 1979, it was introduced by Mercedes-Benz and five years later in the American market. The ABS aims to improve the vehicle safety mechanism, optimizing the minimum stopping distance which could generate a sliding scenario. The system considers the forces on the wheels in the braking scenario [35]. A subsystem called Electronic Brake-force Distribution (EBD) is used to improve the efficiency of the ABS. It has the goal of balancing the brake force over the vehicle wheels avoiding a possible whipping [36]

Consequently, the Traction Control System (TCS) is another good example of early ADAS. This system has the main goal of controlling the slip rate of the driving wheels using torque (controlling the general slip) and the braking pressure (controlling the difference in the slip of the drive wheels) [37]. The Electronic Stability Control (ESC) technology derived from ABS and TCS, and it is in charge of keeping the stability of the vehicle given an action over the steering wheel. The evaluation is done measuring continuously the speed, yaw rate, lateral acceleration, and steering wheel angle. Additionally, it was initially introduced in luxury vehicles, as Mercedes-Benz and BMW, in 1997 [38].

Moreover, the Brake Assistance System (BAS) was introduced in vehicles in 1997 [39]. The system was designed to assist drivers during an emergency braking situation, e.g. when objects suddenly appear in the vehicle's trajectory. To support the drivers, it activates a full braking pressure regardless of the initial position of the braking pedal. This is done under a scenario where the driver intends to full brake and the system verifies it [40]. Years later, the Automatic Emergency Brake (AEB) system is studied and developed to reduce or mitigate the fatal risks or injuries in a collision. Typically the system is used to brake in presence of unexpected pedestrians [41]. It is activated at low speed and it has three key components [42]:

- Sensors to detect the object ahead.
- A control system to classify and decide into the action to be taken.
- The action over the brake pedal to control it automatically

Table 2.1: Summary of some ADAS currently in the market

Type	Some manufacturers	Brief description
Frontal Collision Warning	Continental, Bosch, Mobileye (Intel)	Headway control, collision avoidance, distance and speed monitoring. Detecting critical situations (up to 80 meters away).
Automatic Emergency Braking	Bosch, Nissan, ZF	Automatic emergency braking. Assists in avoiding collision, using front camera, considering pedestrian ahead. Mitigate collisions with other vehicles or pedestrians.
Pedestrian Safety system	Mobileye, Volvo, Continental, Bosch	Full auto brake using cameras. Lidar for pedestrian detection.
Lane Keeping Assistance systems Lane Change Assistance warning Lane Departure warning	Mobileye, Valeo, Bosch, Acura, Continental, infiniti, etc.	The lane alert with sounds and visualy. Steering wheel control in case of the assistance.
Blind Spot Warning	Nissan, Continental, Infiniti	Rear-view camera or rear/side facing radars.
Speed Limit Assistant	BMW, Audi	Cameras and navigation systems for detection.
Traffic Jam Assist	Bosch, Audi	Partial lateral and longitudinal control
Driver Distraction Detection	Nissan, Bosch, Continental, Denso, Autoliv, Valeo	Driver Attention Alert (DAA) system, steering input patterns, monitoring with cameras, steering wheel sensor.
Parking Assistance	Bosch, Valeo, Texas Instruments	Radar sensor, rear camera, multi-camera system, distance sensors for park assist
Night Vision System	Bosch	Pedestrian detection, animal detection, among other things.
Adaptive Light Control	BMW, Bosch, Continental, Volkswagen	Turn indicatorsusing video camera to measure the ambient brightness. Optimal night vision. Follow the angle of your steering wheel, based on cameras.
Collision Avoidance System	Bosch	Cameras, Visibility Around the Vehicle; Radar; Real-time rearview display, any wheather condition, mid-range radar sensor

Another interesting ADAS is Cruise Control (CC). The early days of this technology date back in the 50s. The device was made of mechanical actuators applying pressure to the throttle when driving slower than a set speed. The

modern version of this system appeared around the 80s, including microprocessors and four components: the sensor, user interface, the electronic module, and the actuator of the throttle system [43]. In 1991, the system evolved to the Adaptive Cruise Control (ACC) adding a component to keep a desired distance between vehicles [44].

There is a great variety of system supporting the driver, such as: navigation systems integrated in the vehicle, traffic control management applications, parking aids and parallel/angled parking assistance, lane departure warning and assistance, blind spot warning, traffic sign detection, intelligent speed adaptation, collision warning, driver monitoring, seat belt reminder, among others. A summary of current ADAS in the market is shown in table 2.1. It is expected that the breakthroughs did in the area and its knowledge allows us to accelerate the AD technology and the deployment in regular traffic environments.

2.1.2 Early days of AD

Currently, one of the major concerts of the population is traffic-related death rates. In these terms, the World Health Organization (WHO) has concluded that, at least, 1.2 million people are killed and more than 50 million are injured (in the world) every year as a result of road traffic accidents [45]. In the same work, the authors explained that future estimations are not comforting, as they foresee an increase of 65% in an accident during the upcoming two decades. These are the main reasons for promoting safer vehicles using AD technology.

AD technology was firstly introduced in 1939 when automated vehicles on highways were predicted to be a reality in the upcoming 25 years. This was not true but it introduced the concept and the possibility to have them (Fig. 2.2a) [46]. Futurama was the name given by the industrial designer Norman Bel Geddes to this proposal of the futuristic city, which was shown in the 1939 New York's fair as part of the GM's Highways and Horizons exhibit [47].

In 1956 another milestone of automated driving appeared, as an advertisement of the Central Power and Light Company [49]:

> "*Electricity may be the driver. One day, your car may speed along an electric super-highway, its speed and steering automatically controlled by electronic devices embedded in the road. Highways will be made safe-by electricity! No traffic jams ... no collisions ... no driver fatigue*"

Fig. 2.2b shows the advertisement of a family seated in a vehicle looking at

(a) Model presented in the Futurama

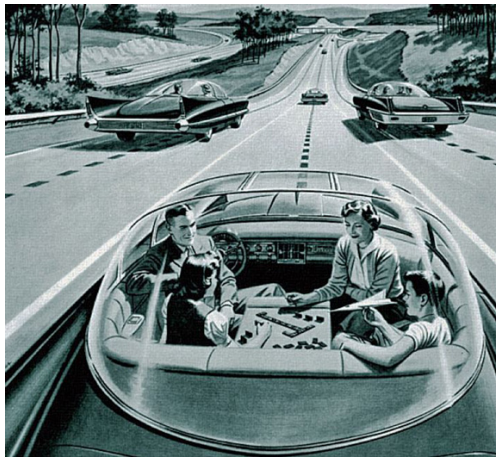

(b) First image of AD in an advertisement [48]

Figure 2.2: Some of the oldest pictures of AD

each other, playing a board game. This picture, from 1956, still prevails in the goals of AD in our days[6].

The first ideas were not just shown many decades ago but a first prototype was tested as well. In September 1968, Continental showed the first prototype of an electronically controlled vehicle in its Contidrom test ground in Lüneburg heath [7]. It was named as the "Ghost car" and the news showed as headlines "the future is here" and "around the banked turn with a ghost in the wheel" describing it. The system was limited in a great number of ways, nevertheless, it was the first prototype of this technology.

Naturally, all these pioneer ideas derived in the first big approaches done in AD. Consequently, the next sections explain these approaches and their relationship with projects, big demonstrations, and exhibitions.

[6] https://spectrum.ieee.org/cars-that-think/transportation/self-driving/watch-general-motors-hilarious-1956-movie-on-smart-roads

[7] https://www.continental-corporation.com/en/company/history/the-ghost-car-145316

2.1.3 Highlight events

One of the biggest events in AD happened in 1986 in the framework of the European consortium "EUREKA". It includes more than 70 industries and 120 universities and research institutes, coming from electronics, components and telecommunication sectors from the European Community members: Austria, Finland, Iceland, Norway, Sweden, Switzerland and Turkey. Some major automotive companies were part of the consortia as well, such as: BMW, Daimler Benz, Fiat, Ford, Jaguar, Matra, Opel, Porsche, P.S.A., Renault, Saab, Steyr-Daimler-Puch and Volvo. The EUREKA consortium was the biggest budget program (650 million euros partly funded by the countries involved) and it was active until 1995 [50]. The main goals were the integration of private and public companies with universities and other institutions as well as the exchange technologies among the different partners and countries [51].

In this perspective, the PROgraM for a European Traffic with Highest Efficiency (PROMETHEUS) initiated in 1986 and focused on road safety and traffic efficiency [52]. PROMETHEUS had impressive objectives such as improving driver's information and its environment (static and moving obstacles), monitoring both road's and driver's state, and enhancing the vehicle vision compared to the driver. Active driver support was another objective of the program considering safety under critical conditions, dynamic vehicle control, and information for assistance. Moreover, the first concepts of intelligent cooperation among automated vehicles were established by intelligent cruise control, intelligent maneuvering and control considering cooperation, intersection crossing management, etc [53].

(a) Navlab5 vehicle used for CMU

(b) Poster of the route

Figure 2.3: Pictures of "No hands across America"

On the other hand, the Carnegie Mellon University (CMU) in the US presented in 1995 the Navlab5 vehicle (1990 Pontiac trans sport minivan), which

had a navigation system called Ralph (refer to Fig. 2.3a) in a challenge called "No Hands Across America". The trip of 3000 miles started in Pittsburgh and ended in San Diego, going by Indianapolis, St. Louis, Kansas City, Denver, Las Vegas and Los Angeles (Fig. 2.3b). Initially, the Ralph system was previously tested in control environments and a shorter trip of 305 miles (from Pittsburgh to Washington D.C.) [54]. Once again, in 1997, CMU led the Free Agent Demonstration (FAD) testing some interesting scenarios such as platooning, trajectory tracking, etc. Two fully automated buses, two fully automated cars, and one partially automated car were the vehicles involved in the demonstration (refer to Fig. 2.4a). Together with US National Automated Highway System Consortium (NAHSC) initiative, all vehicles drove in the I-15 highway (San Diego, California) [55]. The FAD was part of Automated Highway Systems (AHS) event where the California PATH demonstrated a highly automated platoon as well, the scenario is shown in Fig. 2.4b.

(a) CMU's vehicles in the FAD (Navlab10-6) (b) Platoon demonstrated by the PATH

Figure 2.4: Some scenarios of the Automated Highway Systems consortium

In 2003, Toyota launched for the first time a Parking Assistance System (PAS) integrated in its Prius model. The Intelligent Parking Assistance System (IPAS) used as the main sensor a rearview camera, and it was improved, in 2007, using Valeo's ultrasonic sensor (Park4U) assisting the driver during parallel and back parking maneuvers [56]. Around 80% of the customers preferred the Prius version with the IPAS system [57]. However, it was partly solved with the automation of the steering wheel, and the pedals were controlled by the driver.

Some other challenges were hosted by the Defense Advanced Research Projects Agency (DARPA) in 2004, 2005 and 2007. The first one - DARPA's Grand Challenge - was focused on increasing the motivation of the researchers,

(a) Stanley by Stanford University

(b) Sandstorm and H1ghlander by CMU

(c) KAT-5 by Team Gray

(d) TerraMax by Team TerraMax

Figure 2.5: DARPA 2005: finishing teams.

accelerating the development of automated vehicles covering military requirements. The challenge was split into three parts: (1) technical acceptance of the platform (automated vehicle) based on a written report, (2) QID test (qualification, inspection, and demonstration) consisted in a demonstration of path following and obstacle avoidance in the California Speedway in Ontario, California (23 participants applied and 15 vehicles were approved to participate), and (3) the race event awarded with a prize of one million dollars to the first

team capable to drive from Barstow, California to Primm, Nevada in 10 hours or less. In March 2004, the challenge started with a 3000 waypoints mission file to automatically drive the vehicles through the field. All teams did not finish the race, and CMU's Sandstorm achieved the longest distance which was 7 miles of 150 total miles [58].

In 2005, the second DARPA Grand Challenge doubled the total amount of applications (from 106 to 197 participant applications), and only 23 teams reached the final event. It was harder than the previous version with a total distance of 132 miles through the desert of Nevada containing a great variety of non-flat terrain, dust, sharp turns, bridges, long tunnels, obstacles, windy roads, etc. Five teams finished the race. "Stanley", the vehicle of Stanford University, was the winner, driving an average speed of $31km/h$ and driving 6 hours and 53 minutes. The rest of the teams (4 teams) finished the race in less than 10 hours [13]. Fig. 2.5 depicts more details of the finishing teams.

In 2007, DARPA's 3$^{\text{rd}}$ edition - Urban Challenge - milestone was about automated Army's ground vehicles by 2015, based on Congress and Department of Defense requirements. In the first two versions, the feasibility of this technology was proved to cross deserts and avoid natural obstacles [59]. In this context, concepts such as smooth transitions between consecutive trajectories, classification of obstacles, coordination of multiple participants and fault tolerance were established and demanded for the first time [60]. The winner of the challenge was the Tartan Racing Team composed by CMU's students, and staff of GM, Caterpillar, Continental, and Intel. Their vehicle name was "Boss" and it handled average speeds of $48km/h$ [61].

In 2010, during the World Expo "better cities, better life" (Shanghai, May 1$^{\text{st}}$ to October 31$^{\text{st}}$), new ideas in terms of mobility were shown. In this sense, VisLab of the University of Parma established the VisLab Intercontinental Autonomous Challenge that consisted of driving autonomously from Parma (Italy) to Shanghai (China) using the old silk road, passing through Russia and Kazakhstan. More than $13000km$ of data in automated mode was registered, as it is shown in Fig. 2.6. The 15 years experience of this laboratory dealt with two use cases: (1) single-vehicle following autonomously a trajectory and (2) a second vehicle following autonomously the leader [62]. Three months of traveling with 11 vehicles (4 automated vehicles, 4 motor homes, and 3 big trucks) generated 50 terabytes of registered data [63, 64]. This can be considered the first demonstration done under normal traffic circumstances and multiple environmental conditions. It brought more than 98 continuous kilometers driving in automated mode [65], with frequent stops to recharge system batteries and sensor periodical calibration [66].

(a) Team (b) Route

Figure 2.6: Vislab autonomous challenge

In the same year, Google unveiled its Self-Driving car project, later called Waymo, teamed up by engineers coming from DARPA challenges. Its main goal was "help prevent traffic accidents, free up people's time and reduce carbon emissions by fundamentally changing car use" [67]. The most impressive things in the Toyota Prius Google's fleet was the enhancement of the vehicle perception using a LIDAR in the rooftop. The sensor collects a point cloud that rebuilt the vehicle's environment [68]. Later on, Google added Lexus RX450h SUVs to their automated vehicle fleet [69] (refer to Fig. 2.7). In October 2010, Google's car had logged around 225000 kilometers, of vehicle's operation and its environment. Only 1000 miles were driven in totally automated mode, without human intervention [8][9].

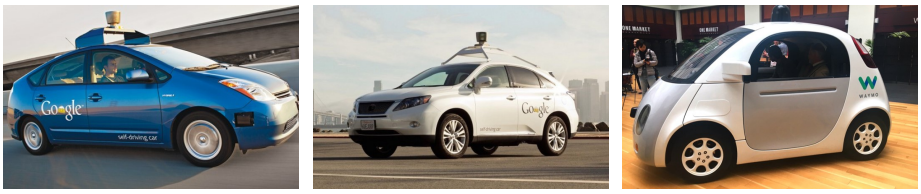

(a) Google's Prius (b) Google's RX450h (c) Google car prototype

Figure 2.7: Some of the vehicles used by Google for testing.

Another good year for AD was 2012 when the state of Nevada modified its Administrative Chapter and the Status Chapter 482A opening the roads to

[8] https://googleblog.blogspot.com/2010/10/what-were-driving-at.html
[9] https://techcrunch.com/2010/10/09/google-car-video/

automated vehicles. The following was required by the Department of Motor Vehicles (DMV) to obtain the automated vehicle license:

- 1 million dollars insurance policy, for up to 5 vehicles.
- An emergency shutdown button.
- A specialized driver at all-time in the vehicle, and at least two passengers when driving in automated mode.
- Proven 10000 miles driving in automated mode.

In 2012, Stanford University together with Volkswagen Automotive Innovation Lab (VAIL) and Electronics Research Laboratory of Volkswagen of America (ERL), modified an Audi TTS vehicle to drive it autonomously at high speeds learning from experienced drivers, who control the vehicle safely under risky conditions (race car and rally drivers). The main objective was to apply advanced and safe control techniques when driving automated vehicles in emergency maneuvers. Stanford did the experiments in the Pikes Peak Hill Climb Course (Colorado) considering a driving behavior on friction limits, achieving high speeds limits in safe conditions [10]. Additionally, considering a real-time target it was found, during these tests, that the control calculation speed (including vehicle's perception) for high and low-speed vehicles must be at least 200 Hz (5 milliseconds). The performance was improved at higher rates but it is limited by sensor technology [70].

In August 2013, the Karlsruhe Institute of Technology (KIT) completed Bertha Benz's memorial-route (done 125 years ago) with a Mercedes-Benz S-Class vehicle named Bertha. The vehicle drove more than 100 kilometers (from Mannheim to Pforzheim) on different types of roads (highways, urban, and countryside), along with German cities and towns [71]. One of the major achievements was driving with close to production sensors and equipment [72].

2.1.4 Recent achievements

In 2015, Delphi, a british automotive supplier, covered the first AD trip in US from coast (Pacific) to coast (Atlantic). The trip started in San Francisco, passing through 15 states including the District of Columbia, and it finished in New York. The vehicle (Roadrunner) drove 99% of the trip on automated mode under all kind of weather conditions and road situations [73].

[10] `https://www.youtube.com/watch?v=YxHcJTs2Sxk`

Tesla unveiled in October 2015 and January 2016 the projects Autopilot and Summon respectively. The Autopilot aims to drive the vehicle in "automated mode" whereas Summon dealt with parking maneuvers, putting the vehicle in resting mode when arriving home. These systems can be considered the first industrial step to improve from level SAE 2 [74, 75].

Unfortunately, in May 2016, the first fatal accident related with AD took place, killing the driver of a Tesla vehicle. The vehicle failed in distinguishing a white tractor trailer crossing the highway against a bright sky background. Some time later, the National Highway Traffic Safety Administration (NHTSA) determined that the vehicle gave the signal, to the driver, of taking back control. The signal was released 7 seconds before the impact, but the driver was watching a movie on the phone and he was not aware [76–78].

The Michigan Institute of Technology (MIT) unveiled the MCity, 13 hectares at Ann Arbor, Michigan (US). This place was built for testing vehicular technology in real conditions without compromising safety of people [79].

Next, in 2016, a software company named nuTonomy deployed the first public automated taxi service, in Singapore, to cover a route of 6 kilometers with designated stops. The vehicles (electrical) were Renault Zoe and Mitsubishi i-MiEV. Some weeks later, the company Uber launched a similar test case in Pittsburgh for an area of 31 square miles. In this case, the total amount of vehicles was 100 taxis using Ford Fusion vehicles [80]. Unfortunately in 2016, Google's vehicle had their first fatal accident, due to the fact that the vehicle did not recognize a pedestrian crossing with a bicycle at night [81].

On the other hand, the DriveMe project got started in 2017. Lead by Volvo, it assigned 100 vehicles to "ordinary" drivers to test them in a specific area of Gothenburg (Sweden), covering a total length of 50 km. The main goals were: (1) SAE Level 4 technology awareness to nonprofessional drivers, (2) collecting vehicle and environment data until 2020, and (3) testing the AD capacity of the vehicles [82].

In 2018, GM had announced its Super Cruise technology with a driver monitor system detecting driver's distraction. This system was installed in the Cadillac CT6 2018 [83, 84]. The same year, Audi has presented its AI Traffic Jam Pilot introducing a commercial and limited version of SAE Level 3 vehicles. The driver can delegate the driving task completely to the vehicle in traffic jams circumstances under $60km/h$. In case of unexpected situations, the vehicle demands driver intervention [85].

Some others upcoming achievements are: BMW in partnership with Mobileye (computer vision company) are planning to introduce automated driving functionalities by 2021 [86], the efforts in artificial intelligence of Hyundai Mo-

tors [87], the alliance between the Renault-Nissan group and Microsoft to have automated vehicles in 2020 [88], and the investments done by Ford in a AI company named ARGO AI [89]. A great number of alliances have been generated in the last years, and they will continue growing.

2.2 AD technology in Europe

2.2.1 European Projects

The European Union has a strong history in research programs and projects related to AD, which can be divided into four main domains: (1) highly automated urban transport systems, (2) ADAS, (3) connectivity and communication and (4) networking and challenges. Fig. 2.8 shows a summary of the recent initiatives promoted by the EU in terms of these domains based on the ERTRAC roadmap of 2017 [3].

One interesting group of projects were the Citymobil (2006 to 2011 [90]) and Citymobil2 (2012 to 2016 [91]) projects. These EU projects have been focused on developing new mobility concepts on urban transportation. The goals were to improve efficiency, safety, and quality of life while reducing energy and pollution [92]. Citymobil pilots took place in La Rochelle (Fr), Heathrow Airport (UK), Castellón (Es), and Rome (It) [93]. The Citymobil2 pilots were in La Rochelle, Vantaa, Trikala, Sophia Antipolis, San Sebastian, among others [94].

The Safe Road Trains for the Environment (SARTRE) project, started in 2009 and finished in 2012, is another action taken by the EU in terms of the seventh framework program (FP7). The main goal of the project was to develop new methods and strategies to establish vehicle cooperation in terms of public road platoons (vehicles following a leader). Hence, the project demanded the use of V2X and V2I with the main goal of improving the scenario in terms of the environment: reducing fuel consumption, safety in case of emergencies, comfort, and road congestion [95–97].

The Grand Cooperative Driving Challenges GCDC2011 and GCDC i-Game goals were to improve the cooperation among automated vehicles considering the platoon and cooperative intersection scenarios. Both events took place in the years 2011 and 2016, respectively, on the highway between Helmond and Eindhoven in the Netherlands. The first edition had the goal of demonstrating the feasibility of two parallel platoons following a leader vehicle, whereas in the second edition three more complicated use cases were validated: (1) the merging of two different platoons in one, (2) actions of two parallel platoons

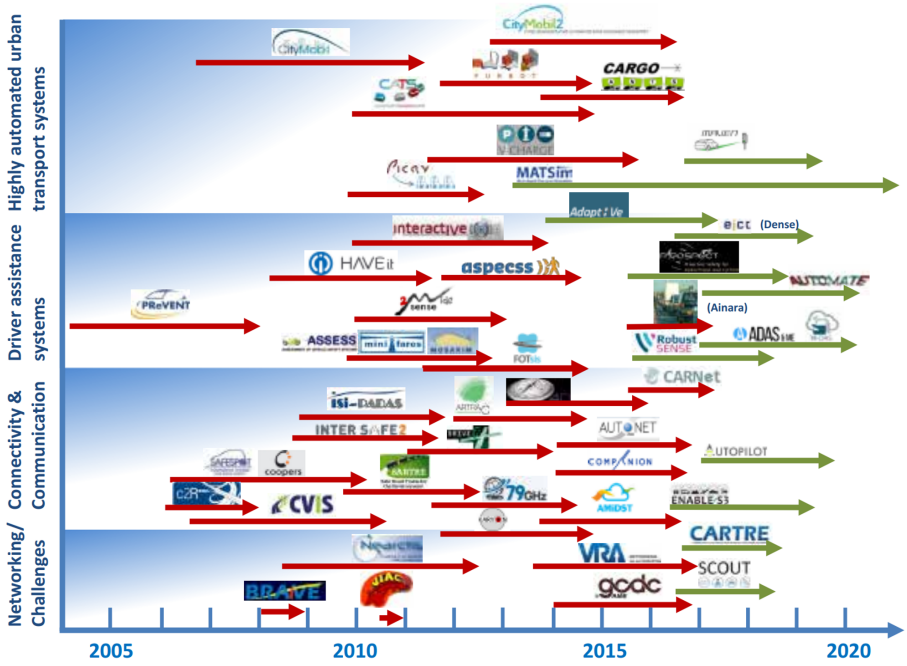

Figure 2.8: Summary of European Projects [3]

with an emergency vehicle, and (3) cooperative intersection [98–100].

Autonet2030 (Co-operative Systems in Support of Networked Automated Driving by 2030) project was another of the recent projects done in the EU between 2013 and 2016. The objectives of the project were in terms of achieving three principal objectives: (1) establishing an on-board sensor architecture for reliable lane-keeping, (2) standardizing V2X message during cooperative maneuvers and (3) generating decentralized techniques for fully automated cooperative maneuvers. Platooning, merging in a platoon, leaving a platoon, and cooperative intersections were the scenarios considered [101].

One of the newest EU projects in terms of automated driving is the Managing Automated Vehicles Enhances Network initiative, also known as Maven. This project started in 2016 and finished in 2019, the main goals of the project were to develop intelligent infrastructure, managing cooperation among vehicles and intersections, increasing safety, and efficiency. This was one of the first projects

analyzing the cooperation among vehicles as a method of negotiation. This represented a novel method to resolve the cooperative AD problem. The scenario studied was limited to platoons in urban environments considering signalized intersections [102, 103].

There are many projects related to AD technologies, but this Ph.D. thesis has been developed in the framework of the ENABLE-S3 and UnCoVerCPS projects which are explained below.

ENABLE-S3 Project

The European project Enable Validation for Highly Automated Safe and Secure Systems (ENABLE-S3) is especially relevant for the current work because it was a framework for developing and testing the proposed methods. It started in May 2016 and finished in May 2019 with a total budget of 65 million euros. The consortium is constituted by 68 partners from 16 different countries, from academia, researching centers, and industry and six different domains: automotive, aerospace, rail, maritime, health care and farming [104]. In general, these six areas can be categorized as ACPS or Automated Cyber-Physical systems.

The general problem aimed at ENABLE-S3 was the importance of Validating and Verifying (V&V) all these ACPS before introducing the technology in the market, hence the main goal was to reduce in 50% the effort demanded to do the V&V task. Two objectives were proposed to achieve it:

- The validation methodology must consider novel approaches for scenario and metric selection, considering optimization of the process and improving system simulations in terms of reducing the time-to-market [105].
- Establishing a general architecture to test and validate and verify ACPS in general terms, considering Model-in-Loop (MiL), Hardware-in-loop (HiL), Vehicle-in-Loop (ViL), and proving ground [106].

UnCoVerCPS Project

Unifying Control and Verification of Cyber-Physical Systems (UnCoVerCPS) project had the objective of improving the V&V process using online methods. In these terms, the goals can be summarized as follows [107]:

- Designing novel methods for on-the-fly verification concepts, strongly based on Model Predictive Control, and standardized models for different domains.

(a) EnableS3 logo

(b) UnCoVerCPS logo

Figure 2.9: Relevant project for this thesis

- Designing novel algorithms for online verification of the control systems.
- Application of the methods and algorithms in 4 different domains, including automated driving, human-robot collaboration, wind turbines, and smart grids.

The automated driving use case dealt with the collaboration of automated driving scenarios including the overtaking, which represented a novelty in European initiatives.

2.2.2 Legal framework in the EU

A great amount of time and effort has been given from the European Commission to improve this technology in Europe, additionally, there are some efforts done for each country individually.

In the case of Spain, in 2015, it was approved a legal framework to test automated driving technologies on public roads. It is a special license, valid for two years, which allows companies, research centers, and universities, to execute tests of AD [11].

France has established an AD national plan for the upcoming years (Horizon 2020) considering a legal framework for executing experiments on roads, and more national budget for projects on this topic [108].

Germany is working in terms of its Pegasus initiative to accelerate AD technology considering the standards. The initiative is strongly based on the Federal

[11] DGT webpage: `http://www.dgt.es/es/prensa/notas-de-prensa/2015/20151116-trafico-establece-marco-realizacion-pruebas-vehiculos-conduccion-automatizada-vias-abiertas-circulacion.shtml`

Ministry for Economic Affairs and Energy, and the country's goals are: (1) standardization of the procedures for testing automated vehicles in simulated and real scenarios, (2) creation of tool-chains for AD, and (3) involvement of the manufacturers in early stages of the designing and testing process [12].

Since 2015, drivers uses AD's functionalities in the Netherlands. The restriction is to have the driver inside the vehicle. In 2017, a new law removed the driver from the vehicle while executing remote operation tests. This accelerated the process of testing AD functionalities and it was a step closer to the market [13][14].

In 2018, the Aurora test ecosystem started in Finland with the main goal of testing AD and infrastructure under extreme weather conditions. It is a corridor of 10km on the public E8 road connecting Pahtonen with Muonio. This road has a great number of sensors, communication devices, and intelligent infrastructure to be used for testing. Furthermore, new pieces of hardware can be added in the road infrastructure [15][16].

Lastly, Sweden established the first full-scale test environment, it was named AstaZero which derived from "Active Safety Test Area Zero". A great variety of traffic situations can be recreated in this environment [17].

2.3 Current AD problem and limitations

The previous sections presented a summary of relevant projects, initiatives, challenges, and milestones achieved. Although, great efforts are still demanded to AD's final deployment under unsupervised conditions. They are grouped into three topics: environment modeling, hardware, and software. Environment modeling is considered a hardware/software problem but out of the vehicle, considering the models used, Road Side Units (RSU), intelligent infrastructure, etc. The hardware domain deals with sensors, actuators, and communication devices (V2X). Finally, the software is split into three tasks: perception, decision, and control.

[12]PEGASUS project webpage: `https://www.pegasusprojekt.de/en/about-PEGASUS`

[13]Government of Netherlands webpage: `https://www.government.nl/latest/news/2017/11/22/new-legislation-allows-for-the-testing-of-cars-with-remote-drivers`

[14]Library of congress webpage: `http://www.loc.gov/law/foreign-news/article/netherlands-legislation-to-allow-more-testing-of-driverless-vehicles/`

[15]Väylä webpage: `https://vayla.fi/web/en/e8-aurora/test-ecosystem#.XH-RQkxFyhc`

[16]Väylä webpage: `https://vayla.fi/web/en/e8-aurora/r-d/arctic-challenge#.XH-RRUxFyhc`

[17]AstaZero webpage: `http://www.astazero.com/about-astazero/`

The vehicles' hardware was deeply studied, and some works are currently under development. On the other hand, the algorithms used for vehicular perception have been analyzed in the past as well. The limitation is still in terms of sensors and computation power. Communications has a well-documented state of the art, and currently, this technology is under market improvements.

Many decision and control techniques were tested in the past and there are still issues to achieve market standards (i.e. the interaction between automated and non-automated vehicles). Therefore, this section presents a summary of the current work developed in the vehicles' decision and control area.

2.3.1 The control problem

All manufacturers' improvements were done in terms of vehicular actuators, such as steering wheel and the pedals. Some techniques such as fuzzy logic [109], linear quadratic controllers [110], and PID [111] were used to control the vehicle in the lateral and longitudinal domains. These techniques are called reactive control because they generate a response based on a calculated error, correcting an event after it occurred.

Currently, Model Predictive Control (MPC) is commonly used due to the advantages of the prediction horizon. The authors of [112, 113] presented MPC methods, based on kinematic models, to control the lateral and longitudinal vehicle actions on a platoon scenario. Other applications were in terms of eco-driving and power management while driving [114]. The drawback of this type of linear model is the low precision of the open-loop actuator signals, demanding the re-calculation of the control actions constantly. Moreover, other authors used a dynamic vehicle model with tires representation to improve the system performance, with the disadvantage of large computation time. Moreover, this type of model does not support low speeds due to an inverse relation of vehicle speed [115].

AD's new-tendencies try to generate decentralized control algorithms for cooperative scenarios, such as platoon. These methods solve individual problems in each vehicle considering the scenario's constraints [116]. In [117] was explained a method to control the vehicle under driving limits, keeping vehicle control in high-stress maneuvers, such as lane changes.

Another tendency is the vehicle's shared control whereas, it switched between driver and vehicle's decisions. Currently, this type of control assists the driver with a mixed action between human and vehicle's judgment, avoiding unsafe future conditions [118].

2.3.2 The Decision problem

The vehicle decision process was deeply studied, as well as vehicle control, and some interesting works concluded: more research is demanded before their commercial deployment [1]. Some scenarios, such as urban or overtaking, are especially complex in terms of maneuvering in the presence of sharp turns or roundabouts, and the interaction with other agents.

The literature uses a large variety of names to separate different decision tasks. Some names are global, path, behavioral, maneuver, local, trajectory, and motion planning or high-level decision-making [119]. In general terms, motion planning is associated with vehicle movement considering: comfort, solutions feasibility, presence of obstacles on the road, etc. The other terms are categorized into three general categories:

Global planning

Also known as route planning, this task relies on the topology of the environment, which is based on the use of maps. It finds the best route to the desired destination. The obstacles considered by the path planning are generally static (blockage of a route) due to the time consumed by recalculating the route in real-time [120]. Most of the techniques used are based on graph search methods.

Dijkstra and A* based algorithms are good examples of path planning methods, which divide the region into a grip, assigning weights or rewards in terms of distance and the lack of obstacle on the paths. Some of them even include techniques such as lattice to move around the grip region with a good efficiency [121].

Another method widely used is Rapidly-exploring Random Trees or RRT (refer to Fig. 2.10a). It is a sampling-based planner which increments a tree from the route to the goal or vice versa, using heuristics or system constraints for its expansion [122].

Behavioral planning

Depending on the approach used, high-level decision assignments are part of the planning module. This task describes the maneuver space using discrete actions, for example: accelerate, decelerate, keep speed, lane change, keep the lane, etc. An approach highly used is the Partially Observable Markov Decision Processes (POMDP), predicting future actions of the participants while generating discrete action sets [125].

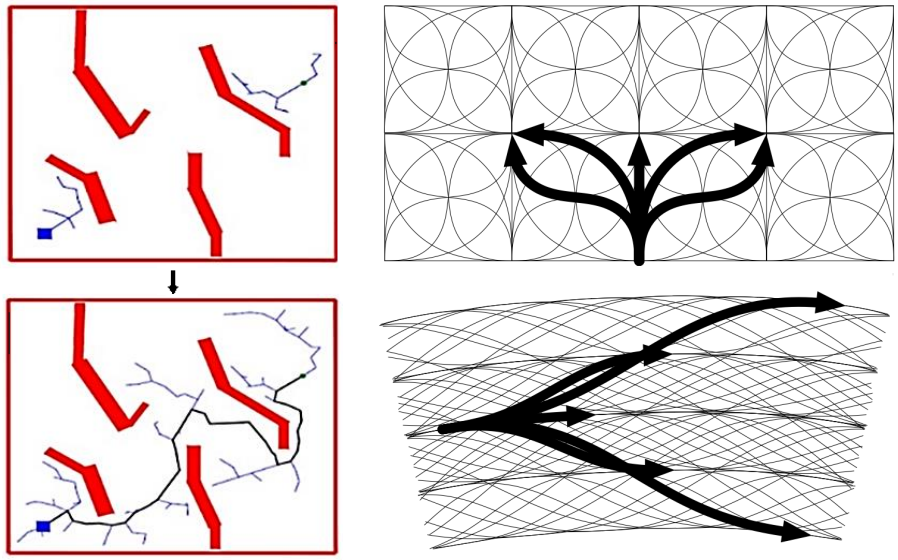

(a) Example of RRT [123] (b) Examples of lattice application [124]

Figure 2.10: Different path and trajectory methods used in literature

Local planning

Also known as trajectory planning, it generates feasible vehicle trajectories, in terms of the lateral and longitudinal domain. Generally, they have constraints, such as: (1) vehicle's dynamics, (2) road's geometry, (3) safety, and (4) comfort. These approaches use models which are kinematic or dynamic. They can be non-holonomic (standard vehicle models) or holonomic ones (more degrees of freedom during the movement).

Interesting approaches use curves to imitate the driving process with a set of constraints, during complex maneuvers such as lane changes [126]. Some of the curves used in the state of the art are clothoid, b-splines, and Bézier (refer to Fig. 2.11). Bézier has special characteristics and benefits (detailed in chapter 3).

Some approaches were proposed using RRT methods based on motion primitives. They used driver, vehicle , and mathematical representations for the generation of the primitives [127, 128]. Lattice was another of the approach

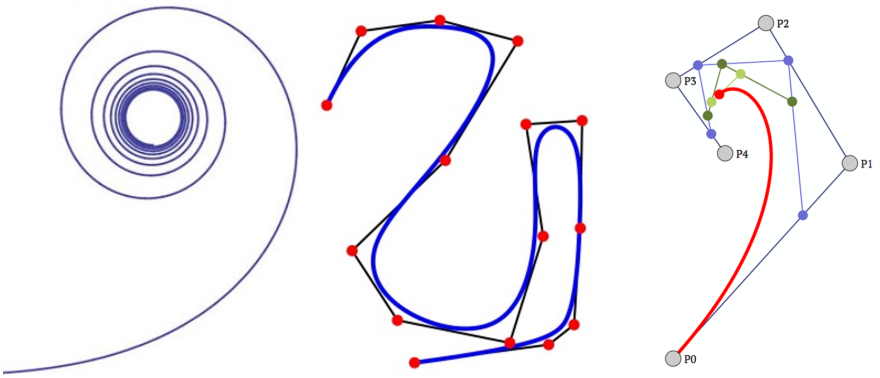

(a) Clothoids (b) B-Splines (c) Bézier

Figure 2.11: Curves used in trajectory planning.

used, and motion primitives were introduced to cover completely the action space (Fig. 2.10b). This method has slower computation-time compared to RRT [129].

Optimal control problems (OCP), such as MPC formulations, are new tendencies to solve the trajectory planning problem. The action space is not limited to a set of discrete actions. OCP delivers a general solution subject to constraints and target goals. These approaches have a large computation cost, although it depends of the model used and the constraint definition [130–134].

Emerging tendencies consider the trajectory planning topic as a cooperative task on the road. Most of them are based on centralized solutions for all the participants in the scenario [135, 136]. Artificial intelligence based on driver information is an interesting approach in this field [137]. Nonetheless, it has some troubles in terms of the regulation and certification process. Fig. 2.12 presents a summary of the advantages and disadvantages of the methods used in the state of the art.

In the framework of this Ph.D. thesis, a formal method has been proposed to ensure safety in the trajectory generation, which represents a possible solution to the AD validation and verification process.

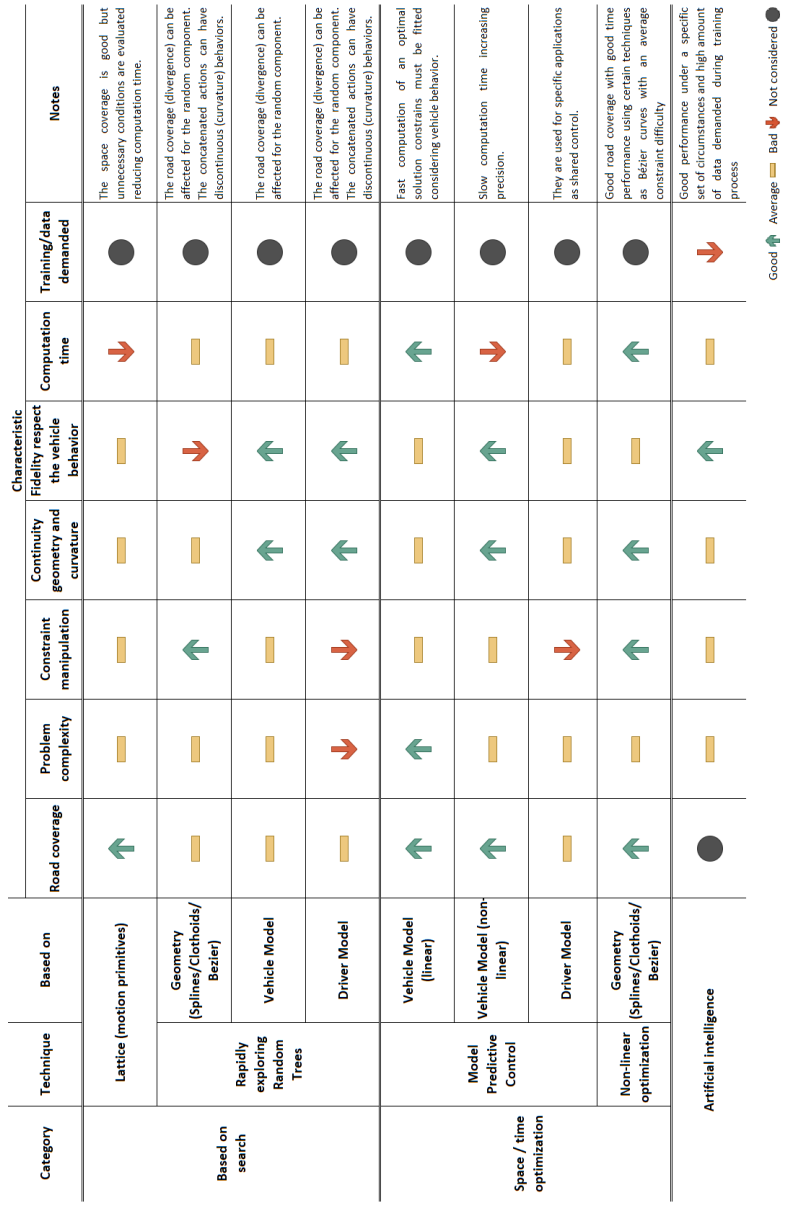

Figure 2.12: Summary of mostly used trajectory planning techniques

2.4 General summary

A large number of decision and control milestones have been achieved in AD technology due to challenges, projects, and public-private initiatives around the world. These technologies have improved the performance of the ADAS on commercial vehicles. It permits a better integration of AD functionalities in structured and unstructured environments.

Furthermore, there are some gaps in technology considering trajectory generation in urban environments and in certain maneuvers such as overtaking. In these terms, UnCoVerCPS and EnableS3 projects are aiming to improve AD technology in urban scenarios, adding cooperation among the agents involved (detailed in chapter 5).

On the other hand, the literature has analyzed different techniques in automated driving, especially in terms of control systems. Fuzzy, PID, and MPC are some of the strategies used in the vehicle's control. Currently, this area is targeting market deployment with applications such as lane departure assistance and adaptive cruise control.

Nevertheless, the decision area demands further research on topics such as trajectory generation and high-level decision making. RRT, lattice, MPC, and parametric curves are some of the techniques used for motion planning. In these terms, this Ph.D. thesis has used the Bézier curves and MPC methods for the generation of safe and comfortable trajectories. They are selected due to the benefits detailed in chapters 3 and 4.

"All the great things are simple, and many can be expressed in a single word: freedom, justice, honor, duty, mercy, hope".

Winston Churchill

3

Dual-modular control architecture for AD

In the last decades, a considerable amount of institutions, research centers, and companies have improved AD functionalities [138, 139]. Lateral and longitudinal controllers [140–142], as well as perception [143, 144], and communications [145] are some of the topics studied on public road demonstrations.

Other topics have received less attention, like vehicles' decision algorithms. This area is a challenging topic in AD due to its large number of tasks. Some examples are the generation of smooth trajectories [146], speed profiles considering fuel consumption and comfort [147], obstacles avoidance [148], coordination with other vehicles [149], among others.

In these terms, this chapter proposes an AD trajectory planning approach based on Bézier curves. State of the art methods are also summarized and described, followed by an explanation of the framework used for testing AD functionalities that was built during this Ph.D. thesis.

The proposed AD software architecture has improved the process of developing and testing new functionalities, for example, the trajectory planning on urban and semi-urban environments.

3.1 Summary of control architectures

In the past, AD functionalities were designed for a specific conditions. This situation required constant modifications of the architecture with every new application or scenario developed. Some authors have generalized and standardized the tasks, hence reducing the time of deployment.

A first approach was a cascade control architecture presented in [109], which aimed to a robust steering wheel control in a wide speed range. The main novelty was the addition of the position and angular speed for the steering wheel control. The authors used a fuzzy logic controller to move the actuators, using an architecture which was divided into three modules: (1) data collection and processing, (2) the high-level fuzzy controller, and (3) the low-level control of the actuators.

The Stadpilot project can be considered a practical case of this cascade architecture. The project aimed to deploy "Leonie" vehicle in urban environments, considering other conventional vehicles (traffic), bicycles, pedestrians, etc [150]. Leonie was partly built by Volkswagen together with Stadpilot consortium, and its architecture was split into: (1) environment recognition, (2) vehicle modeling and map data, (3) decision module, and (4) vehicle's control.

Next, the authors of [151] presented a distributed control architecture for automated vehicles. The main novelty was the introduction of AUTOSAR's methodology during the development. It was validated in the Autonomous Vehicle Competition (AVC) in Korea in 2010 and 2012. In this case, perception, control, planning, system management, and localization were the modules embedded in the architecture. This work did not consider the communications among the automated vehicle and other participants.

In 2013, during the Public ROad Urban Driverless (PROUD) tests [152], the University of Parma tested a new control architecture for automated vehicles. The approach used the methods proposed by the universities of Stanford and Parma in the DARPA challenges. Perception, planning, and control were the modules of this approach. The perception module was rich and complex considering: fusion of different sensors and map information using techniques such as Unscented Kalman Filter (UKF), lane and traffic light information fusion, among others. Planning and control were simple modules, hence lacking details.

The authors of [153] presented a control architecture divided into three components: (1) the perception of the environment and context evaluation of the vehicle operation, (2) the combination of the decision and control of the vehicle motion, and (3) the actuators' low-level control. This architecture added the semantics as part of the perception module, and the decision and control module

considered the diagnosis and fault management.

Another example is the Robust Sense architecture that has been developed to detach the AD tasks [154]. This architecture was focused on perception including fallback strategies in case of unexpected conditions. The novelty in this approach was an online monitor for system state verification. Although, this approach lacked details in the decision, control, and communication modules.

On the other hand, the authors of [155] presented an AD architecture tested, both in a real vehicle platform and simulation environments, considering the decision, control, and actuation modules without communication and perception which are normally used in AD architectures (refer to section 1.4).

In [156], an architecture designed for the platoon scenario was divided into three different modules: (1) a controller which was designed for the maneuver, (2) a communication module for exchanging information, and (3) the HMI. This approach did not considered perception.

Another control architecture was presented in [157], which was divided into three levels: (1) the strategic level or routing, (2) the tactical or maneuvering level, for example, lane changing, cruising, etc, and (3) trajectory generation and tracking. Although this development contained more details than the previous ones, it merged the planning and control modules.

While all these designs were used for specific tests and deployments, the authors of [1] summarizes them in a general architecture based on six modules, i.e. acquisition, perception, communications, decision, control, and actuation.

In these terms, the general AD control architecture inspired the current work, facilitating new developments such as trajectory planning. This Ph.D. thesis aims to improve it. Section 2.3.2 presented some state-of-the-art methods including curves and arcs, clothoid curves, driver models, and vehicle models. The parametric curves had a special interest in this work, due to their simplicity for modeling feasible vehicle trajectories.

3.2 Proposed control architecture

The proposed architecture has been implemented in Matlab®/Simulink® (refer to Fig. 3.1), and it was built with the six main modules of AD: (1) acquisition, (2) perception, (3) communication, (4) decision, (5) control, and (6) actuation. Furthermore, the Human Machine Interface (HMI) was added to interact with the modules. Extra modules can be added as subsystems.

The acquisition module gathers all the data generated by the physical sensors in the vehicle, as well as virtual ones. Some of the information collected by this

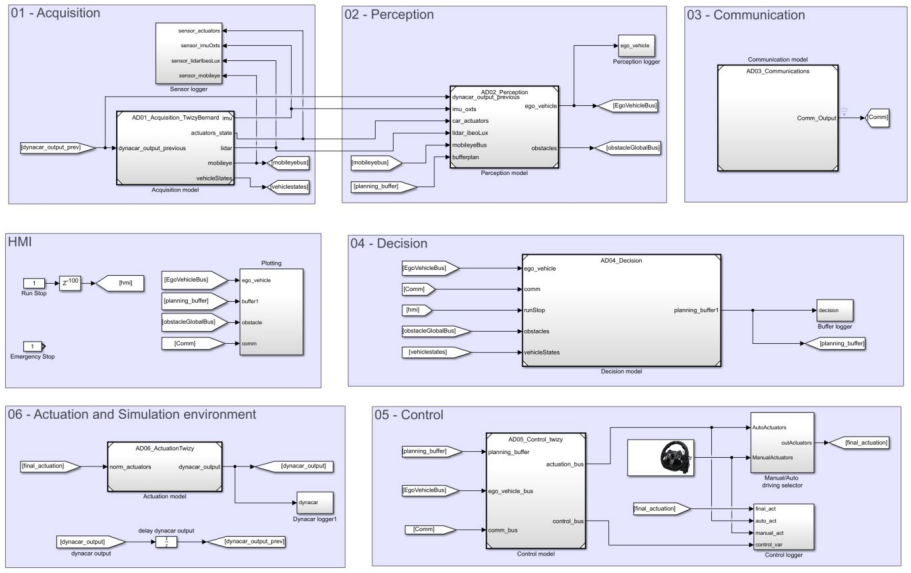

Figure 3.1: Proposed automated vehicles architecture

module is position coordinates, roll-pith-yaw angles, speed in 3 axes, wheel angle, etc. Conventionally, this module reads the data from sensors, such as radars, cameras, LIDAR (Laser Imaging Detection and Ranging), GPS, inertial units, and vehicle odometry.

The perception module combines the information collected from the acquisition module. It mitigates possible errors or information noises during data collection. A great variety of techniques are used in this module with interesting results. Simultaneous Localization And Mapping (SLAM), and prediction filters for future vehicle states are some interesting methods implemented in this module. In this thesis, a Kalman filter was used to obtain a precise vehicle position. This filter was implemented by a commercial device, and it did the fusion of the Intertial Measurement Unit (IMU) signal and a Global Position System (GPS) data.

The communication module gives detailed information about the participants - with communication capacities - around the vehicle. There are different configurations such as communication between vehicles V2V [158], communication Vehicle-to-Infrastructure V2I [159] and Vehicle-to-Pedestrian V2P [160].

This module is especially relevant for the contributions of chapter 4 and 5.

The decision module is divided into three sub-tasks: global planning, behavioral planning, and local planning. Global planning is related to the routing problem, and it identifies a path (using the map). The behavioral planning gives high-level assignments shaped as rules, e.g. lane changing, cruising, and stopping requests. The local planning generates feasible, safe, and comfortable trajectories for the vehicle's controllers. The main approaches of this Ph.D. thesis are in the local planning, precisely in trajectory generation. Additionally, other contributions are focused on behavioral planning, i.e. lane changing, overtaking, and obstacle avoidance (refer to chapters 4 and 5).

The control module tracks the generated trajectory. This action is divided into two parts: lateral control related to the vehicle position and longitudinal control related to the speed. PID, fuzzy, on-off control, among others reactive control techniques, and predictive controllers like MPC and optimization-based controllers were used in this module during the work.

Finally, the actuation module gathers the information generated for the control module to the actuators. This module has low-level control, as well as the models used for the simulation.

This architecture was used in a large number of projects and scientific publications. The time used for developing functionalities was optimized and simplified and validated on these publications: [161], [162], [163], [164], [165], [104], [166], [167], [168], [169] and [170].

3.3 Bézier curves

This Ph.D. thesis is mainly focused on trajectory generation, and a key components in the construction of them were the Bézier curves. They are a type of parametric curves that have been commonly used for computer graphics, animations and path generation in robotics [171]. In general, they are good for real-time implementations, and the computation time is lower than clothoid and other splines curves [172]. Bézier curves are described by the following equation:

$$\mathbf{B}(t|n, P_0, ..., P_n) = \sum_{i=0}^{n} b_i \mathbf{P}_i, \quad b_i = \binom{n}{i} t^i (1-t)^{n-i} \tag{3.1}$$

where $\{b_i \in \mathbb{R}\}$ is the Bernstein polynomial, $\{\mathbf{P}_i \in \mathbb{R}^2\}$ are the control points used to generate the curve, $\{n \in \mathbb{N}^+\}$ is the Bézier order and $\{t \in \mathbb{R}, t = [0, 1]\}$ is the parameter used for curve construction.

This work has used some of the following Bézier curves' properties:

- The starting point of the Bézier curve corresponds with control point $\mathbf{P}_0$, and the ending point corresponds with $\mathbf{P}_n$.
- The first point tangent vector (at $t = 0$) will be given by $\overrightarrow{P_0P_1}$ and the last point tangent vector (at t = 1) will be given by $\overrightarrow{P_{n-1}P_n}$.
- The curve will lie into the convex hull formed by the control points.
- Bézier curves are continuous geometrically and its curvature, $\{C^n \ \& \ G^n, \forall n \in \mathbb{N}^+\}$ which can be preserved in joints of two different curves.
- Bézier curves are symmetric, i.e. the generated curve for $t : 0 \rightarrow 1$ is equal to the one for $t : 1 \rightarrow 0$.

This thesis uses 4^{th} and 5^{th} order Bézier curves due to the fact that they have the best results during trajectory generation. In some special conditions, 3^{rd} degree curves are used. Higher-order curves were not considered because they do not have additional benefits within the current approach, while increasing the computation complexity [173].

A more compact representation of Eq. 3.1 is obtained when it is written as follows:

$$\mathbf{B}(t) = \mathbf{K}_0 + \mathbf{K}_1 t + \mathbf{K}_2 t^2 + ... + \mathbf{K}_n t^n \tag{3.2}$$

$\mathbf{K}_i$ are functions of the control points in fixed positions and the curve order. The values of $\mathbf{K}_i$ coefficients are given in Table 3.1. $\mathbf{K}_1$ and $\mathbf{K}_2$ determine the curvature at the starting point. Similarly, the coefficients determine the curvature in ending points using the property of symmetry (previously mentioned).

Using the information from 3^{rd} to 5^{th} degree Bézier, $\mathbf{K}_1$ and $\mathbf{K}_2$ are defined as follows:

$$\mathbf{K}_1 = n\overrightarrow{v_1} \qquad\qquad \mathbf{K}_2 = \frac{n(n-1)}{2}(\overrightarrow{v_2} - \overrightarrow{v_1}) \tag{3.3}$$

where $\overrightarrow{v_1} = \mathbf{P}_1 - \mathbf{P}_0$ and $\overrightarrow{v_2} = \mathbf{P}_2 - \mathbf{P}_1$ simplify the equations, and n is the degree of the curve.

In general terms, the curvature in $\mathbb{R}^2$ is defined as [174]:

Table 3.1: Compact Bézier polynomial Coefficients "K"

C	Bézier curve order		
	3rd Order	4th Order	5th Order
$\mathbf{K}_0$	$\mathbf{P}_0$	$\mathbf{P}_0$	$\mathbf{P}_0$
$\mathbf{K}_1$	$-3\mathbf{P}_0 + 3\mathbf{P}_1$	$-4\mathbf{P}_0 + 4\mathbf{P}_1$	$-5\mathbf{P}_0 + 5\mathbf{P}_1$
$\mathbf{K}_2$	$3\mathbf{P}_0 - 6\mathbf{P}_1 + 3\mathbf{P}_2$	$6\mathbf{P}_0 - 12\mathbf{P}_1 + 6\mathbf{P}_2$	$10\mathbf{P}_0 - 20\mathbf{P}_1 + 10\mathbf{P}_2$
$\mathbf{K}_3$	$-\mathbf{P}_0 + 3\mathbf{P}_1 - 3\mathbf{P}_2 + \mathbf{P}_3$	$-4\mathbf{P}_0 + 12\mathbf{P}_1 - 12\mathbf{P}_2 + 4\mathbf{P}_3$	$-10\mathbf{P}_0 + 30\mathbf{P}_1 - 30\mathbf{P}_2 + 10\mathbf{P}_3$
$\mathbf{K}_4$	–	$\mathbf{P}_0 - 4\mathbf{P}_1 + 6\mathbf{P}_2 - 4\mathbf{P}_3 + \mathbf{P}_4$	$5\mathbf{P}_0 - 20\mathbf{P}_1 + 30\mathbf{P}_2 - 20\mathbf{P}_3 + 5\mathbf{P}_4$
$\mathbf{K}_5$	–	–	$-\mathbf{P}_0 + 5\mathbf{P}_1 - 10\mathbf{P}_2 + 10\mathbf{P}_3 - 5\mathbf{P}_4 + \mathbf{P}_5$

$$k(t) = \frac{\dot{B}_x(t)\ddot{B}_y(t) - \ddot{B}_x(t)\dot{B}_y(t)}{\sqrt{(\dot{B}_x(t)^2 + \dot{B}_y(t)^2)^3}} = \frac{\dot{\mathbf{B}}(t) \times \ddot{\mathbf{B}}(t)}{||\dot{\mathbf{B}}(t)||^3} \tag{3.4}$$

the function $\mathbf{B}$ is the Bézier equation. Evaluating at $t = 0$, it is obtained:

$$k(t=0) = 2\frac{\mathbf{K}_1 \times \mathbf{K}_2}{||\mathbf{K}_1||^3} = \frac{(n-1)}{n}\frac{\overrightarrow{v_1} \times \overrightarrow{v_2}}{||\overrightarrow{v_1}||^3} \tag{3.5}$$

The previous equation explicitly shows: if the three starting points in a curve are co-linear, the generated Bézier curve will have zero curvature at its starting point $\{k(t = 0) = 0\}$. This affirmation can be extended to the three ending points due to symmetry on the 5^{th} degree curves. This property is useful for designing the intersections, lane changes, and for entering and exiting on the roundabout scenario.

3.4 Trajectory planning method

The proposed trajectories are based on Bézier curves. However, they have additional conditions which are obtained from the map model. Hence, this section explains the map modeling and the construction of lateral and longitudinal trajectories. This method is supported by mathematical demonstrations.

3.4.1 Map definition

This section presents the mapping approach which is demanded by the global planner. Map information simplifies the conditions for the local planning with

Bézier. The map is known as "simple map", and it contains description points defining common road structures. Some of these structures are intersections, roundabouts or lane changes, and they are shown with "×" shape in Fig. 3.2, 3.4, and 3.3. Besides, the principal benefit is the reduction of the total amount of points, keeping the problem geometrically simple.

Intersections

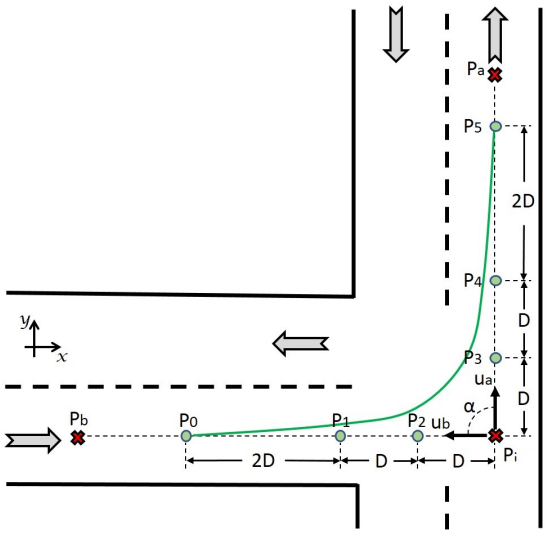

Figure 3.2: Map and trajectory planning on intersection.

Fig. 3.2 depicts the description of an intersection using a simple point. This point represents a junction of two or more straight paths. The unitary vectors u_a and u_b define the intersecting roads, and they are given by:

$$\overrightarrow{u_b} = \frac{\mathbf{P}_b - \mathbf{P}_i}{||\mathbf{P}_b - \mathbf{P}_i||} \qquad \overrightarrow{u_a} = \frac{\mathbf{P}_a - \mathbf{P}_i}{||\mathbf{P}_a - \mathbf{P}_i||} \tag{3.6}$$

where $\overrightarrow{u_a}$ is the unitary vector that goes from intersection $\mathbf{P}_i$ to the previous global point $\mathbf{P}_b$, and $\overrightarrow{u_b}$ is the unitary vector formed with the next simple point $\mathbf{P}_a$ and $\mathbf{P}_i$. The angle α can differ with respect to 90°. Therefore, this approach

models a large number of intersections. The parameter D will be used later on local planning for the Bézier curve modeling.

Roundabouts

Fig. 3.3 shows the definition of a roundabout using a simple point for its description. It uses the roundabout center point $\mathbf{P}_r$, its radius R, entrance angle a_i, and the exit angle a_o. The roundabouts can be modeled using these parameters, with an approximated circular shape.

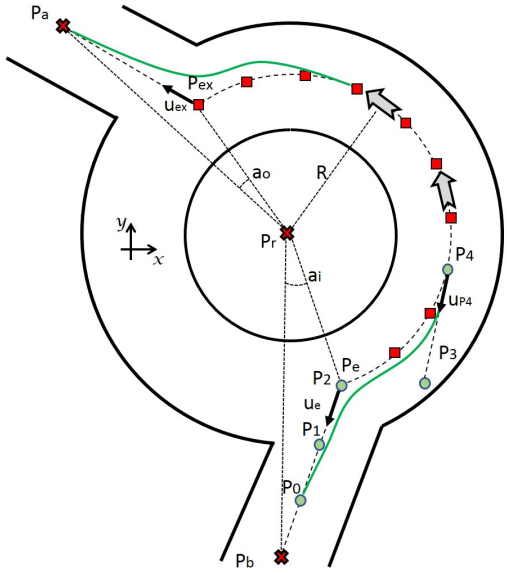

Figure 3.3: Map and trajectory planning on roundabouts.

Roundabout entrance and exit points are defined by:

$$\mathbf{P}_e = \mathbf{P}_r + R \begin{bmatrix} cos(tan^{-1}(\frac{u_{b_y}}{u_{b_x}}) \pm a_i) \\ sin(tan^{-1}(\frac{u_{b_y}}{u_{b_x}}) \pm a_i) \end{bmatrix} \tag{3.7}$$

$$\mathbf{P}_{ex} = \mathbf{P}_r + R \begin{bmatrix} cos(tan^{-1}(\frac{u_{a_y}}{u_{a_x}}) \mp a_o) \\ sin(tan^{-1}(\frac{u_{a_y}}{u_{a_x}}) \mp a_o) \end{bmatrix}$$

where $\mathbf{P}_e$ is roundabout entrance coordinates, $\mathbf{P}_{ex}$ is roundabout exit coordinates, values of $\overrightarrow{u_a}$ and $\overrightarrow{u_b}$ are defined by Eq. 3.6 but the intersection point $\mathbf{P}_i$ is substituted by roundabout points $\mathbf{P}_{ex}$ and $\mathbf{P}_e$ respectively. In these equations, the upper sign is used when traffic is defined counter clockwise and lower one for left-drive traffic [175].

The n_r points (points with square shape in Fig. 3.3) define the route inside roundabout. Following this procedure, the total amount of points, generated with the center point $\mathbf{P}_r$ and radius, is $n_r + 2$.

Lane changes

In this case, the approach considers straight path segments during the maneuver (Fig. 3.4). The vectors of Eq. 3.6 describes the path in the lane-change, and they have the following relation:

$$\overrightarrow{u_b} = -\overrightarrow{u_a} \tag{3.8}$$

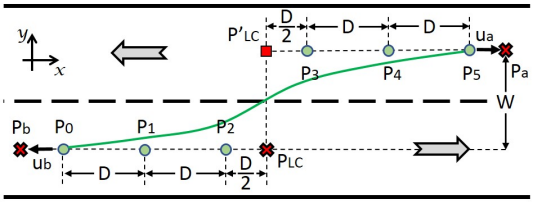

Figure 3.4: Map and trajectory planning on lane change maneuver.

Under these conditions, a new point $\mathbf{P}'_{LC}$ is introduced to handle the maneuver in local planning. This point is defined by the equation:

$$\mathbf{P}'_{LC} = \mathbf{P}_{LC} + w \begin{bmatrix} cos(tan^{-1}(\frac{u_{a_y}}{u_{a_x}}) \pm \frac{\pi}{2}) \\ sin(tan^{-1}(\frac{u_{a_y}}{u_{a_x}}) \pm \frac{\pi}{2}) \end{bmatrix} \tag{3.9}$$

where w is the road width, $\overrightarrow{u_a}$ is the vector presented in Eq. 3.8. The symbol $\pm$ is negative when the lane change is done to the right side and positive to the left side.

3.4.2 Path planning

The main contribution of the current chapter is in terms of the generation of trajectories with smooth and continuous curvature. This goal is achieved with formal definitions for the automated vehicles' trajectories. The work is mainly aiming at urban scenarios, while not limited to them. The subsection is divided into three scenarios: intersections, roundabout, and lane changes.

Table 3.2: Bézier control points for lateral and longitudinal approach for intersections "Int", roundabout entrance "RE", roundabout exit "REx" and lane change maneuver "LC", and speed planning.

Planning		Control points n-order Bézier P_0	P_1	P_2	P_3	P_4	P_5
Lateral	Int	$4D\overrightarrow{u_b} + \mathbf{P}_i$	$2D\overrightarrow{u_b} + \mathbf{P}_i$	$D\overrightarrow{u_b} + \mathbf{P}_i$	$D\overrightarrow{u_a} + \mathbf{P}_i$	$2D\overrightarrow{u_a} + \mathbf{P}_i$	$4D\overrightarrow{u_a} + \mathbf{P}_i$
	RE	$\frac{3D}{2}\overrightarrow{u_e} + \mathbf{P}_e$	$\frac{D}{2}\overrightarrow{u_e} + \mathbf{P}_e$	$\mathbf{P}_e$	$D_{P_3}\overrightarrow{u_{P_4'}} + \mathbf{P}_4$	$\mathbf{P}_r + R\overrightarrow{u_{\theta_e}}$ *	-
	REx	$\mathbf{P}_r + R\overrightarrow{u_{\theta_{ex}}}$ **	$D_{P_1}\overrightarrow{u_{P_0}} + \mathbf{P}_0$	$\mathbf{P}_{ex}$	$\frac{D}{2}\overrightarrow{u_{ex}} + \mathbf{P}_{ex}$	$\frac{3D}{2}\overrightarrow{u_{ex}} + \mathbf{P}_{ex}$	-
	LC	$\frac{5\overrightarrow{u_b}D}{2} + \mathbf{P}_{LC}$	$\frac{3\overrightarrow{u_b}D}{2} + \mathbf{P}_{LC}$	$\frac{\overrightarrow{u_b}D}{2} + \mathbf{P}_{LC}$	$\frac{\overrightarrow{u_a}D}{2} + \mathbf{P}'_{LC}$	$\frac{3\overrightarrow{u_a}D}{2} + \mathbf{P}'_{LC}$	$\frac{5\overrightarrow{u_a}D}{2} + \mathbf{P}'_{LC}$
Longitudinal	Speed	$\begin{bmatrix} s_0 \\ v_0 \end{bmatrix}$	$\begin{bmatrix} s_0 + D \\ v_0 \end{bmatrix}$	$\begin{bmatrix} s_0 + 2D \\ v_0 \end{bmatrix}$	$\begin{bmatrix} s_0 + 3D \\ v_0 + W \end{bmatrix}$	$\begin{bmatrix} s_0 + 4D \\ v_0 + W \end{bmatrix}$	$\begin{bmatrix} s_0 + 5D \\ v_0 + W \end{bmatrix}$

* $\theta_e = tan^{-1}(\frac{P_{e_y} - P_{r_y}}{P_{e_x} - P_{r_x}})$, $\overrightarrow{u_{\theta_e}} = [cos(\theta_e + \frac{D}{R}) \quad sin(\theta_e + \frac{D}{R})]$

** $\theta_{ex} = tan^{-1}(\frac{P_{ex_y} - P_{r_y}}{P_{ex_x} - P_{r_x}})$, $\overrightarrow{u_{\theta_{ex}}} = [cos(\theta_{ex} - \frac{D}{R}) \quad sin(\theta_{ex} - \frac{D}{R})]$

Intersections

Fig. 3.2 shows an intersection defined with a single point. This configuration reduces the number of points in the map, but it demands a trajectory method connecting, smoothly, the two straight segments. Bézier curves of 5^{th} order solves this problem optimally.

Three Bézier control points (from $\mathbf{P}_0$ to $\mathbf{P}_2$), set over the same line, ensure curvature zero in the starting point of the curve $\{K(t = 0) = 0 : P_{y_{0,1,2}} = mP_{x_{0,1,2}} + b\}$, as Eq. 3.5 justifies. This means that the starting segment has straight path properties. The same equation and the symmetry criteria define curvature 0 in the ending part of the curve ($t = 1$) using the control points $\mathbf{P}_n$ to $\mathbf{P}_{n-2}$.

This information concludes that the minimum Bézier order, in an intersection, should be 4^{th} (5 control points). Nevertheless, this case sets the control

point $\mathbf{P}_2$ in the position of the intersection point $\mathbf{P}_i$. Hence, the 5^{th} order is selected as a solution, without the addition of many control points, and it is less restrictive than 4^{th} order. The positions of the control points are shown in Table 3.2 where the vectors $\overrightarrow{u_b}$ and $\overrightarrow{u_a}$ are given by the equation 3.6.

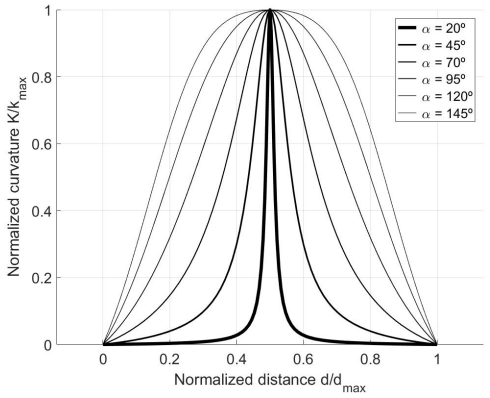

Figure 3.5: Curvature analysis for different intersection angles.

The distance between control points ensures the maximum curvature, of the Bézier curve, in the middle point of the trajectory. This value describes whether the trajectory is feasible or not, considering the maximum curvature radius of a vehicle given its mechanical limits. Fig. 3.5 shows the normalized curvature K/K_{max} (curvature of the generated segment divided by the maximum curvature of this segment) with respect to the normalized trajectory distance d/d_{max} (a total distance of the generated segment divided by the maximum value). It considers angles between straight segments α from 20 degrees to 145 degrees.

It is applied derivative in Eq. 3.4 to find its maximum value, as follows:

$$\frac{d}{dt}K(t) = \frac{(\dot{\mathbf{B}} \times \dddot{\mathbf{B}})(\dot{\mathbf{B}} \cdot \dot{\mathbf{B}}) - 3(\dot{\mathbf{B}} \times \ddot{\mathbf{B}})(\dot{\mathbf{B}} \cdot \ddot{\mathbf{B}})}{||\dot{\mathbf{B}}||^5} \tag{3.10}$$

evaluating the derivative of Bézier curve in $t = 0.5$:

$$\begin{aligned} \dot{\mathbf{B}}(t = 0.5) &= \frac{15}{4} D(\overrightarrow{u_2} - \overrightarrow{u_1}) \\ \ddot{\mathbf{B}}(t = 0.5) &= 10D(\overrightarrow{u_2} + \overrightarrow{u_1}) \end{aligned} \tag{3.11}$$

$$\dddot{\mathbf{B}}(t = 0.5) = 0$$

where D is the design parameter for trajectory and $\overrightarrow{u_{1,2}}$ are unitary vectors defined by Eq. 3.3. From these equations $\dot{\mathbf{B}} \times \dddot{\mathbf{B}} = \dot{\mathbf{B}} \cdot \ddot{\mathbf{B}} = 0$ generate a curvature derivative equal to 0 in $t = 0.5$ (maximum value).

Roundabouts

Fig. 3.3 shows the roundabout based on a simple point description. Their trajectories are modeled with two Bézier curves, and both trajectories connect the straight road with the inner part of the roundabout, which is modeled as a circle with a constant radius. The criteria used for designing the roundabout trajectories considers:

- The curvature points, at entrance $t = 0$ and at exit $t = 1$, must be 0 due to the fact they are straight paths.
- The roundabout's entrance and exit segments must fit its inner part with a curvature equal to the inverse of its radius.
- Bézier joining point angle must be the same as the circle arc angle (continuous trajectory).

Three co-linear control points ensure the first consideration. Another two points are selected in the inner part of the roundabouts, over a segment that is tangent to the circle, assuring curvature and direction continuity (second and third criteria). In summary, three co-linear points generate a curvature of 0, and two points generate a curvature equal to R^{-1}. Therefore, the 4^{th} order Bézier curve ensures the curvature requirements, and Fig. 3.3 depicts it.

Table 3.2 shows the trajectory generation at the entrance (RE) and the exit (REx) of the roundabout, as well as the Bézier control points. The straight paths are designed using similar criteria as in intersections, with D as a designing parameter. Those segments are from $\mathbf{P}_0$ to $\mathbf{P}_2$ in the case of the entrance and from $\mathbf{P}_2$ to $\mathbf{P}_4$ in the exit. The point $\mathbf{P}_4$ (entrance) and $\mathbf{P}_0$ (exit) are selected using the distance D over the arc of the circle.

In the entrance, the point $\mathbf{P}_3$ is separated from point $\mathbf{P}_4$ a distance that is given by:

$$D_{P_3} = \sqrt{\frac{3}{4} \frac{||\overrightarrow{u_{P_4}} \times (\mathbf{P}_2 - \mathbf{P}_4)||}{K_r}} \tag{3.12}$$

where $\overrightarrow{u_{P_4}}$ is the tangent vector (with the circle) in the point $\mathbf{P}_4$ and K_r is the roundabout curvature. In the case of exit, the point $\mathbf{P}_4$ is substitute by $\mathbf{P}_0$ and $\mathbf{P}_3$ by $\mathbf{P}_1$.

Fig. 3.6 shows the behavior of trajectory generation and its curvature using the specifications given in the planning method. Fig. 3.6a depicts three different trajectories generated for different distances D. Fig. 3.6b shows the trajectory's curvature while perfectly fit the inverse of the radius $0.1[m^{-1}]$.

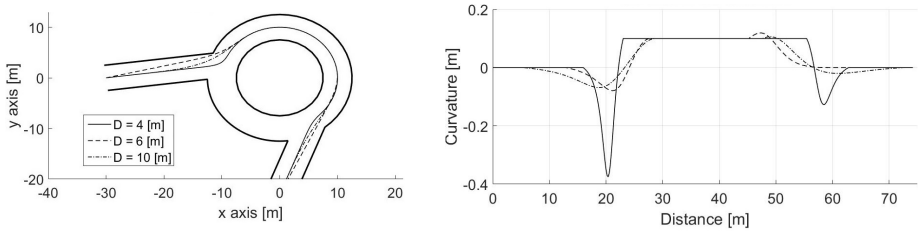

(a) Generated trajectories

(b) Curvature of the different trajectories

Figure 3.6: Examples of roundabout trajectories for different D values

Lane change

The approach uses a similar criteria as intersections, but its control points are aligned on the lane direction and they are separated a distance of D (Fig. 3.4). The unitary vectors u_b and u_a are explained in Eq. 3.8, w is the width of the road, and D is the distance between two consecutive control points $\{D \in \mathbb{R}, D = ||P_{n-1} - P_n||\}$.

Table 3.2 depicts the location of the control points on the lane-change. The minimum value of D is limited to W, and this generates maximum curvature values in $t \approx 0.20$ and $t \approx 0.80$. If a vehicle deals correctly with this lane change due to its physical and dynamical limitations, it can handle any trajectory with $D > W$.

The overtaking is considered as a special case of two-lane changes. First, using the proposed method; next, the opposite lane is kept until the overtaking is done. The returning is executed with the application of the symmetry criteria used as in the first lane change.

3.4.3 Speed planning

Sudden changes on speed reference can affect the speed control. On the other hand, if the changes are smooth and continuous, the controller will have a better performance. In such a way, a speed planner is proposed, also it is based on Bézier curves. It aims:

- To anticipate future conditions on the speed of the road.
- To consider vehicle physical constraints, such as maximum acceleration and maximum deceleration.
- To keep the vehicle velocity under the speed limits safely.
- To take into account the comfort of passengers.

The speed planner approach uses 5^{th} order Bézier curves to keep the advantages of this order and the problem symmetry. Fig. 3.8 depicts the location of control points for a speed profile curve, which is a function of distance in the path. The formulas for each control point are presented in Table 3.2.

The space between consecutive control points P_{i-1} and P_i is defined as $\{D \in \mathbb{R}, D = distance_x(P_{i-1}, P_i) \quad \forall \quad i = 1, 2, 3, 4, 5\}$. Hence, the condition generates curves with the x-coordinates proportional to the parameter t. This can be summarized by the equation:

$$B_x(t) = 5Dt = s \tag{3.13}$$

this equation fixes the distance in x-axis, and the parameter $t \in [0, 1]$ is proportional to this distance. It is introduced the variable $\{s \in [s_0, s_0 + 5D]\}$ to simplify the calculation.

The physical constraints of the vehicle, like acceleration and deceleration, have a direct relation with the generated curve. The definition of acceleration $\frac{dv_l(t)}{dt}$ is used with the change of variable $v_l = ds/dt$, and this change permits the introduction of these constraints. The resulting equation is given by:

$$a_l(t) = \frac{dv_l(t)}{dt} \Rightarrow a_l(s) = v_l(s)\frac{dv_l(s)}{ds} \tag{3.14}$$

where the variable a_l is longitudinal acceleration, v_l is longitudinal speed, t is time, and s the position. A nomenclature change is done using $v_l = B_y$ and $ds = dB_x = 5Ddt$ to simplify the problem, and this results in the equation:

$$a_l(s) = B_y \frac{dB_y}{dB_x} = B_y \frac{dB_y}{ds}, s \in [s_0, s_0 + 5D] \tag{3.15}$$

The maximum points of acceleration are found with the application of the derivative to Eq. 3.15. The resulting equation is:

$$\frac{da_l}{ds} = \left(\frac{dB_y}{ds}\right)^2 + B_y \frac{d^2 B_y}{ds^2} \tag{3.16}$$

The 5^{th} order Bézier equation is introduced in Eq. 3.16, and it has the following roots:

$$s_{a_{max}} = 5D \begin{cases} \frac{0.49\frac{v_o}{W} + 0.88}{\frac{v_o}{W} + 1.41}, & \text{if } \frac{v_0}{W} > 0 \\ \frac{0.52\frac{v_o}{W} - 0.03}{\frac{v_o}{W} - 0.46}, & \text{if } \frac{v_0}{W} < -1 \end{cases}$$

these roots prove a direct solution for the maximum acceleration in the speed curve.

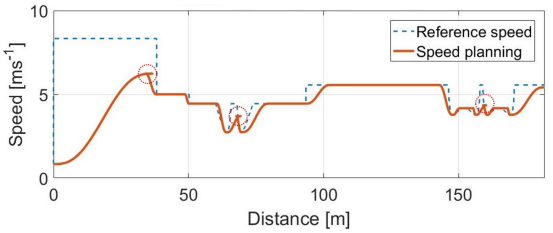

(a) Speed planning with overlapped intersections

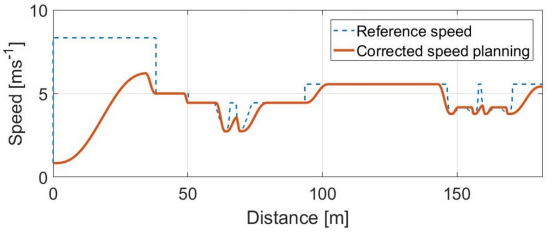

(b) Speed planning with no overlaps

Figure 3.7: Stages of the speed planning approach

The first step in the speed planning method is applying the comfort speed limitation (reference speed) presented in [175] with the equation:

$$a_\omega = \sqrt{(1.4a_x)^2 + (1.4v_l{}^2K)^2 + a_z{}^2} \tag{3.17}$$

where a_ω is the total acceleration felt by the passengers, related to the comfort criteria of the ISO2631-1. The contributions of the longitudinal acceleration and vertical acceleration, a_x and a_z respectively, are zero because they have small changes (≈ 0). The longitudinal speed is described by v_l, and K is the curvature at each point of the path.

Fig. 3.7a depicts the speed planning approach, where some segments overlap one with each other. In this stage, Bézier curves are generated with the consideration of the maximum acceleration criteria on each upward and downward speed change (under the speed limits). Next, the intersections between curves are calculated. In the example, this happens three times. The calculation considering each speed step ensures numerical stability while reducing the accumulation of numerical errors derived from the concatenated curves.

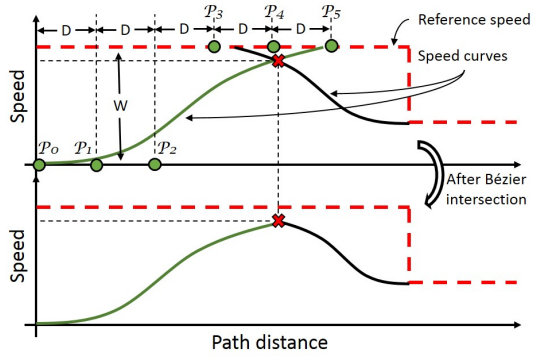

Figure 3.8: Speed planning designing method

Fig. 3.7b depicts the last stage of the speed planning, which generates a new curve based on the intersections on the speed profile. This new curve is smoother than the previous one (refer to Fig. 3.8). Also, the profile is constrained to the acceleration limits of the vehicle, considering comfort during the driving process, and while safely keeping speed under road limits.

3.5 Experimental set-up

A good simulation environment and real vehicles are required for testing AD applications. In these terms, the following section explains the Dynacar simulation environment, as well as the physical vehicle along with their controllers and the proving ground.

3.5.1 Simulation environment: Dynacar

The Dynacar was developed in the Automotive Group of Tecnalia Research and Innovation, and it is a benefit for this Ph.D. thesis in terms of support service. Additionally, it is a very precise model that helps in the validation of the proposed algorithms.

The vehicle dynamics are modeled with a multi-body vehicle formulation. The vehicle movements and forces are calculated in each wheel, suspension, and chassis, improving the precision in case of uneven terrains.

This simulator is used in the relevant stages of automated driving, such as Hardware-in-the-Loop (HiL), Driver-in-the-Loop (DiL), and Model-in-the-Loop (MiL) testing. Furthermore, the simulator has a 3D environment to visualize the vehicle's behavior, as well as the tool for developing new scenarios (Fig. 3.9).

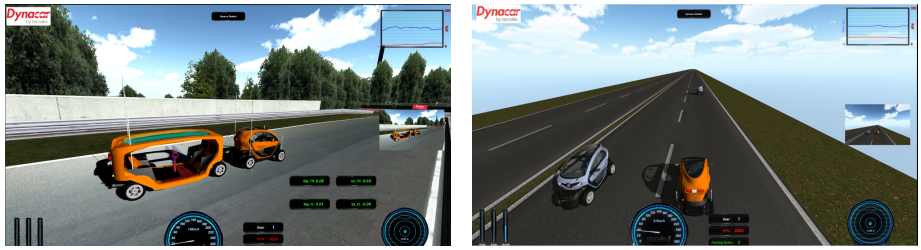

(a) Side view (b) Rear view

Figure 3.9: Dynacar simulation environment

3.5.2 Automated vehicle: Renault Twizy

Today, Tecnalia Research and Innovation has two automated Renault Twizy (refer to Fig. 3.10). They were instrumented to support the automation capabilities of the steering wheel, throttle, and brake actions. Those vehicles drive at

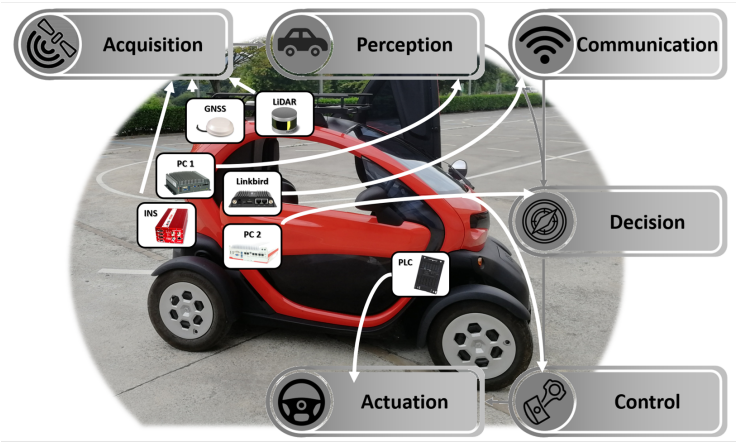

Figure 3.10: Physical Automated vehicle

a maximum speed of 80$[km/h]$, and their size makes them a feasible solution for outdoor and indoor applications, considering one passenger inside the vehicle (or not), such as shuttling, surveillance, cargo movement, etc.

The computer used for automation purposes is a Core^{TM} i7 of 6th generation, and it runs Matlab®/Simulink® with the control architecture. It is connected through a CAN interface to a Programmable Logic Controller (PLC).

The PLC executes the low-level control of the Maxon motors, and they are located on the steering wheel and brake system. In the first case, the motor is in the middle of the tie rod. For the braking system, the motor is coupled to the brake pedal (with a wire), and it pulls the brake pedal according to the action supplied. Furthermore, the PLC controls the throttle system with a central ECU signal.

Both vehicles have a Global Navigation Satellite System with the Inertial Navigation System (GNSS/INS). They are supplied by Oxford Technical Solutions OxTS, and the GNSS/INS system achieves a precision of two centimeters along with a differential station. This component must be set in a permanent position for precise corrections.

Other sensors are installed in the vehicle, like lasers or LiDARs, but they are out of the scope of this Ph.D. thesis. Also, the communication capabilities are assured using third-party hardware, and it was provided in the project H2020 UnCoVerCPS (LinkBird Device).

3.5.3 Proving ground

Tecnalia has a closed test track (refer to Fig. 3.11) used for developing and testing automated driving functionalities. It is located in Derio at Biscay, Basque Country. The proving ground has approximately 85 meters of length, 18 meters wide, and 3 meters of road width. It can be used for testing the proposed algorithm in the automated Twizy platform.

The test track has 4 circular turnings with roundabout aspect, lane change sections, two lanes paths, and some intersections.

(a) Top view

(b) Side view

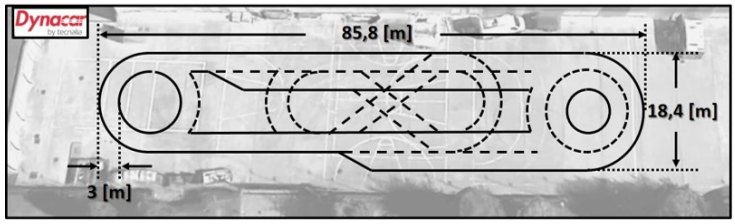

(c) Quotas

Figure 3.11: Tecnalia's test track

3.5.4 Vehicle's controller used

The typical automated vehicle control variables are lateral error, angular error, and curvature (refer to Fig. 3.12). The lateral error is the shortest distance between the heading point and the trajectory (the heading point is a projection, some meters ahead, of the vehicle frontal point). The angular error

is the difference between the trajectory angle and the vehicle angle. Lastly, the curvature is calculated over the shortest distance path point P_t.

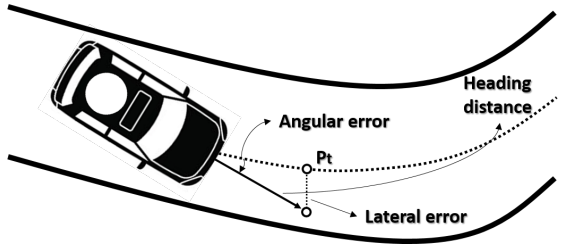

Figure 3.12: Vehicle's control variables

All the tests have considered a linear controller for the steering wheel action and a fuzzy controller for throttle and brake systems. The first controller is called double proportional plus curvature, and it is a feedback controller, based on a linear combination of the lateral error and angular error, with a feed-forward component based on curvature. The formula of this controller is:

$$c_v = \max\{-1, \min\{1, k_1 e_{lat} + k_2 e_{ang} + k_3 \kappa\}\} \tag{3.18}$$

this controller is limited between -1 and 1, for a total action of the steering wheel to each side. The values of e_{lat}, e_{ang}, and κ are lateral error, angular error and curvature respectively. The controller gains are defined by k_1, k_2, and k_3. A large number of publications proved the robustness of this controller [20] and [176].

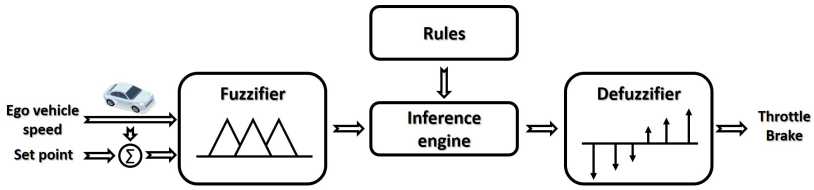

Figure 3.13: Vehicle's speed control (fuzzy) diagram

In the case of the longitudinal domain, a fuzzy logic controller was used due to its robustness in delayed systems [109]. It considers the speed error between the reference and the vehicle one, and the current vehicle speed. The triangular shapes define the membership functions, each variable with three tags, and the

output was characterized using singletons (refer to Fig. 3.13). The algorithm 1 defines the set of rules used.

Algorithm 1 Set of rules for the longitudinal control

1: IF the speed error is NEGATIVE AND vehicle speed HIGH THEN maximum deceleration
2: IF the speed error is NEGATIVE AND vehicle speed MEDIUM THEN medium deceleration
3: IF the speed error is NEGATIVE AND vehicle speed LOW THEN soft deceleration
4: IF the speed error is ZERO THEN keep acceleration
5: IF the speed error is POSITIVE AND vehicle speed LOW THEN soft acceleration
6: IF the speed error is POSITIVE AND vehicle speed MEDIUM THEN medium acceleration
7: IF the speed error is POSITIVE AND vehicle speed HIGH THEN maximum acceleration

3.6 Experimental results

This section presents the experimental results, which are divided in three subsections: (1) virtual testing, (2) real validation, and (3) a comparison between virtual and real environments.

3.6.1 Virtual tests

This section explains the simulation results using Dynacar and the AD modules, described in section 3.2. The test location is depicted in Fig. 3.14, and it corresponds with an urban scenario of Bilbao in Spain. Furthermore, it has 2 roundabouts, 3 right turns and 6 left turns.

The map has its points divided among: 1 starting point, 1 ending point, 9 intersections, and 2 roundabouts. These points result in 13 points defining all the route. Table 3.3 shows x-y coordinates in meters (simulator absolute coordinate system), the reference speed in $[m/s]$, and the type of point (1 for intersections and 2 for roundabouts). The roundabout global planning requires

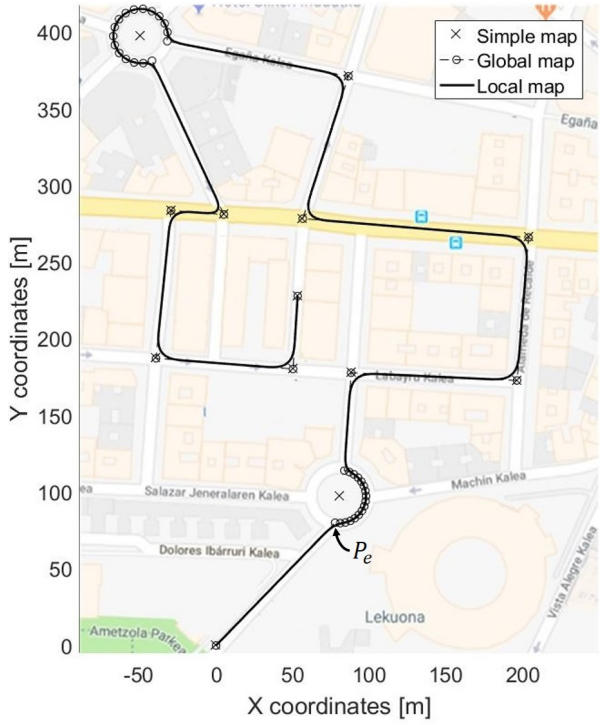

Figure 3.14: Virtual testing: Map, global and local planning.

additional information for its description: the radius (meters), the angles of the entrance, and the exit (radians). The previously described points are shown in Fig. 3.14 with a cross marker.

Global planning is generated with the information collected from the map, and it gives a better description of roundabouts considering bend segments (completion of the circle arc). The global planning points coincide with the map points for an intersection. These are depicted as circles in Fig. 3.14.

The local planning is depicted with the soft and continuous black line (Bézier trajectory). The values of D (designing parameter of the approach) are set by hand ith values between 8 and 10 meters. Also, they could be selected using an optimization algorithm as in [20].

An example of the roundabout is located in $[80.48; 97.09]$ absolute coordi-

Table 3.3: Virtual test map points' description

X $[m]$	Y $[m]$	V $[m/s]$	Type [-]	R $[1/m]$	a_i $[rad]$	a_o $[rad]$
0.00	0.00	11.11	1	–	–	–
80.48	97.09	11.11	2	17.29	0.52	0.09
88.04	177.90	11.11	1	–	–	–
196.21	172.89	11.11	1	–	–	–
203.72	266.16	11.11	1	–	–	–
56.55	278.46	11.11	1	–	–	–
86.24	371.34	11.11	1	–	–	–
−49.30	397.61	11.11	2	17.76	0.00	0.00
5.08	281.16	11.11	1	–	–	–
−29.37	283.73	11.11	1	–	–	–
−39.17	187.34	11.11	1	–	–	–
50.16	180.36	11.11	1	–	–	–
53.19	227.94	11.11	1	–	–	–

nates (roundabout center). It uses the definition of the entrance angle for its description (Eq. 3.7):

$$P_e = \begin{bmatrix} 80.48 \\ 97.09 \end{bmatrix} + 17.29 \begin{bmatrix} cos(-2.26) \\ sin(-2.26) \end{bmatrix} = \begin{bmatrix} 69.4 \\ 83.8 \end{bmatrix}$$

The entrance point was used to present a numerical example. The exit point can be calculated with the same Eq. 3.7.

The speed planning defined for that trajectory generates a longitudinal acceleration profile shown in Fig. 3.15. The continuous line is the acceleration given the comfort parameter $a_\omega = 0.5[m/s^2]$. Based on [175], this amount of acceleration a_w corresponds with a value between "not uncomfortable" and "a little uncomfortable" for vehicle passengers.

Results show a successful tracking of the generated speed profile in terms of acceleration. These are good results due to the fact the speed profile considers the maximum acceleration and deceleration (red bounds of Fig. 3.15).

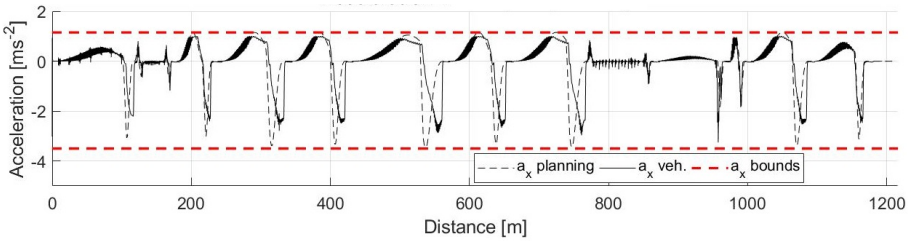

Figure 3.15: Virtual testing: acceleration profile.

The Fig. 3.16 depicts different lateral acceleration profiles considering several maximum values, and its relation with the comfort parameter a_w. Five different values of a_ω were used: 0.5, 1.0, 1.5, 2.0, and 2.5$[m/s^2]$ which match with profiles "not uncomfortable", "a little uncomfortable", "fairy uncomfortable", "uncomfortable", and "very uncomfortable" used in [175]. The approach aimed a maximum a_ω under the selected comfort limit, and the generation of a smooth profile.

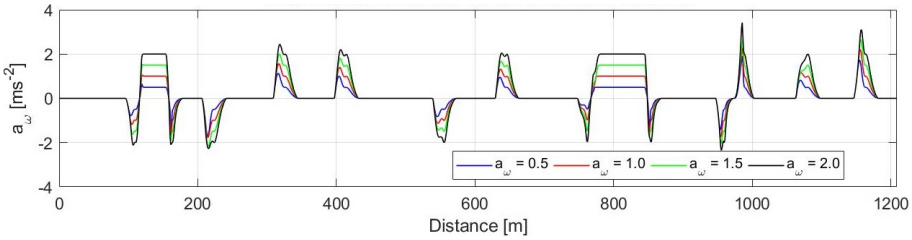

Figure 3.16: Acceleration profiles in the virtual test's path

An overshoot over the acceleration limit is observed in the case of tight junctions, roundabout entrances, and roundabout exits. This event appears due to the filtering process of the overlapped segments. The lateral acceleration levels are exceed due to numerical errors obtained during the filtering process. These values over the limits are detected for a short distance, and its total effect is not relevant. A more precise speed profile, based on an optimization method, is presented in section 4.3.

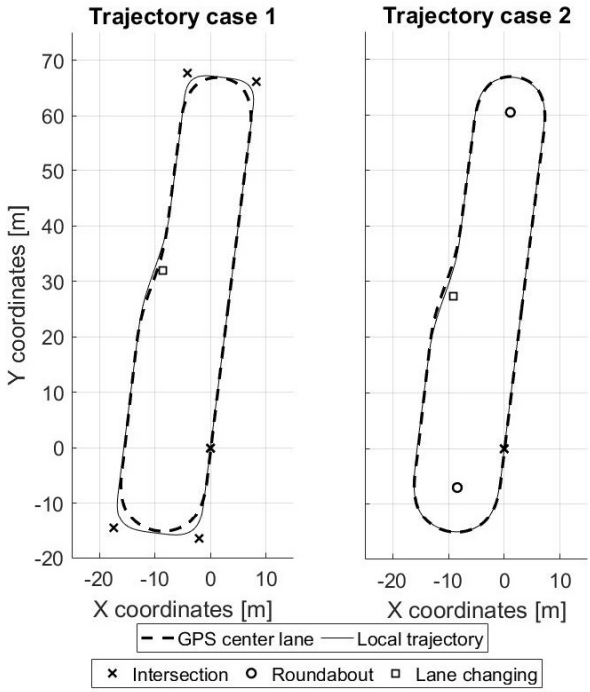

Figure 3.17: Comparison in trajectory definition.

3.6.2 Real tests

This section shows the trajectory planning approach integrated into the vehicle. Two route definitions were implemented (refer to Fig. 3.17). The center of the lane - guide trajectory - was recorded using a DGPS.

The first case is shown on the left side of Fig. 3.17. The trajectory uses intersection points in the 180[°] turn (roundabout). In this case, the error in the turning points (top and bottom of the test track) is greater than in the definition of the curve with roundabouts (right side Fig. 3.17).

The scenario of the right side of Fig. 3.17 was tested at five different speed profiles. Fig. 3.18 depicts the curvature value that results from each test. The vehicle curvature is depicted with a gray line, and it is calculated as follows:

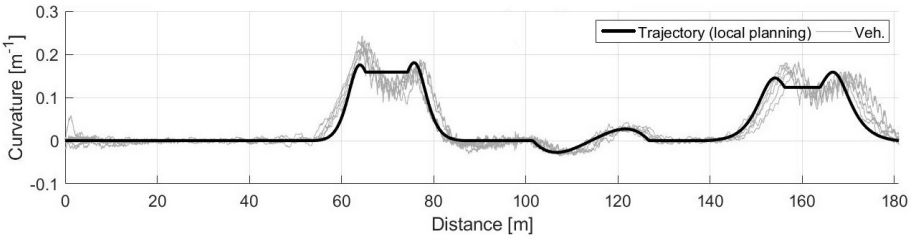

Figure 3.18: Curvature profile

$$K(t) = \frac{\omega(t)cos(\Phi(t))}{V_l(t)} \tag{3.19}$$

where K is the curvature, ω is the rate of change of yaw, Φ is the roll angle of the vehicle, and V_l is the longitudinal speed. The path curvature is depicted in black. These results show that the vehicle is capable of following the generated trajectory, in terms of curvature, at different speed profiles (the overshoots in curvature are caused by the controllers).

3.6.3 Comparison between the virtual and real environment

One of the main benefits of the architecture is the interconnection between the AD modules, the automated platform, and the simulator Dynacar. A comparative study has been conducted to test the benefits of a precise multi-body vehicle model embedded in the AD platform during algorithm validation (decision and control).

The controller explained in section 3.5.4 has been tested with and without the feed-forward component. A trajectory has been generated and tested in the simulator with the same test track presented in subsection 3.5.3. Fig. 3.19a depicts the trajectory tracking of the cases with feed-forward and without it. The performance of both controllers was measured in terms of the lateral error, angular error, and speed tracking (refer to Fig. 3.19c, 3.19e, and 3.19g, respectively).

The maximum, average, and median lateral errors are presented in table 3.4. The best results are shown in the controller with curvature compared to the one without the curvature. The curvature-based controller's errors reduce the

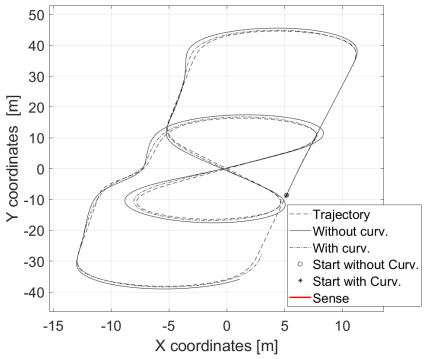

(a) Trajectory tracking of both controllers using virtual environment

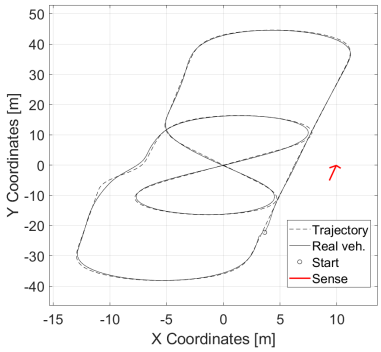

(b) Trajectory tracking of the controller with curvature in real platform

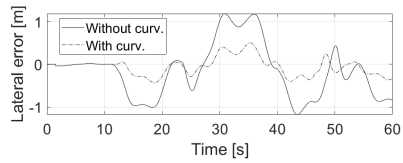

(c) Lateral error in virtual test

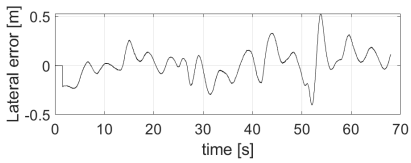

(d) Lateral error in real test

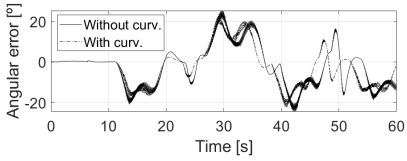

(e) Angular error of virtual tests

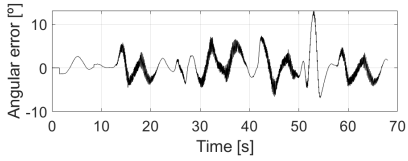

(f) Angular error of real test

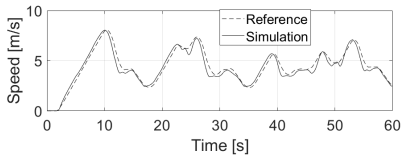

(g) Speed in virtual test

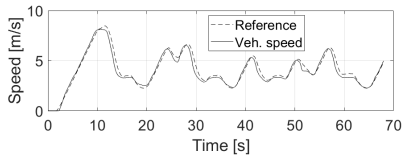

(h) Speed in real test

Figure 3.19: Comparative results considering virtual and real tests

maximum, average, and median values, in 57.6%,67.3%, and 65.8% respectively, respect to the controller without the curvature.

Table 3.4: Lateral error in simulation and real vehicle

Controller	Max.	Average	Median
Virtual Without Curv.	1.18 [m]	0.49 [m]	0.41 [m]
Virtual With Curv.	0.50 [m]	0.16 [m]	0.14 [m]
Real With Curv.	0.53 [m]	0.11 [m]	0.08 [m]

The controller with curvature has been tested on the real platform. It shows the vehicle tracking results in Fig. 3.19b, and the lateral error in Fig. 3.19d. The maximum, average, and median values are shown in table 3.4. They are similar to the simulation results, with a maximum value of 0.53 meters and 0.11 meters on average.

The maximum, average, and median values of the angular error are presented in table 3.5. The results have shown better performance in the case with curvature. The angular error results have improved a 10.1%,9.2%, and 21.1% respect to the maximum, average, and median values. The result of the angular error is shown in Fig. 3.19f. The maximum, average, and median are shown in table 3.5, and those are 13.1°, 1.96°, and 1.49° respectively.

Table 3.5: Angular error in simulation and real vehicle

Controller	Max.	Average	Median
Virtual Without Curv.	25.21 [°]	7.92 [°]	7.73 [°]
Virtual With Curv.	22.65 [°]	7.19 [°]	6.10 [°]
Real With Curv.	13.10 [°]	1.96 [°]	1.49 [°]

The tracking of the speed has been implemented using the fuzzy controller presented in section 3.5.4. Refer to Fig. 3.19g and 3.19h for the results of virtual and real speed tracking, respectively.

3.7 Summary

This chapter has introduced the control architecture and the tools used during this Ph.D. thesis, especially related to the high fidelity simulation environment Dynacar. The main contribution is in terms of trajectory generation that is part of the decision module. Bézier curves have been used to generate the trajectories for its simplicity and benefits on this task. The modeling process of these trajectories has been formally defined.

Additionally, different tests have been performed considering urban environments and closed test tracks. A comparative study of the system performance in simulation and the real platform has been conducted with a close performance between the algorithm tested in the simulation environment and the real platform. The tests have shown good performance in the real platform with tracking errors under 0.53 meters and an average error under 0.11 meters, the curvature changes were smooth and feasible for the vehicle.

In terms of the longitudinal planning, the method has presented good results but it demands long computation-time for comfort verification. Consequently, the next chapter presents a complementary method for lateral and longitudinal real-time trajectory planning in case of lane change maneuvers (e.g. overtaking and obstacle avoidance).

"Knowing what is big and what is small is more important than being able to solve partial differential equations".

Stanislaw Ulam

4

A hybrid approach using parametric curves and MPC

4.1 Introduction

People's mobility is one of the major concerns since many decades ago and it has great importance in the regular activities of the society. Somehow, Advanced Driver Assistance Systems (ADAS) were built to fulfill this demand. In these terms, Automated Driving (AD) presents a possible evolution of the ADAS, encouraging enhancement of traffic safety, transport efficiency, and comfort. Nonetheless, Lane Change (LC) and obstacle avoidance scenarios are a challenge due to their complexity.

The obstacle avoidance maneuver is executed as consecutive lane changes on the road (structured environments defined by lanes and traffic rules). Similarly, the overtaking is defined as two consecutive LCs, and it is explained in chapter 5. In these terms, the questions in AD, about these maneuvers, are: when and how is the maneuver executed? [177].

The United States (US) recorded a total number of 240 000 vehicle crashes per year due to LC maneuvers, where 60 000 people were injured, and a large

number of properties were damaged [178]. Worldwide was quantified that 90% of the total accidents are directly linked to human errors due to wrong decisions in the driving process. The leading causes of accidents are incorrect estimations of the vehicle environment as well as the execution of the maneuver itself [179].

Automated LC involves longitudinal and lateral dynamics during its execution. First implementations only considered lateral control by introducing a fixed offset in the steering wheel control [180]. The basic drawback of these methods lies in the evaluation of: the driver's attitude emulation, the current vehicle state, and surrounding vehicles as well as the road information [179].

Today, trajectory planning is widely used in obstacle avoidance or LC maneuvers, aiming optimal solutions with collision-free methods. Some authors have considered a direct evaluation, using a finite set of rules or predefined trajectories. However, the problem is constrained to specific solutions. Model Predictive Control (MPC) has been successfully used in different domains, generating optimal solutions for continuous models. Furthermore, the MPC can generate time-affordable collision-free trajectories during LC and obstacle avoidance [20].

In these terms, this chapter presents one MPC method merged with the Bézier trajectory planning framework (refer to chapter 3). This approach is efficient and obtains optimal solutions in the case of LC and obstacle avoidance maneuvers. A linear model was used based on integrator chains. This model simplifies system complexity with a reduction of the computation time. On the other hand, it supports road and vehicle constraints, which are mandatory for safe maneuver execution. A deterministic and active evaluation of possible collisions is taken into account to keep safety on the maneuver execution.

This chapter is organized with an introduction of MPC, including its mathematical definition, and some applications in tracking controllers and trajectory planning. Next, the proposed method is presented along with the explanation of the model used, the collision evaluation, constraints manipulation, and reference assignment. Then, the deployed controller is described. Finally, real vehicle results and simulation tests are presented considering a risky situation and some alternatives to mitigate these circumstances. The simulation results are described at the end, introducing the approach presented in chapter 5.

4.2 Model Predictive Control in AD

MPC, also known as Receding Horizon Control (RHC), is a method where the current control action is obtained when solving a finite horizon Optimal Control Problem (OCP) at each sample time [181]. MPC's model defines the

case of study, plant, or scenario, while it is projected on the horizon. The main difference between MPC and traditional control is the capacity of using a model to compute the optimal control signals. Other MPC's advantages are its capacity to support multi-variable systems, constraints manipulation, and boundaries of the permissible states. In the past, MPC was a discarded solution for the amount of time demanded by its execution. Currently, there is a great number of methods, such as Sequential Quadratic Programming (SQP), that make online and real-time computation possible [182].

Commonly, the problem is defined with the continuous-time state-space representation of the system. In the case of linear models, the definition is:

$$\begin{aligned} \dot{\mathbf{x}(t)} &= \mathbf{A}\mathbf{x}(t) + \mathbf{B}\mathbf{u}(t) + \mathbf{E}\mathbf{d}(t) \\ \mathbf{y}(t) &= \mathbf{C}\mathbf{x}(t) + \mathbf{D}\mathbf{u}(t) + \mathbf{G}\mathbf{d}(t) \\ \mathbf{x}(t) &\in \mathbf{X}, \quad \mathbf{u}(t) \in \mathbf{U} \end{aligned} \tag{4.1}$$

where $\dot{\mathbf{x}}$ is the derivative of the state vector $\mathbf{x}$ and $\mathbf{y}$ is the output vector. $\mathbf{X} \in \mathbb{R}^{m\times 1}$ is the bounded set of all possible states and $\mathbf{U} \in \mathbb{R}^{n\times 1}$ is the bounded set of all possible control inputs. The matrices $\mathbf{A}$ and $\mathbf{C} \in \mathbb{R}^{m\times m}$ are associated to the state vector, $\mathbf{B}$ and $\mathbf{D} \in \mathbb{R}^{n\times n}$ are matrices associated to the control input, and $\mathbf{E}$ and $\mathbf{G} \in \mathbb{R}^{w\times w}$ are time invariant matrices (as $\mathbf{A}$, $\mathbf{B}$, $\mathbf{C}$ and $\mathbf{D}$) associated to the system disturbances $\mathbf{d} \in \mathbb{R}^{w\times 1}$.

In this work, the state-space representation is defined using discrete-time without disturbances in the form of:

$$\begin{aligned} \mathbf{x}_{k+1} &= \mathbf{A}\mathbf{x}_k + \mathbf{B}\mathbf{u}_k \\ \mathbf{y}_k &= \mathbf{C}\mathbf{x}_k + \mathbf{D}\mathbf{u}_k \\ \mathbf{x}_k &\in \mathbf{X}, \quad \mathbf{u}_k \in \mathbf{U} \end{aligned} \tag{4.2}$$

The cost function used to define the optimization process is given by:

$$\begin{aligned} \Omega(\mathbf{x}, \mathbf{x^{ref}}, \mathbf{u}, \mathbf{u^{ref}}) = {} & (\mathbf{x}_{k+N|k} - \mathbf{x}^{ref}_{k+N|k})^T \mathbf{Q}_{k+N|k} (\mathbf{x}_{k+N|k} - \mathbf{x}^{ref}_{k+N|k}) + \\ & (\mathbf{u}_{k+N|k} - \mathbf{u}^{ref}_{k+N|k})^T \mathbf{R}_{k+N|k} (\mathbf{u}_{k+N|k} - \mathbf{u}^{ref}_{k+N|k}) + \\ & \sum_{j=0}^{N-1} ((\mathbf{x}_{k+j|k} - \mathbf{x}^{ref}_{k+j|k})^T \mathbf{Q}_{k+j|k} (\mathbf{x}_{k+j|k} - \mathbf{x}^{ref}_{k+j|k}) + \\ & (\mathbf{u}_{k+j|k} - \mathbf{u}^{ref}_{k+j|k})^T \mathbf{R}_{k+j|k} (\mathbf{u}_{k+j|k} - \mathbf{u}^{ref}_{k+j|k})) \end{aligned} \tag{4.3}$$

where the notation $(\cdot)_{k+j|k}$ is used to describe the value of each variable $(\cdot)$ in the sample time $k+j$ given an observation in the sample k. The vector $\mathbf{x^{ref}}$ and $\mathbf{u^{ref}}$ define the state and control action references respectively. The matrices $\mathbf{Q}$ and $\mathbf{R}$ are weighting matrices and the notation $(\cdot)^T\mathbf{M}(\cdot)$ describes the weighted norm of the vector $(\cdot)$ with $\mathbf{M}$ a generic square matrix (weights).

The optimization problem can be described as:

$$\begin{aligned} &\min_{\mathbf{u},\mathbf{u^{ref}}} \{\Omega(\mathbf{x}, \mathbf{x^{ref}}, \mathbf{u}, \mathbf{u^{ref}})\} \\ s.t.: \quad &\mathbf{x}_{k+j|k} \in \mathbf{X}_{k+j|k} \\ &\mathbf{u}_{k+j|k} \in \mathbf{U}_{k+j|k} \\ &j \in \{0, 1, 2, ..., N-1, N\} \end{aligned} \tag{4.4}$$

where the aim is to minimize the cost function $\Omega(\mathbf{x}, \mathbf{x^{ref}}, \mathbf{u}, \mathbf{u^{ref}})$ using the control inputs $\mathbf{u}$. $\mathbf{X}_{k+j|k}$ and $\mathbf{U}_{k+j|k}$ are convex sets. The condition of convexity will be explained in section 4.3.4.

The concepts behind the MPC are relatively new for AD applications. However, there are some interesting results obtained in the academic field, especially in terms of the tracking controllers of automated vehicles and for trajectory generation.

4.2.1 Tracking control

Stanford University presented one MPC designed to control the vehicle in its driving limits [183]. The controller can determine the steering wheel commands ensuring stability and tracking of a nominal path, adding the possibility of executing emergency collision avoidance maneuvers. In these terms, two different constraint sets or envelopes for the trajectory generation and tracking problems were used. The collision avoidance was stated as an emergency maneuver problem, i.e. incorporating it in the tracking controller.

In the work conducted by authors of [184], a nonlinear MPC approach for the autonomous steering of ground vehicles was presented. The model included front and rear tire lateral forces. This study was a basis for researching in the field of emergency acceleration and braking maneuvers.

In [185], another MPC formulation was presented and it considered the Adaptive Cruise Control (ACC) scenario. The objective of this formulation was to keep an inter-vehicle distance among the participants. The method considered this maneuver as a problem of the longitudinal domain.

One MPC framework was presented to solve the problem of path tracking in Automated Ground Vehicles (AGV) in [186]. The control architecture considered two different types of models: a kinematic model for low speeds and a dynamic model for the rest of the cases. Also, the work compared two different types of linear kinematic models to use it in the low-speed definition of the framework. One of those controllers was based on a successive linearization concept and the second one is based on a local reference frame with a path strategy. The results of this work have been simulated in a wide range of speeds. In the real tests, the maximum speed was under $10km/h$.

On the other hand, the authors of [187] have proposed a robust tube-based MPC tracking controller. A linear vehicle representation was used besides a constant speed approximation. The computation time was reduced in this approach, the comfort of the passengers was considered with the rate of change of the steering wheel, and reliable tracking conditions were fulfilled with the tube model. The approach was tested only in simulation environments at a maximum speed of $120km/h$.

The authors of [188] have studied the influence of a centralized MPC tracking control for dense traffic zones. The MPC oversees the generated control signals of each vehicle. It has considered all the participants at once, minimizing the reference speed error in each vehicle (improving traffic flow) and minimizing the fuel consumption (efficiency). The results have been tested in a microscopic traffic simulator called AIMSUN.

Finally, another MPC tracking controller has been proposed in [189]. It has a piecewise approximation of the tire forces, which considers the linear part and saturation in the boundaries. The MPC was implemented as different controllers that switch from linear tire model to saturation model. The approach has been tested in low-friction surfaces using a real vehicle platform.

4.2.2 Trajectory generation

In the case of the trajectory planning field, there are some approaches done at the moment but their results are not good enough for a real deployment. For instance in [190], the MPC formulation has been designed considering feasible corridors only in the lateral domain and at a constant speed.

The authors of [191] have presented a MPC lane change trajectory planning algorithm. However, the authors did not provide details regarding the proposed algorithm, computational complexity or its applicability on real-time implementation on a vehicle.

In [20], the authors were interested in designing an active safety system which

has trajectory planning and tracking in the same module. They used a non-linear MPC formulation and potential fields to consider the information about road and obstacles. Additionally, constraints in terms of yaw rate and sideslip were used to stabilize the system. The problem behind this approach was the complexity of the models. Some of the non-linearity and approximations were of difficult consideration in real vehicle applications. Virtual tests were conducted with the CarSim simulator.

In the work conducted by the authors of [192], a MPC method has been presented considering a non-linear bicycle model in simulation environments. The path planning method has the capacity of dealing with different scenarios without conditioning them to a discrete subset of possibilities, e.g. lane change, intersection, crossing, etc. The main problem of this approach was the relaxed constraints used to keep the system stable. Hence, the safety decreased in the case of real-life deployments.

4.3 Problem formulation

The chapter 3 has explained the benefits of using Bézier curves for trajectory planning on automated vehicles, such as tracking improvements, comfort, and safety. Nevertheless, the non-linearity of these polynomials makes them difficult to be resolved on real-time, considering unexpected conditions such as lane changing, obstacle avoidance, and overtaking maneuvers. On the other hand, some methods can be quickly resolved to accomplish this demand. MPC formulations based on Quadratic Programming (QP) solvers permits to find an optimal in short time.

The approach proposed in this Ph.D. thesis uses a "nominal trajectory" built with Bézier curves and in case of unexpected conditions. The MPC approach is overlapped to this nominal trajectory. The combination of both trajectories is known as hybrid trajectory. The approach decouples the longitudinal and lateral dynamics of the vehicle to simplify the problem, obtaining real-time solutions.

The general idea of this approach is depicted in Fig. 4.1. In the case of verifying a possible blockage of the nominal trajectory, the ego vehicle evaluates whether the opposite lane is available and safe to overtake the obstacles. A lateral offset signal is generated by the MPC to control the vehicle movement. In parallel, the longitudinal model avoids any collision with other participants.

In these terms, 5 key components are demanded to build the hybrid trajectories:

1. A linear model for lateral and longitudinal dynamics (section 4.3.1).

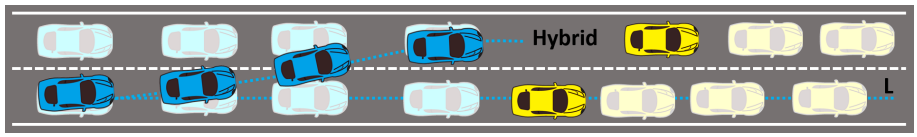

Figure 4.1: The hybrid approach using Bézier curves and MPC for trajectory planning

2. The projections on the road of other participants and the ego vehicle (section 4.3.2).
3. An evaluation of possible collisions (section 4.3.3).
4. Constraints and references manipulation (section 4.3.4).
5. Implementation of the method with the nominal trajectory based on Bézier (section 4.3.5).

4.3.1 Model used

One key component of MPC is the model used, which increases the computation time with the precision of the model (losing real-time properties). Villagra et al., in [193], showed the relation between the longitudinal jerk and comfort while driving. On the other hand, in [175] was explained a similar effect over the comfort, considering the lateral acceleration felt by passengers. This permits us to increase safety as well. This work has used a triple integrator chain in the longitudinal domain, using comfort and safety in the optimization problem. The double integrator chain was used in the lateral domain because further studies must be done in terms of the lateral jerk to add it. Both models are shown below:

$$d_x(t) = \iiint j_x(t)dt^3 \quad d_y(t) = \iint a_y(t)dt^2 \tag{4.5}$$

the variables $d_{<x,y>}$, $v_{<x,y>}$, $a_{<x,y>}$, j_x mean distance, speed, acceleration and jerk, whereas sub-indexes $< x, y >$ mean longitudinal and lateral domain respectively. In these terms, $\mathbf{x}_x$ and $\mathbf{x}_y$ are the state vectors described as $\mathbf{x}_x = [d_x, v_x, a_x]^T$ and $\mathbf{x}_y = [d_y, v_y]^T$ where the super-index T means vector transpose. The control input vectors in longitudinal and lateral domain, $\mathbf{u}_x$ and $\mathbf{u}_y$ respectively, are defined as $\mathbf{u}_x = j_x$ and $\mathbf{u}_y = a_y$.

The models showed in the Eq. 4.5 can be described in terms of Ordinary Differential Equations (ODE) such as:

$$\dot{d}_{<x,y>} = v_{<x,y>} \quad \dot{v}_{<x,y>} = a_{<x,y>} \quad \dot{a}_{<x,y>} = j_{<x,y>} \tag{4.6}$$

Consequently, the ODE can be represented as a linear combination of the states and control inputs, given the state space representation of Eq. 4.2:

$$\begin{aligned} \mathbf{A}_x &= \begin{bmatrix} 1 & 0 & 0 \\ 0 & 1 & 0 \\ 0 & 0 & 1 \end{bmatrix} \qquad \mathbf{A}_y = \begin{bmatrix} 1 & 0 \\ 0 & 1 \end{bmatrix} \qquad \mathbf{B}_x = \mathbf{B}_y = \begin{bmatrix} 0 \\ 0 \\ 0 \end{bmatrix} \\ \mathbf{C}_x &= \begin{bmatrix} 0 & 1 & 0 \end{bmatrix} \qquad \mathbf{C}_y = \begin{bmatrix} 1 & 0 \end{bmatrix} \qquad \mathbf{D}_x = \mathbf{D}_y = \begin{bmatrix} 0 \\ 0 \end{bmatrix} \end{aligned} \tag{4.7}$$

The complete formulation of the problem is obtained introducing these values in the state-space formula:

$$\begin{aligned} \begin{bmatrix} \dot{d}_x \\ \dot{v}_x \\ \dot{a}_x \end{bmatrix} &= \begin{bmatrix} 0 & 1 & 0 \\ 0 & 0 & 1 \\ 0 & 0 & 0 \end{bmatrix} \begin{bmatrix} d_x \\ v_x \\ a_x \end{bmatrix} + \begin{bmatrix} 0 \\ 0 \\ 1 \end{bmatrix} j_x \qquad y_x = \begin{bmatrix} 0 & 1 & 0 \end{bmatrix} \begin{bmatrix} d_x \\ v_x \\ a_x \end{bmatrix} \\ \begin{bmatrix} \dot{d}_y \\ \dot{v}_y \end{bmatrix} &= \begin{bmatrix} 0 & 1 \\ 0 & 0 \end{bmatrix} \begin{bmatrix} d_y \\ v_y \end{bmatrix} + \begin{bmatrix} 0 \\ 1 \end{bmatrix} a_y \qquad y_y = \begin{bmatrix} 1 & 0 \end{bmatrix} \begin{bmatrix} d_y \\ v_y \end{bmatrix} \end{aligned} \tag{4.8}$$

The objective function was defined using Eq. 4.3 in the form:

$$\begin{aligned} \Omega(v_{xk}, d_{y_k}, v_{x_k}^{ref}, d_{y_k}^{ref}) = & \\ & \begin{bmatrix} v_{xk+N|k} - v_{x_{k+N|k}}^{ref} \\ d_{y_{k+N|k}} - d_{y_{k+N|k}}^{ref} \end{bmatrix}^T \begin{bmatrix} 1 & 0 \\ 0 & 1 \end{bmatrix} \begin{bmatrix} v_{xk+N|k} - v_{x_{k+N|k}}^{ref} \\ d_{y_{k+N|k}} - d_{y_{k+N|k}}^{ref} \end{bmatrix} + \\ & \sum_{j=0}^{N-1} \begin{bmatrix} v_{xk+N|k} - v_{x_{k+j|k}}^{ref} \\ d_{y_{k+N|k}} - d_{y_{k+j|k}}^{ref} \end{bmatrix}^T \begin{bmatrix} 1 & 0 \\ 0 & 1 \end{bmatrix} \begin{bmatrix} v_{xk+N|k} - v_{x_{k+j|k}}^{ref} \\ d_{y_{k+N|k}} - d_{y_{k+j|k}}^{ref} \end{bmatrix} \\ & = \sum_{j=0}^{N} \begin{bmatrix} v_{xk+j|k} - v_{x_{k+j|k}}^{ref} \\ d_{y_{k+j|k}} - d_{y_{k+j|k}}^{ref} \end{bmatrix}^T \begin{bmatrix} 1 & 0 \\ 0 & 1 \end{bmatrix} \begin{bmatrix} v_{xk+j|k} - v_{x_{k+j|k}}^{ref} \\ d_{y_{k+j|k}} - d_{y_{k+j|k}}^{ref} \end{bmatrix} \end{aligned} \tag{4.9}$$

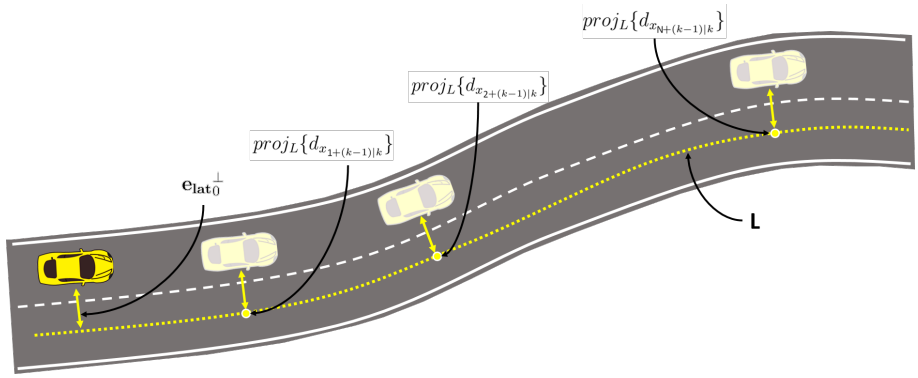

Figure 4.2: Road projections

from this formulation is inferred that all samples' weight have the same value. Furthermore, the lateral and longitudinal dynamics are decoupled in the model and the optimization function. This aims to minimize the squared error of the reference speed, and the squared error of the lateral offset (executing the lane change).

4.3.2 Road projections

The future longitudinal positions of the ego vehicle ($\mathbf{V}_0$), at sample time T_k, are defined using the information obtained at sample time T_{k-1}. These position states are written as $\{d_{x_{i+(k-1)|k}}, i \in 1, 2, ..., N\}$. The future positions of the vehicle are described in terms of the ego vehicle projections over the nominal trajectory L (considering the position $d_{x_{i+(k-1)|k}}$), and the vector formed by the lateral displacement (in the current time T_k) which is named as $\mathbf{e_{lat}}_0^{\perp}$. Fig. 4.2 depicts these elements. The ego vehicle future prediction can be mathematically described as:

$$\mathbf{V}_{0i} = proj_L\{d_{x_{i+(k-1)|k}}\} + \mathbf{e_{lat}}_0^{\perp} \tag{4.10}$$

In the case of the other vehicles $\mathbf{V}_j$, the predictions are built with a kinematic vehicle model which is a function of their current position, speed, and acceleration. The predictions are calculated over the center of the lane, considering the lateral error as in the ego vehicle case. The mathematical representation is given by:

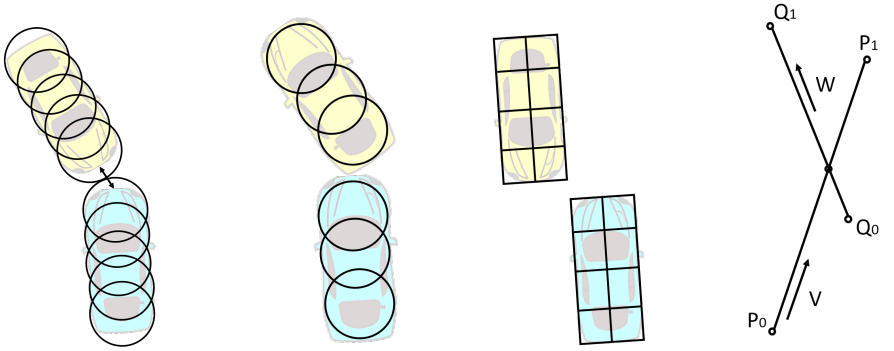

(a) Collision using circumscribed circles

(b) Collision using inscribed circles

(c) Collision using line segments

(d) Intersection between segments

Figure 4.3: Collision evaluation using different methods

$$\mathbf{V}_{j\,i} = proj_{L_{v_j}}\{d_{j0} + v_j T_{i+k} + \frac{a_j T_{i+k}^2}{2}\} + \mathbf{e_{lat}}_{j0}^{\perp} \tag{4.11}$$

4.3.3 Collision evaluation

The evaluation of the collisions can be done with three different methods that have different advantages and disadvantages. Those are:

- Circumscribed circles in vehicle's area (Fig. 4.3a).
- Inscribed circles in vehicle's area (Fig. 4.3b).
- Collision using line segments to define vehicle boundaries (Fig. 4.3c and Fig. 4.3d).

Circumscribed and inscribed circles evaluate the collisions by considering the intersections of the circles modeling the vehicle, whereas circumscribed method is pessimistic due to generates long distances (separation) between the vehicles, and the inscribed method is very optimistic, in some cases, this could generate a collision between vehicles.

Therefore, the method used in this work was the line segments intersection. This method has some drawbacks in the case of small-sized objects, which could

not be detected if dimensions are significantly smaller compared to vehicle size, humans for instance. However, the approach aims the overtaking scenario, where pedestrians are not foreseen in this Ph.D. thesis.

Each vehicle is described with n vertical and m horizontal segments. A potential collision is detected when one vehicle's segment intersects another vehicle's segment. A similar method was used in the past to trigger an overtaking maneuver or brake the vehicle [194]. The intersection between the two segments is shown in Fig. 4.3d where vectors $\mathbf{V} = \mathbf{P}_1 - \mathbf{P}_0$ and $\mathbf{W} = \mathbf{Q}_1 - \mathbf{Q}_0$ describe the segments:

$$\begin{aligned} \mathbf{P}_0 + t\mathbf{V} &= \mathbf{Q}_0 + s\mathbf{W} \\ t &= \frac{(\mathbf{Q}_0 - \mathbf{P}_0) \times \mathbf{W}) \cdot (\mathbf{V} \times \mathbf{W})}{||\mathbf{V} \times \mathbf{W}||^2} \\ s &= \frac{(\mathbf{P}_0 - \mathbf{Q}_0) \times \mathbf{V}) \cdot (\mathbf{W} \times \mathbf{V})}{||\mathbf{W} \times \mathbf{V}||^2} \end{aligned} \tag{4.12}$$

if the scalar values t and s are in $[0, 1]$, a intersection between segments is confirmed.

4.3.4 References and constraints manipulation

The finite horizon OCP was solved in terms of a constrained optimization problem for keeping the maneuver feasible, the passengers' comfort, and mitigating possible collisions. The general problem of lane change due to obstacles interference is non-convex. A general form to transform this problem in convex is using envelopes or tubes defining possible collision-free trajectories [195].

Fig. 4.4a explains the definition of a convex function, where the line segment $\{t\mathbf{P}_0 + (1-t)\mathbf{P}_1, t \in [0,1], \mathbf{P}_0 \in \mathbf{A}, \mathbf{P}_1 \in \mathbf{A}\}$ intersects the function only in the points $\mathbf{P}_0$ and $\mathbf{P}_1$ for all the points contain in the boundaries of the space set $\mathbf{A}$.

The ego vehicle will generate envelopes for a safe collision-free space, when a potential collision with an obstacle is detected on the road. The envelopes are non-convex if they surround the obstacle. This situation generates challenging optimization problems (Fig. 4.4b). In such a case, the approach uses a safe envelope or tube around the other lanes based on traffic rules, avoiding the obstacle, and making the problem convex (Fig. 4.4c).

The constraints associated with the longitudinal domain can be summarized with the inequalities:

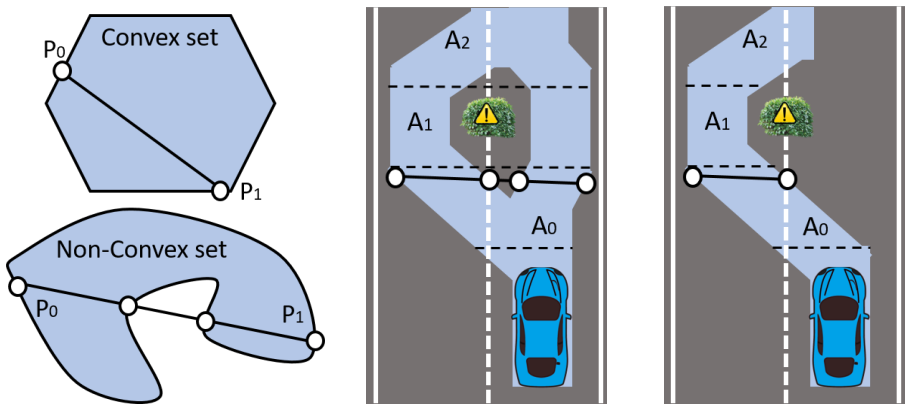

(a) Convex and non-convex set

(b) Non-convex vehicle envelope

(c) Convex vehicle envelope

Figure 4.4: Collision evaluation using different methods

$$\begin{aligned} 0 \leq d_{lon} &\leq D_{veh_{front}} \\ 0 \leq v_{lon} &\leq v_{SP} \\ -|a_{min}| \leq a_{lon} &\leq |a_{max}| \\ -|J_{min}| \leq J_{lon} &\leq |J_{max}| \end{aligned} \tag{4.13}$$

the longitudinal domain acceleration and jerk have static constraints that are unmodified during execution time. The vehicle dynamics were considered in terms of the acceleration limits. The acceleration has considered the maximum vehicle acceleration a_{max} as upper bound and the maximum deceleration a_{min} as lower bound. The jerk constraints have been used to consider the comfort of the passenger with smooth acceleration changes. The upper and lower jerk bounds were set symmetrically with a value of $|J_{max}|$. The maximum jerk value is related to the passenger's comfort [193]. The speed is bounded considering the road speed limits which keeps the safety during maneuver execution and a maximum lateral acceleration criterion keeping comfort [175].

The longitudinal distance is one of the most important variables to execute a maneuver safely. The distance is constrained to the maximum value from the sample, where an unfeasible solution is detected, adding the component of

safety in the maneuver execution. Unfeasible solutions are confirmed when they are out of the constraint limits (bounds).

The lateral dynamics are constrained in terms of the following inequalities:

$$\begin{aligned} -\frac{1}{2}|Road_W| + \frac{1}{2}Veh_W \leq d_{lat} \leq \frac{3}{2}|Road_W| - \frac{1}{2}Veh_W \\ -|v_{max}| \leq v_{lat} \leq |v_{max}| \\ -|a_{max}| \leq a_{lat} \leq |a_{max}| \end{aligned} \tag{4.14}$$

in this case, v_{max} and a_{max} define static boundaries, and the maximum rate of change of the steering wheel is related to these values (in terms of its response time, delay and a safe rate-of-change). The variable d_{lat} is dynamically defined during execution, but its limit values are shown in the inequality, considering the road's width $Road_W$ and the vehicle's width Veh_W.

The maneuver generation was limited to two lanes inspired by human drivers, which solve the overtaking with concatenations of lane changes in case of consecutive overtaking maneuvers. In these terms, the approach can be extended to n-lanes easily. In the case of detecting an obstacle in the nominal lane, the boundaries are moved to $\frac{1}{2}Road_w + \frac{1}{2}Veh_W$ (lower bound) and $\frac{3}{2}Road_W - \frac{1}{2}Veh_W$ (upper bound). If the obstacle is detected in the other lane, the lateral offset boundaries are moved to $-\frac{1}{2}Road_w + \frac{1}{2}Veh_W$ and $\frac{1}{2}Road_W - \frac{1}{2}Veh_W$.

The algorithm 2 summarizes the adaptation process over the references and constraints. It considers a number of samples n_s, where $V_{ego} \cap V_k$ and $V_{ego_{proj}} \cap V_k$ terms refer to:

1. $V_{ego} \cap V_k$ is the collision verification made between the ego vehicle and one of the n_v obstacles. It is named c_l.

2. $V_{ego_{proj}} \cap V_k$ is the collision verification made between the ego vehicle projection over the other lane and one of the other n_v vehicles. It is named c_o.

4.3.5 Implementation using the control architecture

The MPC planning method was added into the AD architecture (presented in section 3.2), as an intermediate module shared between decision and control. The MPC evaluates the decision process of the vehicle on the road (for example collision verification, lane-changing, etc.), along with the generation of commands to execute the maneuver safely (control module), such as the lateral

Algorithm 2 Constraint and reference manipulation

```
1: // Constraints
2: n_limit ← ∞
3: for i ← 1 to n_s do
4:    for k ← 1 to n_v do
5:       c_l ← V_ego ∩ V_k
6:       c_o ← V_ego_proj ∩ V_k
7:       if c_l then
8:          move lat. offset bounds opposite lane
9:       end if
10:      if c_o then
11:         move lat. offset bounds nominal lane
12:      end if
13:      if state unfeasible then
14:         break
15:      end if
16:      if c_l and c_o then
17:         move lat. offset bounds nominal lane
18:         break
19:      end if
20:   end for
21: end for
22:
23: j ← i
24: while j ≤ n_s do
25:    limit longitudinal distance upper bound to distance in sample i
26:    j ← j + 1i
27: end while
28:
29:
30: // References
31: for i ← 1 to n_s do
32:    set lateral offset reference in middle of bounds
33:    set reference speed considering road limits and lateral acceleration criterion
34: end for
35:
```

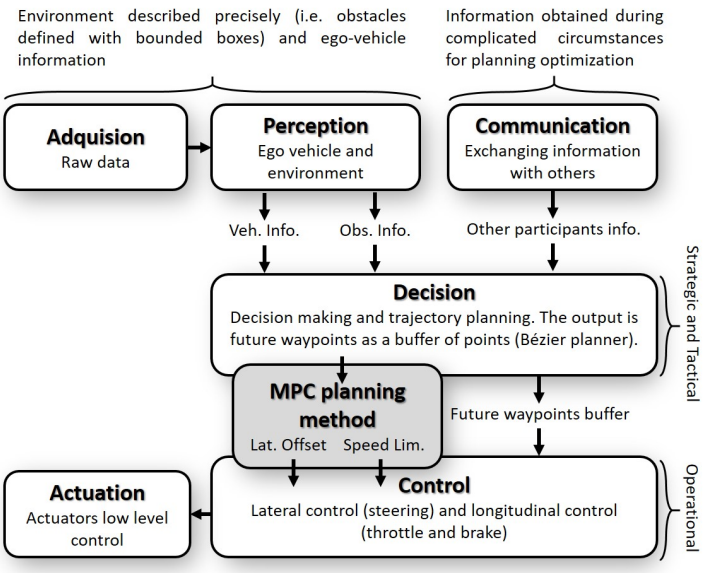

Figure 4.5: Inclusion of the MPC approach in the control architecture

error command and the speed setpoint. This module is observed in gray color in Fig. 4.5.

Splitting the approach in decision and control permits to merge the Bézier and the MPC trajectories easily. While Bézier is completely built in the decision module, the MPC is shared between the decision process (collision calculation) and the control module.

Fig. 4.6 shows an example of an overtaking scenario. The ego vehicle (vehicle 1) is moving over a nominal trajectory that was built with Bézier curves, and a slower vehicle (vehicle 2) is moving some meters ahead. This scenario triggers a lane-change process adding a lateral offset to the control commands. This lateral offset is based on the MPC trajectory. Another vehicle (vehicle 3) was detected during the maneuver execution, regulating the speed.

The MPC outputs will be the longitudinal jerk j_x and the lateral acceleration a_y. Therefore, the outputs must be integrated so as to reconstruct the vehicle states (position, speed, and acceleration). Lateral offset d_y and longitudinal speed v_x are the demanded states, as shown below:

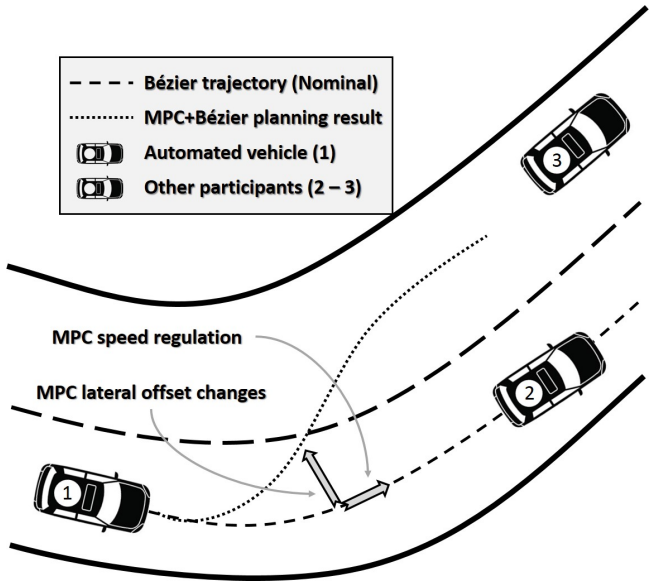

Figure 4.6: Example of the hybrid trajectory generated

$$v_x(t) = \iint j_x(t)dt^2 \quad d_y(t) = \iint a_y(t)dt^2 \tag{4.15}$$

4.3.6 ACADO Toolkit

The MPC formulation was made using ACADO toolkit software (C/C++ library), which aims to solve OCP applications. It is a complete toolchain that offers a great variety of possible configurations with efficient execution times. This software is open-source, and all the demanded packages are contained in the library. It is compatible with the platform Matlab®/Simulink®. It has a fast learning process due to its user-friendly interface and the number of examples [196, 197].

This toolkit solves the following typical control problems:

1. Offline multi-objective control problems or finding an optimal open-loop control law for given dynamics.

2. Parameter and state estimations (model identification problem).
3. Online optimal control problems solution, such as Model Predictive Control.

ACADO uses some of the methods listed below when solving the problems [198]:

1. Multiple shooting method, which is more stable (numerically) than a single shooting method.
2. Complex non-linear models and optimization functions are solved using Sequential Quadratic Programming (SQP).
3. Problems based on linear models are solved in small time intervals.
4. The system integrates the discrete computed states using a Runge-Kutta method.

4.4 Control model

Lane change maneuvers are risky due to the good driver skills demanded, and they have a direct relation with obstacle avoidance (refer to section 4.5.1) and overtaking (refer to chapter 5). Furthermore, they must consider road traffic rules. In these terms, the correct execution of these maneuvers demands a reliable trajectory. A good solution is obtained with the inclusion of models on the trajectory generation due to the reduction of the solution space to the vehicle's feasible possibilities.

Additionally, a good controller is demanded to keep a stable trajectory tracking. The selected controller is a linear function with a curvature component. Double proportional controller plus curvature (explained in section 3.5.4) is the name of the controller used. However, the curvature component was substituted with a model-based feed-forward controller, which makes it more robust.

The feed-forward control has a dynamic bicycle model that can be very precise at low and moderate speeds [199]. Fig. 4.7 represents this model along with the trajectory. The frontal and rear tire slip angles $\alpha_{f,r}$ are given by:

$$\begin{aligned} \alpha_f &= \delta_f - \frac{v_y + \omega a}{v_x} \\ \alpha_r &= \frac{b\omega}{v_x} - \frac{v_y}{v_x} \end{aligned} \tag{4.16}$$

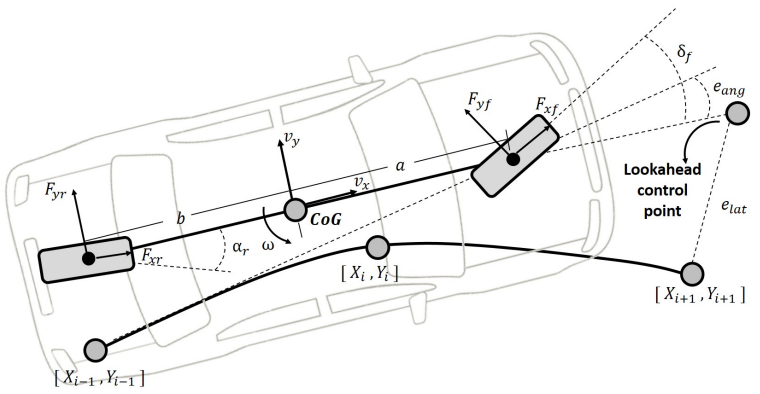

Figure 4.7: Feed forward bicycle model

where a and b are the distances from the Center Of Gravity (COG) to the front and rear wheel respectively, $v_{x,y}$ are the longitudinal and lateral velocities, and δ_f is the steering wheel angle. The resulting force over the tire is given by:

$$C_{f,r} = c_{f,r}\frac{d_{a,b}}{L}Mg \rightarrow F_{y_{f,r}} = C_{f,r}\alpha_{f,r} \tag{4.17}$$

where $C_{f,r}$ is the cornering stiffness of the frontal and rear tire and $c_{f,r}$ are the normalized values of the cornering.

Next, the sum of lateral forces is obtained:

$$\frac{F_{yt}}{M} = \frac{F_{yf}}{M} + \frac{F_{yr}}{M} \rightarrow \frac{F_{yf}}{M} = \frac{F_{yt}}{M} - \frac{F_{yr}}{M} \tag{4.18}$$

The lateral and longitudinal accelerations can be computed using the reference speed v_s, the trajectory curvature k, the acceleration a_x (given by the trajectory), and the angle error between vehicle and the trajectory e_α. The resulting equations are:

$$\begin{aligned} a_{xt} &= a_x \\ a_{yt} &= v_s^2 k cos(e_\alpha) + a_x sin(e_\alpha) \end{aligned} \tag{4.19}$$

Combining Eq. 4.17, 4.18 and 4.19:

$$c_f \frac{a}{L} g \left(\delta_{ff} - \frac{v_y + \omega a}{v_x} \right) = a_{yt} - \frac{C_r \alpha_r}{M}$$
$$\delta_{ff} = \frac{a_{yt} - \frac{C_r \alpha_r}{M}}{c_f \frac{a}{L} g} + \frac{v_y + \omega a}{v_x} \tag{4.20}$$

the feed-forward contribution for the steering wheel angle, which uses the bicycle model and trajectory information.

This controller was tested in a double lane change maneuver considering the feed-forward controller with and without the feedback controller. The performance of the vehicle was measured considering the conformance testing approach [199]. This method evaluates the open-loop model used in the feed-forward part comparing it with real vehicle data traces. The values must be under a certain bound (acceptance criteria) during the designing process (Fig. 4.8a). Once the open model is validated, the system is verified with the tracking correction given by the feedback part. Consequently, the states must remain under the acceptance boundaries (Fig. 4.8b).

The position x, y, and yaw angle ψ bounds are fixed using typical sensor errors. Those values are 10 centimeters of position error and 1 degree of angle error in case of a differential GPS. The speed, yaw rate ω, longitudinal acceleration a_x, and the angle of the frontal wheel δ bounds were set according to vehicle tests.

The experiments have been done using the Dynacar multi-body vehicle model [200] (refer to sections 3.5.1). The real platform was not available during the execution of the tests. The simulation data and the real platform data varies in a small percentage in both cases, and in general, the feed-forward controller has a good performance on real vehicle scenario.

4.5 Experimental validation results: Real tests

This section presents the experimental results using the Renault Twizy real platform (refer to section 3.5.2), and other vehicles modeled with the Dynacar simulator. The approach uses either V2X information or perception. In the case of using perception, vehicles' width and length measurements errors, derived from sensors' data, are considered.

The experiments are divided into a low-medium and a medium-high speed tests. For the first group, static and moving obstacles have been considered on

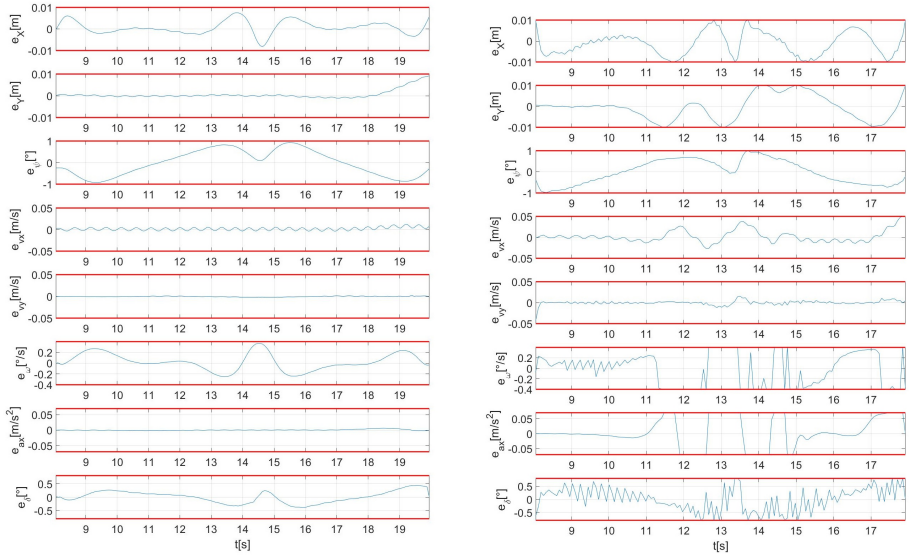

(a) Open loop trace conformance

(b) Close loop trace conformance

Figure 4.8: Formal verification of the feed-forward controller

Tecnalia's test tracks (refer to section 3.5.3). The maximum speed of this track is $30km/h$ due to its dimension. The second tests were done on a long straight lane track.

4.5.1 Low-Medium speed tests

The low to medium speed tests, conducted in Tecnalia's proving ground (refer to section 3.5.3), were in conditions under $30km/h$ due to the physical space limitation. Nevertheless, the test space has been maximized as much as possible to cover obstacle avoidance in straight path and bend segments.

Static obstacles

The first set of tests is depicted in Fig. 4.9. This test has been conducted in a path that overlaps in the center with two roundabouts in the edges. The main trajectory was model using Bézier curves and is depicted in the dashed line. The blue line describes the hybrid trajectory using Bézier plus the MPC.

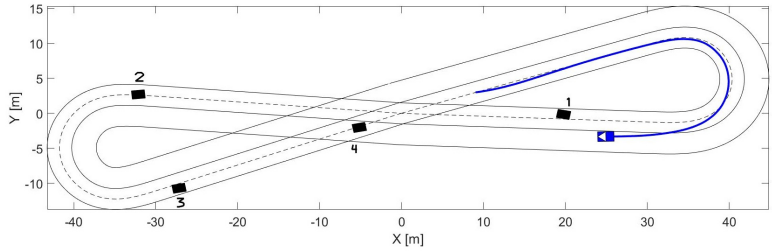

(a) Experiment at 17 seconds

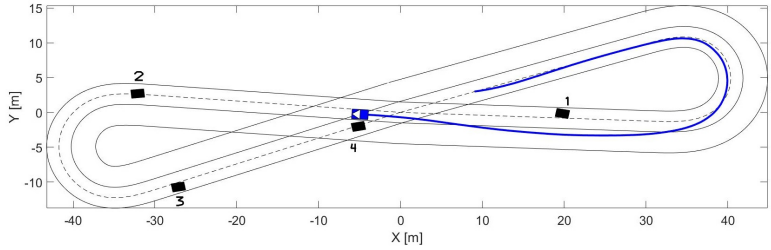

(b) Experiment at 23 seconds

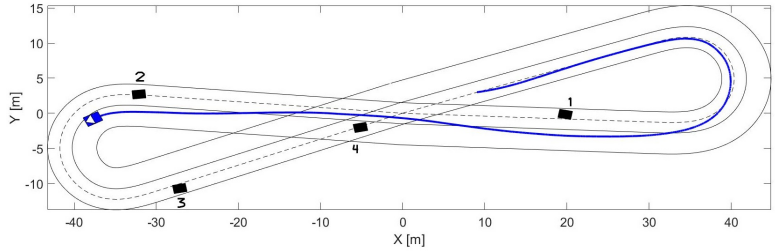

(c) Experiment at 26 seconds

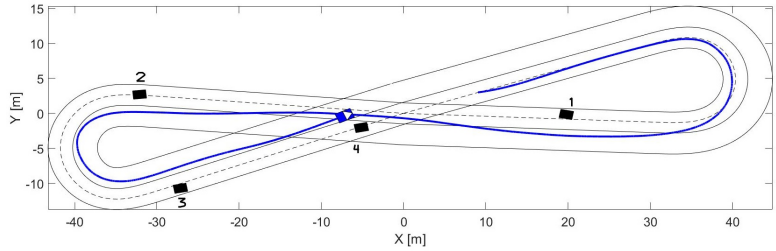

(d) Experiment at 37 seconds

Figure 4.9: Low-medium speed: test results with static obstacles.

Fig. 4.9a shows the vehicle tracking over the nominal trajectory (dashed line). A static obstacle was detected in the nominal lane at the exit of the bent segment (described with a roundabout). The vehicle dynamically has adapted the constraints for moving the lateral offset boundaries to the opposite lane, avoiding the obstacle, and reducing its speed if needed (avoiding a possible collision).

Fig. 4.9b and 4.9c depict the returning process to the nominal lane where the ego vehicle has avoided the static vehicle (number 4). Furthermore, the approach has determined an optimal trajectory without totally returning to the main lane due to the upcoming obstacle number 2.

Fig. 4.9d shows the ego vehicle returning to the main lane, when vehicle 3 has been detected. The ego vehicle has overtaken vehicles 3 and 4 without returning to the nominal lane. Finally, the vehicle returns to the nominal lane, completing the test.

The lateral offset (generated by the MPC approach), the lateral error and the MPC speed setpoint were monitored during the test execution. The lateral offset is shown in Fig. 4.10a which depicts the dynamic adaptation of the system avoiding a lane returning process. This task is not possible with a discrete set of conditions due to the complexity of multiple obstacles closed to each other. Additionally, the obstacles were in difficult positions, i.e. entrance and exits of bend segments and in the middle of the maneuver. During the period of time between 15 seconds and 25 seconds, the vehicle partially returns to the nominal lane, when the presence of another obstacle pushes the ego vehicle back to the opposite lane.

The overall tracking error increases when compared to no obstacles tests (refer to section 3.6.2). Fig. 4.10b depicts the lateral error. Again, its maximum value was around 0.6 meters, which are 10 centimeters over the previous measurements. Values around $0.6m$ happened 10% of the time during the test, the histogram presented in Fig. 4.10c verifies this event. However, these results are acceptable because the lateral tracking error is frequently under the median value of $0.3m$. Moreover, this scenario was complex in terms of decision making on whether staying at the nominal lane or not.

Fig. 4.10d depicts the speed setpoint and the vehicle's speed during the test. Periods between 10 and 15 seconds, as well as 27 and 30 seconds, show MPC's speed setpoint below the maximum speed limit. This is because the vehicle reduce the speed when the solution is unfeasible.

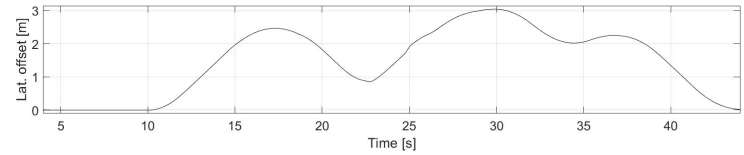

(a) MPC lateral offset

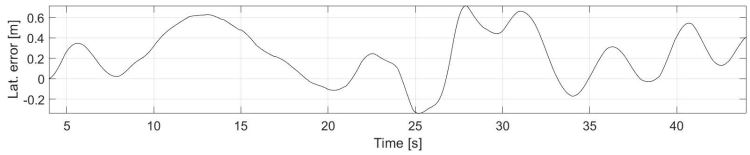

(b) Total lateral error (tracking)

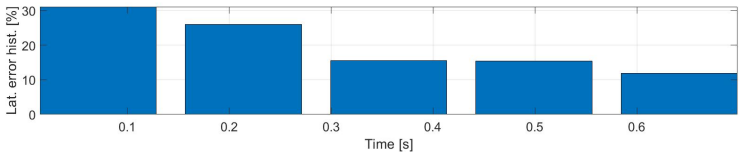

(c) Histogram of the lateral error

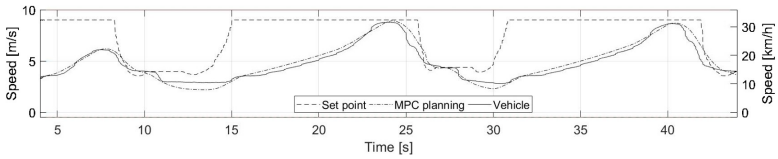

(d) Speed set point

Figure 4.10: Low-medium speed: control variables with static obstacles.

Moving obstacles

Fig. 4.11 shows a low-medium speed test with moving vehicles. The obstacle vehicles were in the opposite lane, driving on the opposite direction. Also, a static obstacle was on the nominal lane. The first part of the experiment is appreciated in Fig. 4.11a to 4.11c. The ego vehicle has reduced the speed to yield the right-of-way to the second vehicle. The ego vehicle continued the maneuver when the opposite lane was available. This experiment showed the execution of the maneuver as stop-and-go, without modifying the algorithm or any other special consideration.

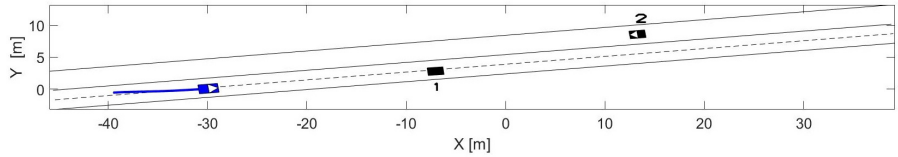

(a) Experiment at 5 seconds

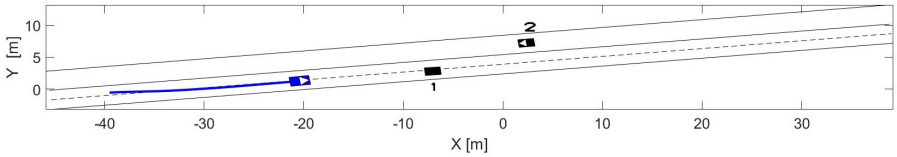

(b) Experiment at 7 seconds

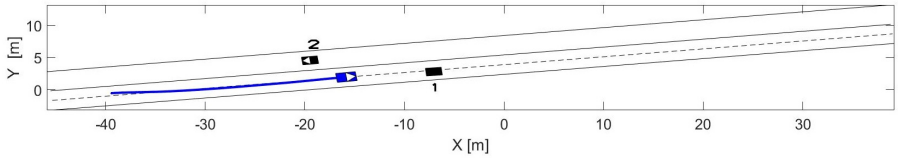

(c) Experiment at 11 seconds

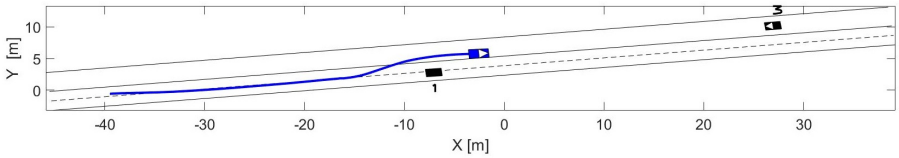

(d) Experiment at 19 seconds

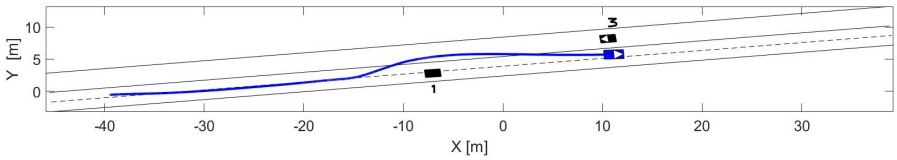

(e) Experiment at 22 seconds

Figure 4.11: Low medium speeds: test results with moving obstacles.

Fig. 4.11d and 4.11e show the process of overtaking the static obstacle and returning to the nominal lane. This maneuver considered a 3rd moving obstacle

rushing the process of returning to the nominal lane.

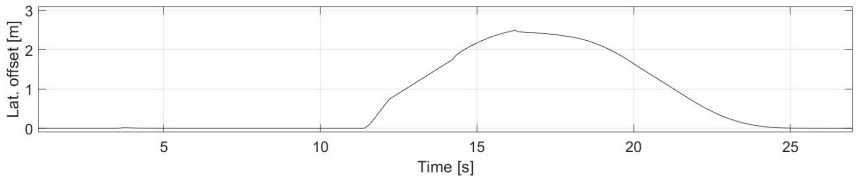

(a) MPC lateral offset

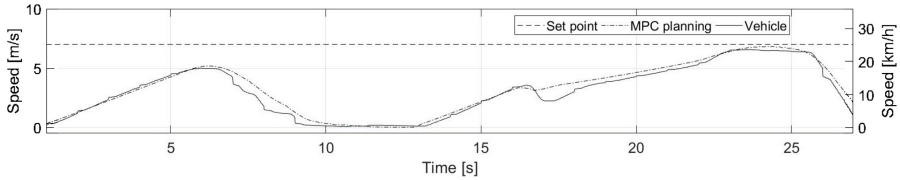

(b) MPC reference speed

Figure 4.12: Low medium speeds: control variables with moving obstacles.

Fig. 4.12a and 4.12b depict the MPC control variables. The first figure depicts the MPC lateral offset. It was not modified before the time 11 seconds to yield the right-of-way to the other vehicle. After, the lateral offset reached 2.5 meters which was a value good enough to avoid the obstacle, returning fast to the nominal lane and avoiding a frontal collision.

The speed has shown a similar behavior reducing the setpoint until 0, yielding the right-of-way in the opposite lane, and avoiding a rear-end collision. After, the vehicle increased its speed until the maximum test track limits (it was around $7m/s$). After 18 seconds, the vehicle returned to the nominal lane avoiding a frontal collision with the vehicle 3.

4.5.2 Medium-High speed test

During the execution of the UnCoverCPS project's live demonstration, the Renault Twizy was shipped to the headquarters of one of the project's partners: DLR (Germany). Real tests were carried out at $60km/h$ ($16.66m/s$) during a cooperative overtaking maneuver of three vehicles on a two lanes test track (both lanes in the same direction). Although the Twizy can reach $80km/h$, it drove automatically at $60km/h$ for its first time.

Figure 4.13 shows the test results on medium-high speeds avoiding obstacles

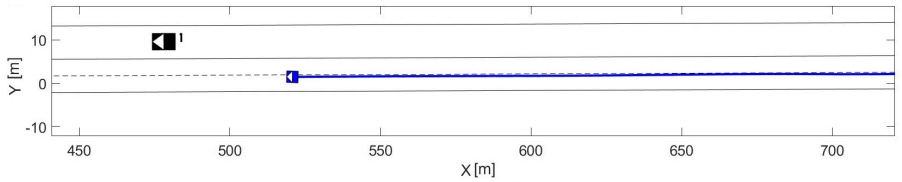

(a) Phase 1 of the experiment

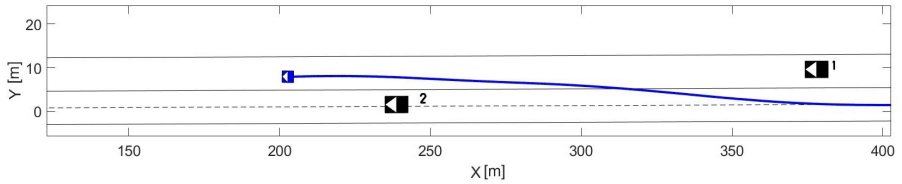

(b) Phase 2 of the experiment

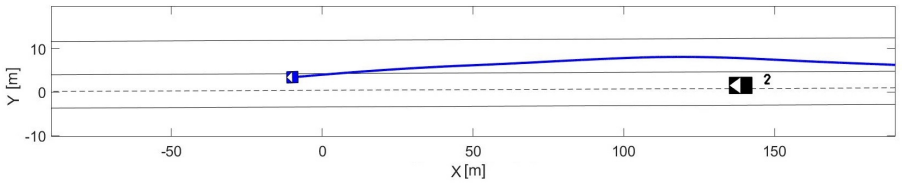

(c) Phase 3 of the experiment

Figure 4.13: Medium-high speed: test results.

while driving on a $4m$ width road. During the first part of the experiment (Fig. 4.13a), The Twizy was driving on its nominal lane and another vehicle (1) appeared in the opposite lane.

In the second phase (Fig. 4.13b), the experiment showed that the nominal lane was blocked by a driving obstacle (2) while obstacle (1) remains on the opposite lane and the right-of-way must be respected during the maneuver. Lastly, the third phase of the experiment (Fig. 4.13c) shows the ego vehicle returning to the nominal lane.

Fig. 4.14a shows the lateral offset. It almost reached the maximum road width which was $4.0m$. In the period between 22 and 27 seconds, a speed reduction has been generated in the MPC to reach safely the opposite lane, without approaching obstacle 2 and avoiding a collision with vehicle 1.

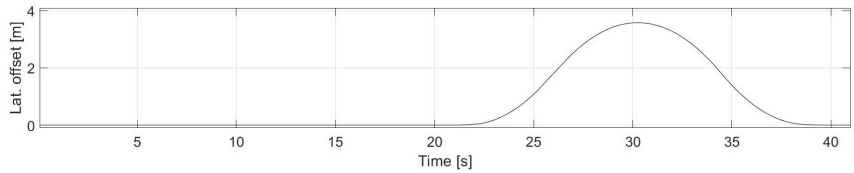

(a) MPC lateral offset

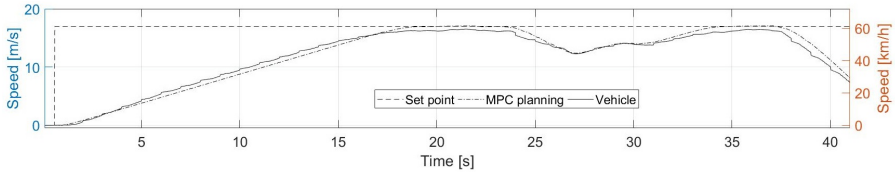

(b) MPC reference speed

Figure 4.14: Medium-high speed: control variables.

4.6 Experimental validation results: Virtual tests

Additional to the real platform tests, a simulation test case has been evaluated using the hybrid approach. In this case, a risky maneuver has been set up where two high speed vehicle (driving around $50km/h$) were involved and a slow speed vehicle (driving around $15km/h$) was blocking the nominal lane. This results are shown in Fig. 4.15.

In this sequence, the ego vehicle (blue box) starts an overtaking maneuver considering the slow vehicle 1. The vehicle 2 was not detected at this moment for multiple conditions as: communication link not established due to the distance among the vehicles or the limited prediction horizon of 5 seconds (considering the relative speed is more than $100km/h$ with both vehicle over $50km/h$). Consequently, an overtaking maneuver started. When vehicle 2 was detected, the ego vehicle returned partially to the nominal lane remaining close to the opposite lane (vehicle 2). At this moment, the scenario could look risky for passengers. After this event, the scenario continued normally finishing the overtaking process safely.

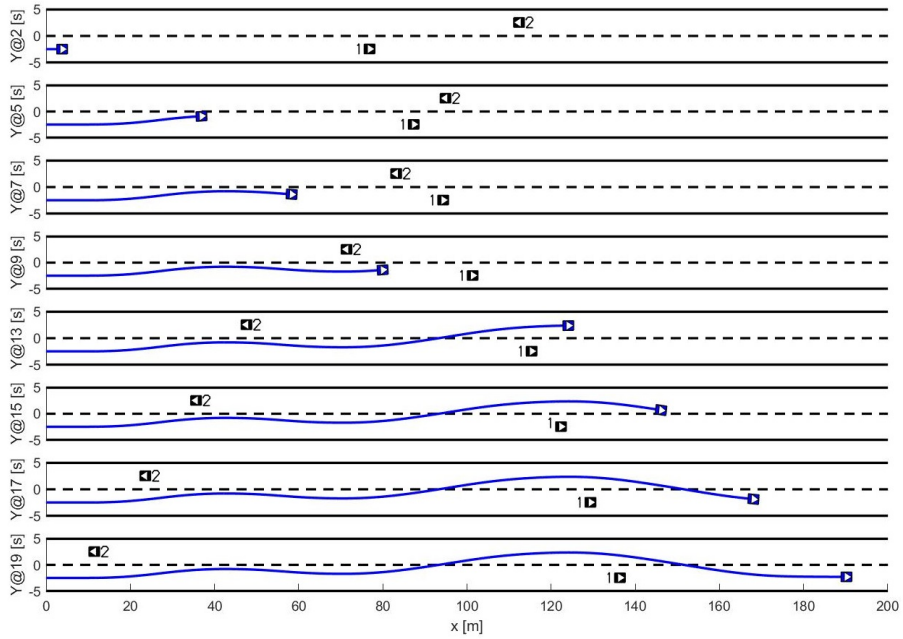

Figure 4.15: Simulation test case

4.7 Discussion and summary

In this chapter, a dynamic planning method has been described considering a hybrid approach based on Bézier curves and MPC. This approach has shown good results in terms of collision avoidance and lane changing maneuvers. Additionally, the method can also be used during overtaking scenarios.

An interesting result is the capacity of adapting the vehicle trajectories on real-time, without coding all the discrete possibilities (previous methods). The bounds' adaptation and the feasibility evaluation help to obtain these good results.

Discrete and specific scenarios as stop-and-go and normal cruising are considered during the trajectory planning. Maneuvers as emergency braking can be considered, for instance, increasing jerk boundaries in the longitudinal domain (compromising comfort). Naturally, these changes mitigate or reduce the impact of a possible collision.

The reliability of the approach has been demonstrated in different platforms and scenarios, like intersections, roundabouts, lane changes, ACC, stop-and-go, emergency braking, etc.

Furthermore, the tracking error was kept at a low magnitude during the maneuver execution, due to the MPC approach. Therefore, the model used in the optimization method is good enough for these automotive applications along with fast response time.

The recorded maximum speeds, through these tests, have been the maximum ones in automated mode at the moment (using Tecnalia's platform). Before, the maximum speeds have never passed $15km/h$.

The time horizon was finite and with a low number of samples (10 samples separated every $0.5s$) in the test cases because these values permitted to reach the planning time-demands. In these terms, a cooperative approach must be implemented to reduce the impact of risky scenarios, reserving future spaces for maneuver planning. The cooperation approach will be presented in the next chapter.

"Coming together is a beginning; keeping together is progress; working together is success".

Henry Ford

5

Cooperative planning for automated vehicles

5.1 Introduction

One of the main goals of AD is to increase safety on roads while improving and optimizing mobility. Today, the technology is based on unconnected vehicles to ensure safety levels during system execution. These approaches have considered vehicle dynamics information navigating with sensors. Nevertheless, the connectivity can extract all the potential of the technology. In these terms, cooperative automated vehicles are one of the most expected developments, increasing safety while improving sub-optimal solutions obtained from unconnected methods.

Projects as the Grand Cooperative Driving Challenge (GCDC) i-Game 2016 [100], the Managing Automated Vehicles Enhances Network (MAVEN) project [102], and the Co-operative Systems in Support of Networked Automated Driving by 2030 (AutoNet2030) [101] have been relevant in terms of cooperative and automated vehicles. GCDC i-Game has considered the scenario of the cooperative platoon on the highway including the merging of two

platoons. This project aimed to improve the traffic flow, while emergency vehicles and intersection crossings were considered as part of the general scenario of driving. The MAVEN project was related to the standardization of cooperation messages for the platoon maneuver. On the other hand, AutoNet2030 studied methods for cooperative maneuvers in terms of merging a vehicle in a platoon and additionally, lane changing out of the convoy. Most of the newest projects have been defined in terms of the cooperative platoon but there are still gaps in some scenarios such as the overtaking.

Overtaking is one of the most challenging and hazardous maneuvers while driving a vehicle. It improves the traffic flow mitigating the impact produced by low-speed vehicles. Additionally, overtaking improves passengers' comfort while reducing the acceleration/deceleration events in keeping the desired speed [201]. However, these benefits demand good driving skills due to risks during the execution of the overtaking. The percentage of accidents is between 4 and 10 %, and the main factor is failing in the decisions during its execution [202, 203].

The work done by Park et al. confirmed that lane change and overtaking maneuvers are risky and they could trigger an accident [204]. Therefore, some authors (e.g. [205, 206]) have separated the maneuver in the following three stages, to simplify and reduce the probability of error:

1. A first lane change to the opposite side of the road.
2. The overtaking process.
3. Returning to the original lane.

splitting it into these three steps makes the problem easier to solve, in comparison with the methods used in the mobile robot field considering fixed obstacles [201] (predefined trajectory).

Sezer et al. presented a novel method to address the decision-making process in the overtaking scenario [207]. It was based on Mixed Observable Markov Decision Process (MOMDP) which is a variant between a Markov Decision Process (MDP) and a Partly Observable MDP. This method is computationally complex making it non-viable for real-time implementations. In [208] was proposed a Rapidly-Exploring Random Tree (RRT) algorithm to avoid obstacles. A model of the vehicle and the control loop were demanded for the planner. The approach has two problems, time demanded and power of calculation. Other authors have used techniques based on intelligent control, like fuzzy logic, to control the steering wheel under overtaking maneuver, as well as obstacle avoidance processes [205, 209]

Many different approaches for automated overtaking can be found in literature. However, most of them have considered this as connected vehicles or, in the worst case, as an unconnected vehicle problem. Sub-optimal solutions, limited discrete solutions, and offline previously calculated trajectories are some of the methods that cannot solve the problem stably and safely, as a human driver does.

In this context, this chapter will present a method to generate cooperation among automated vehicles. It considers Model Predictive Control and space-time reservations of road areas to solve the problem. The approaches presented in chapter 3 and 4 are the basis of the generated trajectories, including a space-time negotiation protocol to complement it. The negotiation improves safety while reducing the impact over the traffic.

5.2 Review of cooperative methods

Non-cooperative overtaking methods produce sub-optimal or dangerous situations, for example, the safety conditions are more conservative, compared to human drivers' decisions (refer to Fig. 5.1a). Moreover, some errors should be considered due to signal disturbances from other participants. This produces a conservative solution, aborting the overtaking process with an impact over traffic flow (refer to Fig. 5.1b). Lastly, another common fault in non-cooperative algorithms is the optimistic prediction of other participants' behavior. Typically, they assume other participants' behavior like yielding the right-of-way (Fig. 5.1c), and this could end in an accident.

Some authors have paid attention to the possible failures in connected and unconnected overtaking methods, and they have proposed some cooperative solutions. In these terms, this section explains some of the strategies used for cooperative automated vehicles. Based on the literature, these methods are separated in hybrid automaton approaches, signalized approaches, and cooperative negotiation.

5.2.1 Hybrid automaton

This approach is related to the generation of a discrete set of events during the system execution, which originates changes in the software used for the automation. It can be seen as different software used for automation and switching in case of different conditions. In this sense, the continuous system dynamic is

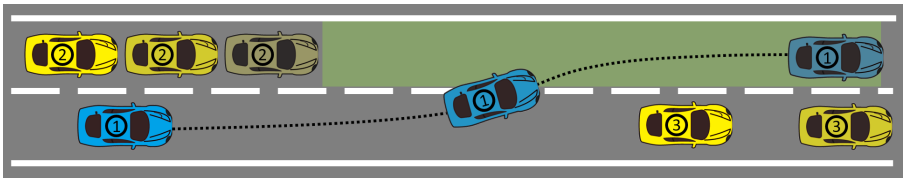

(a) Sub-optimal solutions or lack of motion primitives

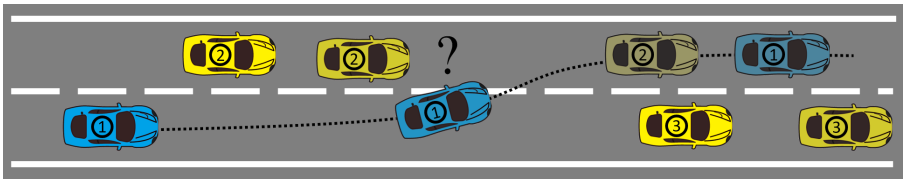

(b) Error during estimation of other participants states (pessimistic)

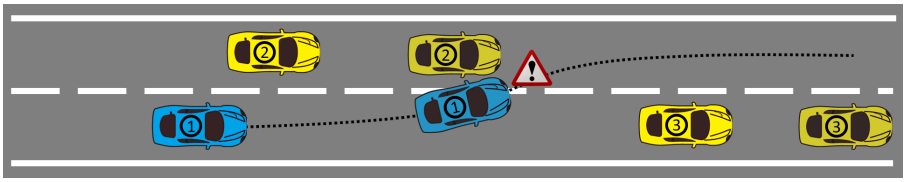

(c) Error during estimation of other participants states (optimistic)

Figure 5.1: Some of the errors originated in non-cooperative overtaking approaches.

governed by "multiple control configurations" depending on discrete conditions or rules.

In these terms, Huang et al. have established this technique for cooperative maneuvers considering the conditions of platooning or normal driving [210]. These two configurations are controlled by merging and splitting events. The vehicle sends a merging event to the vehicle in front. This information is accepted and verified for establishing the presence in the platoon. In the case of splitting, the vehicle generates a new platoon configuration using the cruise condition. The problem with this approach is its limitations due to requiring specific software architectures for all the vehicles. Every scenario of cooperation is treated as a platoon, limiting other scenarios, and requiring a specific message to perform this. Furthermore, the message is limited to platoon content and some variables used for triggering the event (switching dynamics). Finally, the

approach demands periodic messages which saturate the message queue with specific content.

Menendez-Romero et al. proposed another complex hybrid system [211]. It considered the merging scenario. The vehicles assumed cooperation (all the time) before merging. The automated vehicles have their dynamics divided into cruising normally, decelerating while keeping the lane, and changing the lane. On the other hand, the upcoming vehicle dynamics were separated in yielding the right-of-way for the merging, normal merging in the available space, and opening space for the upcoming merging scenario. This approach showed good results introducing a novel aspect such as the "courtesy". Nevertheless, the approach supposed available cooperation among the participants continuously. This condition generates problems on real vehicle applications, due to the limited available time for sending, receiving, and processing the messages. Additionally, the approach demanded the same software for verification of the cooperation in all the participants.

5.2.2 Signalized approach

Other methods used for cooperation are based on traffic signals and rules. These approaches are mostly used in urban environments where the traffic flow is constantly interrupted. Intersections regulated by traffic lights or signals, roundabouts, among other urban scenarios are some examples of disturbance in the urban flow.

Some of the methods using traffic signals for cooperation were reviewed in [212], and some examples are: cooperation among multiple connected vehicles, unconnected vehicles, and manually driven vehicles in terms of mixed traffic. This method is strongly based on extending green light to improve cooperation, introducing it where a signal limiting the traffic flow exist. This also changes the status of some signals, and it starts some conditions before the programmed time (for example changing the traffic light to red or green). In this approach all the vehicles must follow the traffic rules. It improves traffic flow, and appealing characteristics can be added such as reducing power consumption [213].

The main problem of these methods is the inclusion of new pieces of hardware that execute the algorithm. Furthermore, they must include sensors that increase the price of traditional infrastructure.

5.2.3 Cooperative negotiation

In a natural way, drivers negotiate their intentions among other participants on the road. Thus, this topic is relevant in the field of cooperative automated vehicles. Gupta et al. established the negotiation in three terms [214]:

1. Perceiving other participants' intention, for example: pedestrian when crossing a road.

2. Considering other participants' behavior, for example: in the case of aggressive drivers, the driving profile must be adapted to a defensive one.

3. Establishing some kind of agreement between drivers to improve the traffic flow, for instance: merging a roundabout in traffic jams conditions.

Different centralized and decentralized methods have been studied in maneuver negotiation. They have used techniques as: optimization, rule-based approaches, adaptive control, heuristics, fuzzy logic, genetic algorithms, etc [215]. The problem, with most of them, is the strong link that exists between the approach and a specific scenario. Good examples are the approaches for negotiation in case of an intersection [216], they lack generality for all the scenarios of AD. In these terms, a negotiation protocol is one of the possible solutions to generalize completely the cooperation of automated vehicles, as in [217].

5.3 Importance of the cooperation messages

The existence of a specific type of message for establishing the cooperation is needed. In these terms, CAM message (presented in chapter 4) is a complement but, not sufficient for cooperation.

Also, another type of standardized message is the Decentralized Environmental Notification Message (DENM). DENM message is well explained in the ETSI standard [218]. Briefly, this message was built specifically for ITS application and it is triggered in case of road hazards or abnormal traffic conditions. Also, it is broadcast by a vehicle or infrastructure advising other participants to take appropriate actions with sufficient time. This type of message is divided into four possible ones:

1. New: it gives new attributes and creates an event. It assigns an action tag, also called the action ID.

2. Update: it is used to update the information broadcast in a previous "new" message.

3. Cancellation: the participant, who has generated the message, can cancel it.

4. Negation: it is similar to the cancellation message but it is proposed for another participant. It is used when the source of the message is no longer available.

These messages advice other vehicles in case of road hazardous situation. Those are triggered or published, and not necessarily updated, depending on the road conditions. Furthermore, the containers or payloads of the message do not consider cooperative driving.

Consequently, the GCDC i-Game 2016 proposed a cooperation message, additional to CAN and DENM messages. It was called i-Game Cooperative Lane Change Message (iCLCM), which was sent with a frequency between 1 and 25 Hz. These frequencies permit to accomplish safety requirements during difficult cooperative maneuvers such as platoon merging [219]. This approach aimed the cooperation for the platoon scenario without considering the general driving process, which was its main problem. Moreover, the message payload was big and it had specific information on platoon scenarios: objects, lanes, merge conditions, type of scenario, dynamics of the vehicle (redundant to the CAM), etc.

A newer version of cooperative messages was given in the project MAVEN with the name of Maneuver Coordination Message (MCM). The concept of cooperation is related to the coordination at the longitudinal, lateral, and right-of-way domains. The main goal of the approach was to use this type of message during all driving circumstances and not only on specific scenarios. Another advantage was the consideration of the map in all participants on the road since the approaches can diverge from vehicle to vehicle but not the maps [220].

One of the main disadvantages of the proposed MCM messages in MAVEN was to split up the cooperation into three possibilities. This demands a standardized algorithm to detect and classify the type of maneuver. It could represent a problem among OEMs in this early stage of the technology (limitations given by a standardized algorithm). In these terms, the UnCoVerCPS project proposed a cooperation technique improving the driving process. Although, the approach was tested on the overtaking scenario, it is not limited to it [221].

5.4 Cooperation algorithm between vehicles

Previous sections have explained the importance of using cooperation in automated vehicles, especially when dealing with maneuver negotiation. In the past, some approaches were used in specific scenarios, generating protocols for maneuver cooperation, as in the GCDC i-Game 2016 and MAVEN projects. Nevertheless, this work proposes a new method to negotiate a cooperative maneuver for AD, considering the general case of driving. The approach has been tested and validated using two different platforms, with different software and hardware architectures, in a real cooperative overtaking scenario.

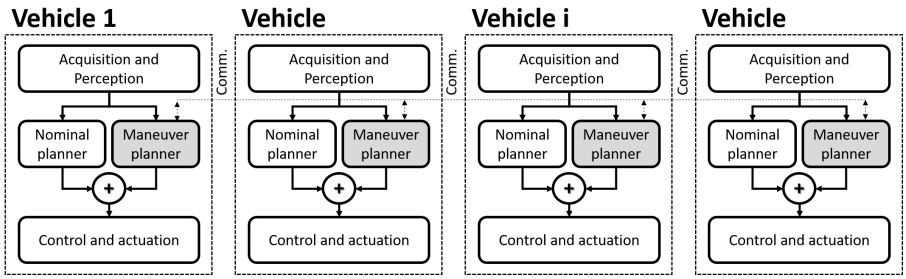

Figure 5.2: General architecture of cooperation among multiple vehicles

In this section, an explanation of the proposed negotiation method is done, considering multiple vehicles and space/time reservations. The vehicle does not demand the same specific architecture. The method requires a nominal planner and a fast maneuver planner (dynamic) ensuring the time specifications during risky maneuvers. A general architecture for vehicle cooperation is shown in Fig. 5.2, which is compatible with the architecture of the automated vehicle shown in section 3.2 .

5.4.1 The negotiation protocol

The negotiation method is based on human driver behavior, in terms of showing an intention on the road which is replied with positive or negative actions (actions taken by other participants). Based on Fig. 5.2, vehicle “i” generates a demand of executing a certain maneuver (for example an overtaking), and the other vehicles start a negotiation of the maneuver with vehicle “i”. In a positive answer, the vehicle “i” can discard or reduce the constraints

around the accepted vehicle (trajectory planning). When the agreement is not established, the other participant must be considered during the trajectory planning, and its motion must be evaluated conservatively. In the case of negative responses, the automated vehicle must drive normally in its lane.

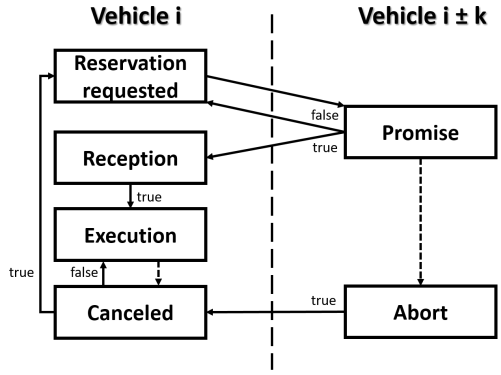

Figure 5.3: Maneuver negotiation protocol.

Fig. 5.3 depicts the process of negotiation of two vehicles "i" and "i ± k" where the vehicle "i" sends a reservation of a space area for a time gap. Vehicle "i ± k" has two possible choices under this *request*, it can *promise* to keep the area available for vehicle "i" (during the time gap), or the vehicle can refuse the reservation. Consequently, the vehicle "i" can send again other reservation message or keep the lane safely until the vehicle achieves another opportunity to send a reservation.

In case of a positive *reception* from vehicle "i ± k", vehicle "i" can remove or reduce the constraints around vehicle "i ± k", and this optimizes the trajectory planning (vehicle "i ± k" must considered as a static obstacle in case of an emergency). In case of keeping the motion conditions conservatively in vehicle "i ± k", the real improvement of the negotiation will not be appreciated. In this stage of *execution*, the vehicle "i ± k" could *abort* the negotiation in case of estrange conditions, as for example an emergency vehicle passing. In this case, the vehicle "i" must *cancel* the reservation and execute the trajectory planning with no cooperation among the vehicles.

5.4.2 The reservation message

The information of the cooperation messages includes a unique identifier of the message from the requester (vehicle) and a specific identifier of the vehicle. The type is included, and describes a *request*, *promise* or *abort message*. Additionally, a description of the space and time reservation must be done, the initial time t_0 and final time for the reservation are included ($t_1 = t_0 + t_k$).

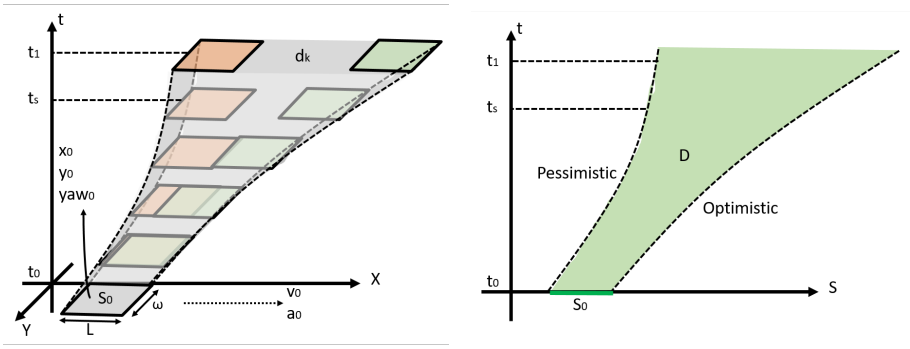

(a) Disturbances of the reservation XY plane vs time

(b) Disturbances of the reservation in 2D, S vs time

Figure 5.4: Representation of the disturbances in the reservation area.

In this context, the reservation cannot be static in the time gap between t_0 and t_1 to obtain an optimal response during the trajectory generation. In such a way, it is added the initial condition for the reservation with the data x_0, y_0, v_0, a_0 and yaw_0, which are the x and y initial position, speed, acceleration, and yaw angle respectively. Also, the reservation width ω and the length L are added to model the space gap (x_0 and y_0 are considered in the center).

This description is enough for executing cooperation while driving (moving this space during the reserved time). However, the disturbances in the initial conditions should be considered to guarantee safety in the execution. Those disturbances are described in terms of minimum initial speed ($v_0 - \Delta v_0^-$), maximum speed ($v_0 + \Delta v_0^+$), minimum acceleration ($a_0 - \Delta a_0^-$), and maximum acceleration ($a_0 + \Delta a_0^+$).

Disturbances are shown in Fig 5.4a. Considering the reservation worst-case scenario (minimum speed and acceleration) shown in red color. This will move the reservation less than the optimistic one considering the maximum speed and

Table 5.1: Maneuver negotiation message's payload

Tag	Definition
$MesID$	Message ID
$VehID$	Vehicle ID
$MesType$	Message type
t_0	Initial time of the reservation
t_1	Final time of the reservation
x_0	Initial X position (space reservation)
y_0	Initial Y position (space reservation)
yaw_0	Initial orientation of the space reservation
ω	Space reservation width
L	Space reservation length
v_0	Initial speed
a_0	Initial acceleration
Δv_0^-	Lower bound of the initial speed
Δv_0^+	Upper bound of the initial speed
Δa_0^-	Lower bound of the initial acceleration
Δa_0^+	Upper bound of the initial acceleration

acceleration (green reservation). In these terms, the space reserved modifies its configuration during t_0 to t_1, as described by the equations:

$$Pessimistic \quad red : \{s_c = s_0 + (v_0 - \Delta v_0^-)t + (a_0 - \Delta a_0^-)t^2/2, \quad t = [t_0, t_1]\} \tag{5.1}$$

$$Optimistic \quad green : \{s_c = s_0 + (v_0 + \Delta v_0^+)t + (a_0 + \Delta a_0^+)t^2/2, \quad t = [t_0, t_1]\} \tag{5.2}$$

a simpler representation of this disturbance boundaries is shown in 5.4b. The XY plane is replaced by the plane S to simplify the problem. This approach is correct in short cooperative time gaps. In the case of a long cooperation times, the disturbances will have a direct impact and variations over time, which

will reduce the efficiency of the approximation (propagation of the initial disturbances over the time horizon), demanding non-linear representation of the disturbances.

In the case of accepting or aborting the message, the information of the container (payload) remains the same. The ID of the vehicle and message type are changed (vehicle answering). The requester verifies the information received, comparing it with the request message (previously sent). This determines the relation of the message received with the requested gap. In conclusion, the message payload is summarized in table 5.1.

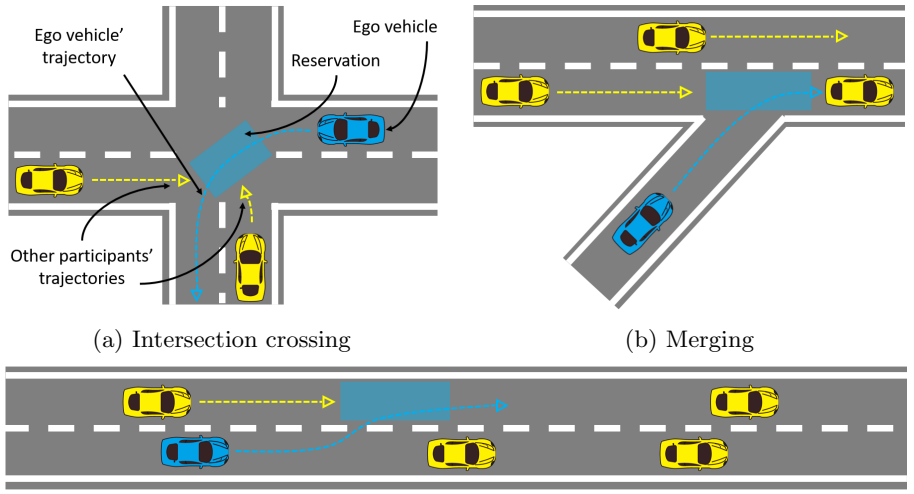

(a) Intersection crossing

(b) Merging

(c) Overtaking

Figure 5.5: Some examples of space and time negotiation.

5.4.3 Some examples using the negotiation protocol and maneuver reservation

The proposed space-time reservation method can be used on intersection crossing (Fig. 5.5a), lane merging (Fig. 5.5b), lane changing or overtaking scenarios (Fig. 5.5c). This method can increase safety in the areas where non-cooperative scenarios do not have a good performance.

In the case of the intersection crossing (Fig. 5.5a), the vehicle requesting permission to turn left submits a message with the reservation. In case of acceptance of any of the vehicles, the compromise of the acceptor vehicle increases the safety and this event permits to relax the constraints around that participant. Furthermore, propagating the future states could incur in driving mistakes due to its stochastic behavior.

In the case of merging (Fig. 5.5a), the vehicle demanding the space gap requests permission to the vehicle which has the right-of-way. The vehicle in the lane can yield the space to the requester, improving the driving process.

This Ph.D. thesis considered the overtaking scenario which was tested for the UnCoVerCPS project (Fig. 5.5c). The vehicle demanding a space gap will use its generated trajectory to send the space and the time, from the start of the lane change to the end of it. This is possible because the lateral and longitudinal domains are considered in the generated trajectory. On the other hand, the receptor of the request message evaluates whether the vehicle can execute this maneuver safely or not. Possible negative replies can be produced due to an unfeasible solution on the space-time gap, for instance: violation detected in the comfort or safety constraints.

5.5 Cooperative planning test

This section describes the platforms used for the validation, the test location, and two different types of scenarios performed. First, the tests were done at low speed, replicating turns as urban environments, and then the other experiment highway scenarios at high speed. The results are presented on two real vehicles, validating and verifying the performance of the method in different software and hardware architectures.

5.5.1 Testing AD platforms and tracks

Cooperative planning maneuvers were physically tested using two AD platforms (refer to Fig. 5.6a) driving at low and high speeds in two different testing tracks (refer to Fig. 5.6b and 5.6c respectively). The Deutsches zentrum für Luft-und Raumfahr (DLR) used a Volkswagen Passat, and it has the following differences, compared to Tecnalia's AD platform (refer to section 3.5.2):

1. In terms of hardware, the communication devices were different in both vehicles. Furthermore, the actuator interfaces were different in both vehicles. DLR's vehicle used the ACC ECU for controlling the throttle and

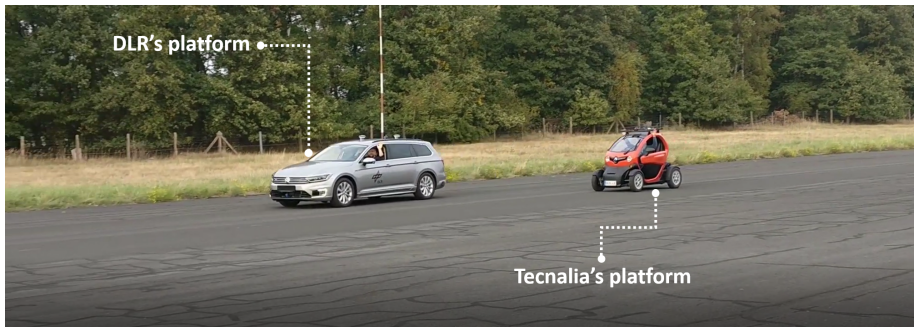

(a) AD vehicle platforms (DLR and Tecnalia)

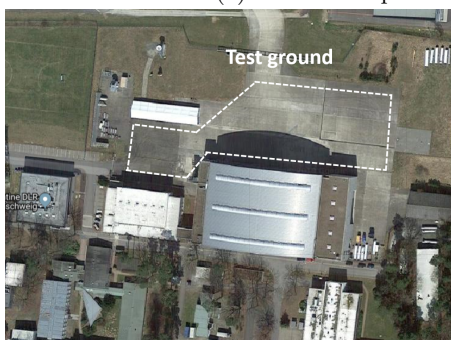

(b) Low speed proving ground at DLR

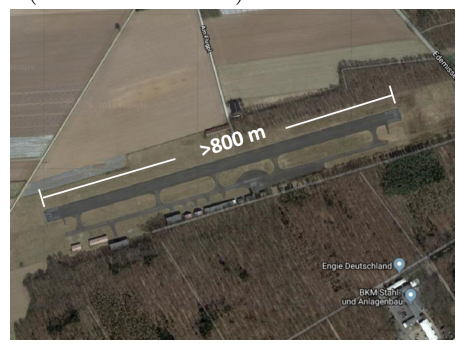

(c) Edimissen airport proving ground

Figure 5.6: Cooperative planning experiments.

brake, and the steering wheel by steer-by-wire. In the case of the Tecnalia's vehicle, the actuators were controlled with external motors and the throttle via ECU.

2. Software architectures were different in both platforms, whereas DLR's vehicle used a distributed architecture based on a software called "Dominion", and Tecnalia's vehicle used Matlab®/Simulink® interfaces programmed in C/C++ (refer to section 3.2).

3. In terms of the algorithm, slightly different trajectory planning methods were implemented, i.e. whereas DLR used the MPC methods and Tecnalia used a hybrid approach with parametric curves and MPC (refer to chapter 4). Additionally, the logic of the negotiation method was implemented in

different forms (programming structures and language) while standardized rules of the negotiation method were used.

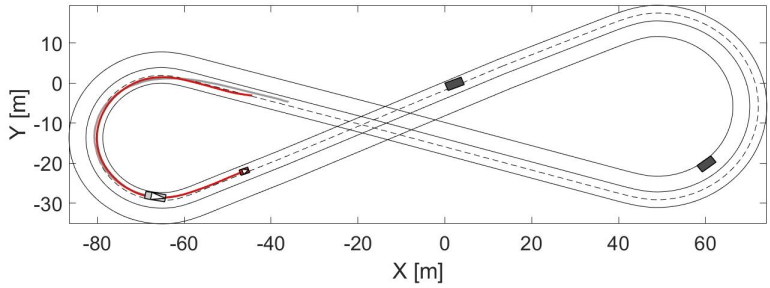

(a) Experiment at 12 seconds

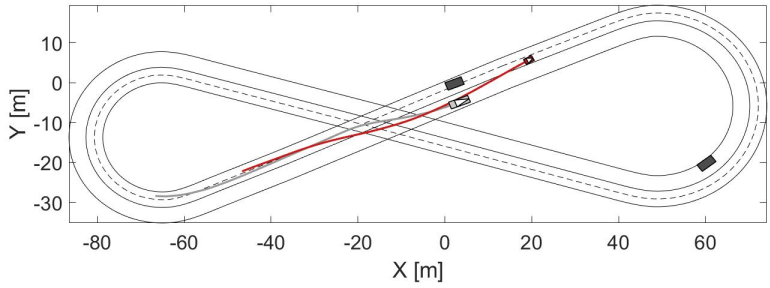

(b) Experiment at 25 seconds

Figure 5.7: Cooperation at low speeds: results of the obstacle avoidance.

Fig. 5.6b shows the proving ground used for the low-speed tests, located in a private airport near DLR's main campus in Braunschweig, Germany. It recreated a scenario with conventional urban environments turns but surrounded by a hangar. This building has reduced considerably the precision of GPS navigation during the tests.

On the other hand, Fig. 5.6c shows the airport field of Edemissen, 60 km from the DLR campus. This field recreated a long straight path for high-speed overtaking maneuver (emulating a highway scenario).

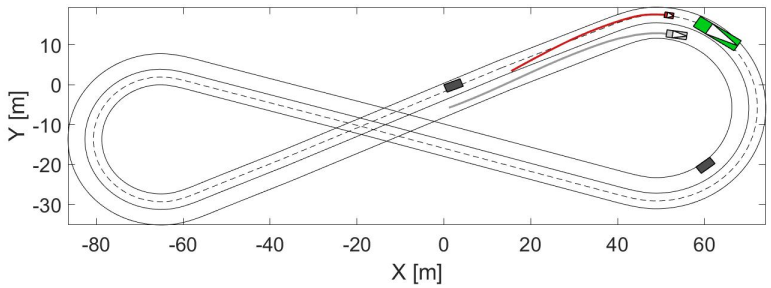

(a) Experiment at 32 seconds

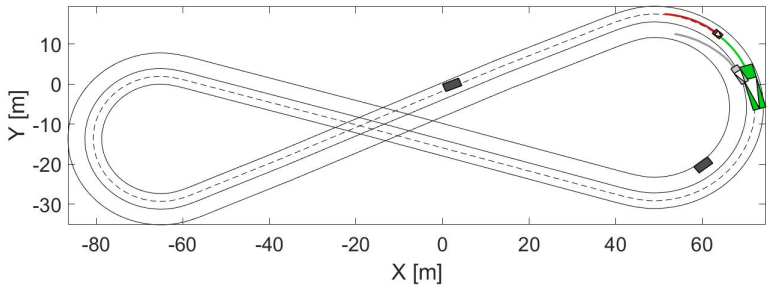

(b) Experiment at 36 seconds

Figure 5.8: Cooperation at low speeds: overtaking negotiation.

5.5.2 Low speeds experimental results

Cooperative planning tests at low speeds covered a test track with two curves overlapped in the middle. The curves segments have been defined using the simple points for the global map describing two roundabouts (see section 3.4.1). In order to maximize the testing track, the vehicles circulated in a 4 meters wide road, and as in left-hand driving countries. This meant that the overtaking started from the left side. Fig. 5.7, 5.8, and 5.9 depict the results obtained with cooperation at low speeds.

The initial conditions of the scenario are shown in Fig. 5.7a. The Renault Twizy (vehicle in red) starts in front of the Passat (light gray vehicle). Two static vehicles (dark gray) have been strategically positioned in the field, one in a straight path and the other one in the bent segment (bigger radius). These first results were related to the Twizy's nominal driving behavior, and there

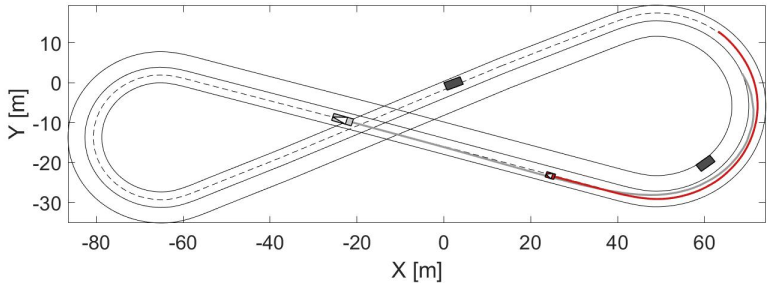

(a) Experiment at 42 seconds

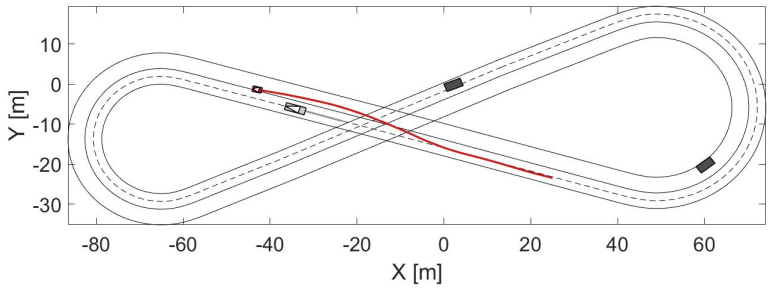

(b) Experiment at 60 seconds

Figure 5.9: Cooperation at low speeds: end of the test.

were no major interactions between the vehicles.

Fig. 5.7b shows the obstacle avoidance capability of both vehicles considering static obstacles. The approach used for the Twizy was the one presented in chapter 4. In such a way, each vehicle starts from the left lane and the right one was taken to avoid the obstacle. The Twizy returned to the main lane after avoiding the obstacle.

Next, Fig. 5.8a and 5.8b depict the process of negotiation the overtaking maneuver. While the Twizy stayed in the left lane, the Passat aimed to overtake the right lane obstacle. The intention of executing this maneuver was transmitted to the Twizy. It verified whether was feasible or not to open the space-time gap. After the verification, the Twizy generated an acceptance message. The reservation was considered with the acceptance of the message, and it started its movement from time t_0 to t_1 (improving the traffic flow).

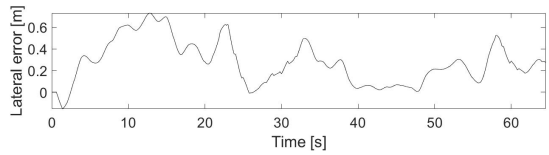

(a) Lateral error

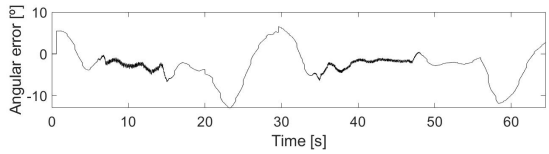

(b) Angular error

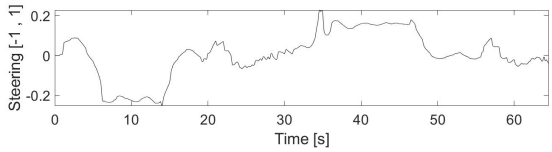

(c) Steering wheel action

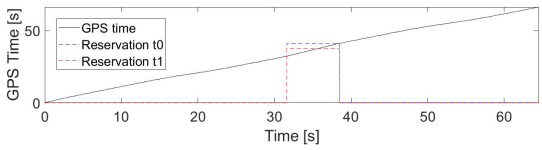

(d) Time reservation

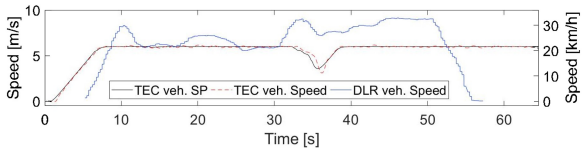

(e) Speed of both vehicles

Figure 5.10: Cooperation at low speeds: control variables.

In the final part of the experiment, the Passat has already overtaken the Twizy and stopped at the start position (Fig. 5.9a). The Twizy performed a final obstacle avoidance maneuver, returning back to the lane (Fig. 5.9b). Next, the scenario started again.

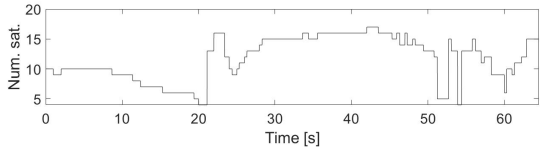

(a) Number of satellites

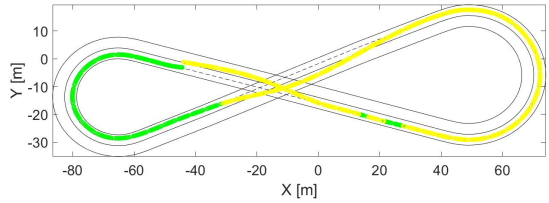

(b) GPS quality

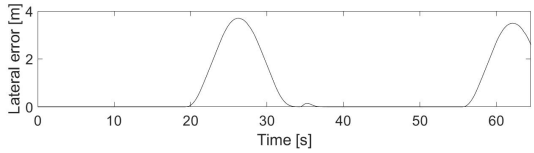

(c) Trajectory lateral error based on open-loop MPC

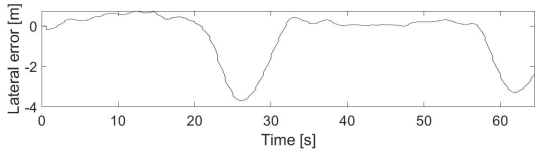

(d) Trajectory lateral error based on Bézier

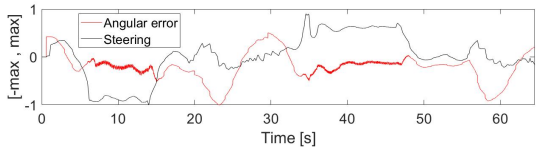

(e) Comparison between the normalized angular error and steering wheel action

Figure 5.11: Cooperation at low speeds: some drawbacks.

The control variables during the experiment were monitored and they are shown in Fig. 5.10. The lateral error is shown in Fig. 5.10a with a maximum

value of 70 centimeters for around 10 seconds (from 10 to 20 seconds) and the rest of the time the lateral error was under 40 centimeters. The angular error is shown in Fig. 5.10b with values under the 15 degrees. The steering wheel action is shown in Fig 5.10c, some perturbations in the smoothness were found in all the experiment, due to the low quality of the GPS signal.

The negotiation is accepted after 32 seconds since starting the experiment. Fig. 5.10d shows the moment of the reception with the value $t_0 = 35s$ (in red) and $t_1 = 38s$ (in blue). The reservation has affected the speed of the Twizy (Fig. 5.10e) by reducing it, opening the gap to the Passat.

Some of the weaknesses found during the low-speed tests were in terms of the low quality of the GPS signal due to the drop in the precision. Fig. 5.11a shows how in some parts of the circuit the number of satellites dropped under 10, restoring a value over it for a few seconds. A reflection with a big building surrounding the test track was the cause. The low quality of GPS is shown in Fig. 5.11b in yellow and in green is an acceptable GPS quality considering the RTK mode (differential).

This low quality has affected the lateral error compared to the main trajectory (Fig. 5.11d). The MPC trajectory was not affected by the GPS quality lost (Fig. 5.11c). Generally speaking, this has affected the steering wheel action, along with sharp changes in the angle calculation (refer to Fig. 5.11e).

5.5.3 High speeds' experimental results

Fig. 5.12 and 5.13 depict the results obtained when considering cooperation at high speeds. The tests have been performed in the test track shown in Fig. 5.6c. The circuit has been modeled as long straight path in the airport field to achieve target speeds around $60km/h$. The road width was set at 4 meters.

The initial conditions of the scenario are shown in Fig. 5.12a, where both vehicles have started in parallel, one on each lane. At 15 seconds from the start, the Passat requested a reservation to generate an overtaking of a vehicle that is blocking the right lane (dark gray obstacle in Fig. 5.12b). The Twizy has used the constraints for the generation of the trajectory. After verifying a feasible solution, the Twizy generates an acceptance message.

When the reservation achieved the time t_0, it started the movement until t_1. Fig. 5.12c shows this condition. In Fig. 5.13, the lane change process was completed and the vehicles drove normally on their lanes.

The control variables during the experiment were monitored (Fig. 5.14). The lateral error is shown in Fig. 5.14a with a maximum value of 1 meter for less than 5 seconds. For the rest of the experiment, the lateral error was under

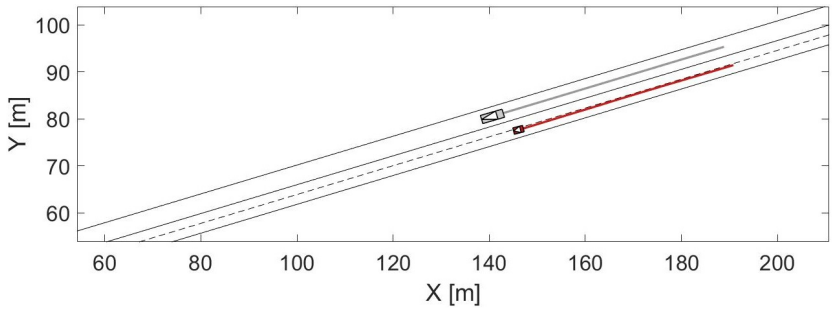

(a) Experiment at 10 - 14 seconds

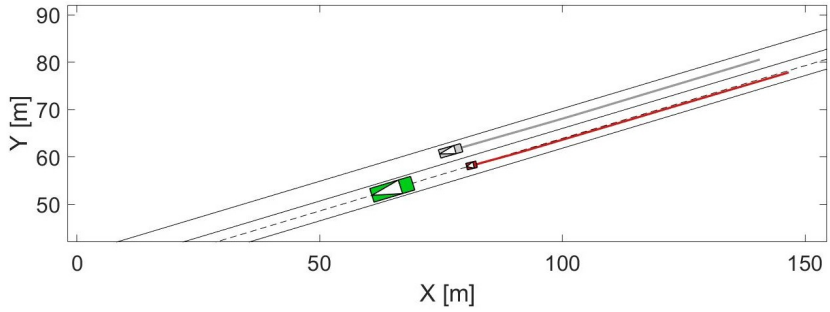

(b) Experiment at 14 - 19 seconds

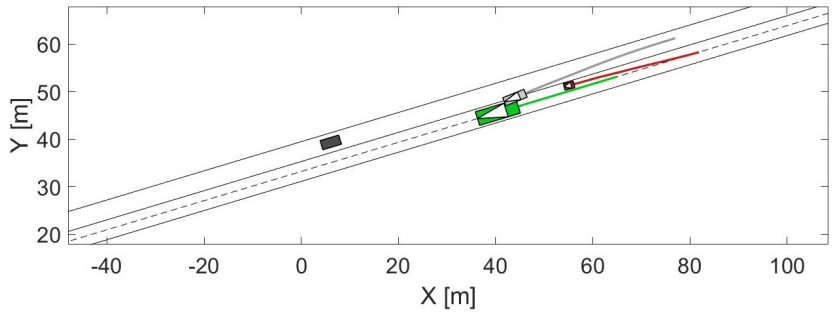

(c) Experiment at 19 - 22 seconds

Figure 5.12: Cooperation at high speeds: overtaking negotiation.

50 centimeters. The angular error is shown in Fig. 5.14b with values below 10 degrees of error. This value is lower than in the low-speed tests due to the

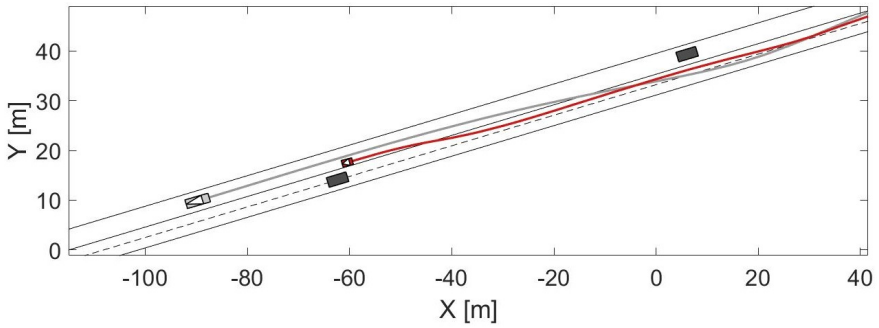

(a) Experiment at 22-32 seconds

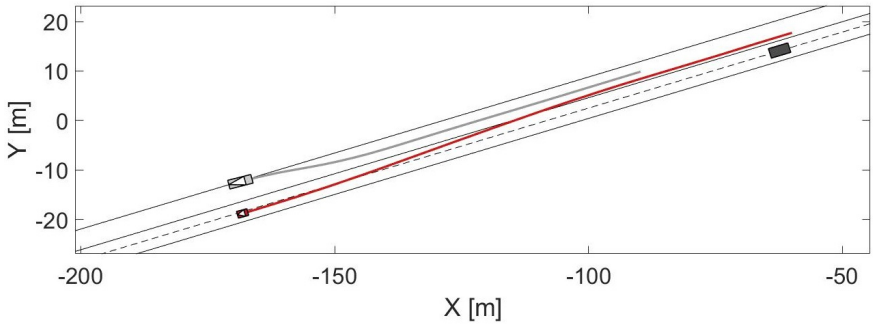

(b) Experiment at 32-41 seconds

Figure 5.13: Cooperation at high speeds: end of the test.

straight path. The resulting steering wheel action is shown in Fig 5.14c. Some perturbations in the smoothness of the steering wheel action were found at 20 seconds. This value is due to a sharp change in the angle (Fig. 5.14b) during a failure in the GPS quality.

The negotiation is accepted at 15 seconds after starting the experiment. Fig. 5.14d shows the moment of the reception with the value t_0 in red and $t_1 = t_0 + t_k$ in blue. The reservation has affected the speed of the vehicle (Fig. 5.14e) reducing it because the Twizy opened the space gap for the Passat. After this event, the speed has increased again to $60km/h$.

5.6 Summary

This chapter has presented a novel method for cooperative planning of automated vehicles. It has consisted of space-time reservations and their negotiation

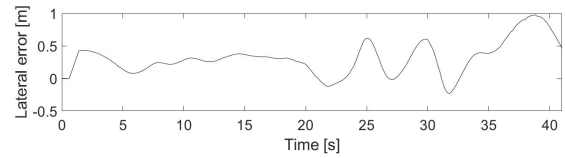

(a) Lateral error

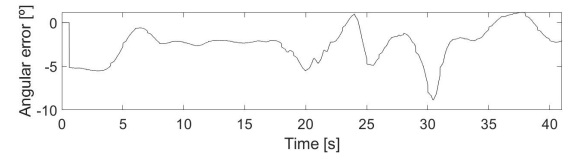

(b) Angular error

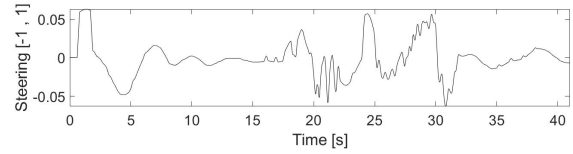

(c) Steering wheel action

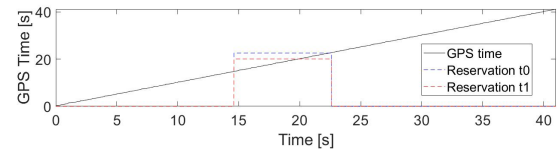

(d) Time reservation

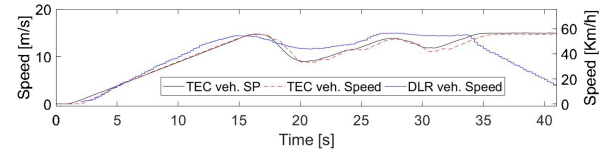

(e) Speed of both vehicles

Figure 5.14: Cooperation at high speeds: control variables.

with other participants on the scenario. The method is a good complement of the MPC + Bézier trajectory method because the space-time reservations are verified as another moving obstacle [162].

The tests conducted at low speed have provided interesting results in terms of the overtaking on bend road segments. The approach yielded a road gap for an overtaking maneuver while a safe distance was kept. The maneuver improved the traffic flow, avoiding a possible brake situation of the Passat.

The high-speed test reached interesting results in terms of vehicle performance, but few problems were found related to the disturbances. They must be very precise for longer reservation times. The calculation of the disturbances will be considered in future works, avoiding divergence between the requester vehicle and the reservation at high speeds (Fig. 5.12c).

"It Always Seems Impossible Until It's Done".
Nelson Mandela

6 Conclusions

This Ph.D. thesis is enclosed with the remarks of the presented state-of-the-art review, proposed methods, and validation results. Thereafter, the future works derived are described.

6.1 Relevant conclusions

The increasing interest in solutions for highly automated driving has pushed forward the deployment of cutting-edge technologies on vehicles, such as Tesla's or Audi's automation methods. Additionally, novel strategies are developed to improve safety and passengers' comfort.

In particular, this work reviewed the most relevant milestones of AD state of the art, going from the trajectory planning and control systems to real vehicle demonstrations. Consequently, the EU PROMETHEUS initiative and the US DARPA challenges are relevant due to the development of methods and techniques that are currently used. Moreover, the Google self-driving project aroused the public interest considering demonstrations in real-traffic conditions. Nonetheless, there are still pending issues to achieve smooth, safe, and comfortable driving for passengers. A solution to this problem is the improvement of the

trajectory planning strategies used on automated vehicles. Hence, this Ph.D. thesis has developed some methods to achieve better automated vehicles in real scenarios, especially under risky situations.

In these terms, Tecnalia's previous works have used an automated Renault Twizy platform for researching in AD. The vehicle's hardware and the test tracks were set up. Nonetheless, the system was only capable of tracking GPS-waypoints files that define the trajectory, limiting the performance to scenarios of lane following at speeds under $10km/h$. Moreover, software architecture lacked modularity which complicates actions such as changing the scenarios, generation of lane-change maneuvers, or testing in simulation environments. Consequently, a novel modular architecture was developed in this Ph.D. thesis to mitigate the problems previously mentioned, including the Dynacar simulator as part of the algorithm validation and verification process.

A new method for map construction has been introduced and tested. This approach describes an urban scenario in terms of simple points connected by line segments and circles (roundabouts, intersections, and lane changes). After, a trajectory planning method was proposed, considering the parametric curves of Bézier. The approach has benefits, such as: smooth curvature and fast computation-time. Moreover, a speed profile method was developed, considering the same type of curves. Some of the main attributes of this speed profile are smooth changes and the integration of the lateral and longitudinal domains in the same trajectory. The proposed algorithm was tested both in simulation and the Twizy platform.

Moreover, this Ph.D. thesis has presented a novel method for trajectory generation using the Bézier trajectories with a Model Predictive Control (MPC) approach. This method decoupled the lateral and longitudinal dynamics of the vehicle, achieving fast computation-times in lane-change based maneuvers. The MPC was modeled using an integrator chain description and a collision verification system based on segment intersection. This strategy has permitted the execution of obstacle avoidance and lane-change maneuvers with the generation of safe trajectories at a rate of $10ms$. Additionally, vehicle speeds over $60km/h$ were achieved using the Twizy platform.

Lastly, a cooperation method was proposed to mitigate unsafe conditions derived from the interaction of automated vehicles. A new message for general maneuver negotiation was included, improving others such as CAM or DENM. This message is a representation of a reserved driving space during a specific time gap. The vehicles have used the GPS time to avoid synchronization problems. Disturbances in the speed and acceleration were included to improve the calculation of the other vehicles' movement. Modeling other participants is a

key factor in collision evaluation. The tests were conducted in two different automated driving platforms in the framework of the UnCoVerCPS project, demonstrating the robustness of this approach.

6.2 Future works

Connected and automated vehicles will take an important role in European transportation in the next years. They will support several of the EU objectives such as road safety, reduction of congestion, social inclusiveness, etc. The overall efficiency of transport systems will increase thanks to automation, considering electric and shared vehicles by 2050 [222]

This Ph.D. thesis has proposed a solution for reliable and comfortable trajectories that mitigate safety issues in automated vehicles. Nevertheless, further research is still demanded in decision and control areas to achieve commercial vehicles with AD capacities, specifically in subjects such as:

- The simple map presented in this thesis has good results for the definition of specific routes or scenarios which are easily defined with geometry. More complex scenarios demand a complete map considering: road entrances or exits, multiple lanes, merging lanes, sidewalks, among others. Further research must be done in this direction to increase, without saturating, the amount of information provided by the map. The methods and knowledge, derived from this thesis, can be used as a basis for approaches with more complex maps.

- Another fundamental aspect is the evaluation of the movement intention of other vehicles and pedestrians in order to define the vehicle's trajectories. The movement intention is a task demanded if maps, with more environment information, are considered.

- The proposed method for maneuver negotiation should be studied in scenarios as the intersections and roundabout merging. Additionally, the case of Cooperative Adaptive Cruise Control (CACC) could be improved considering maneuver negotiation.

- Another important topic is the maneuvers in case of emergencies. This topic is interesting for decision and control tasks, which should consider possible failures of the vehicle's perception. These mechanisms must take into account system fall-backs, simplifying future regulatory processes.

- Future decision and control algorithms should support any platform (freight vehicles, trucks, buses, logistics vehicles, and interaction with drones) regarding the expansion of the operational design domain (ODD [31]) of automated driving.
- More research efforts must be given to vehicle shared control. Strategies to take back control in case of possible risks or to give back the control to the driver must be developed considering real scenarios and its near market deployment.

Bibliography

[1] D. Gonzalez, J. Perez, V. Milanes, and F. Nashashibi, "A review of motion planning techniques for automated vehicles," *IEEE Transactions on intelligent Transportation Systems*, 2016.

[2] J. Schrepfer, J. Mathes, V. Picron, and H. Barth, "Automated driving and its sensors under test," *Springer ATZ worldwide*, vol. 120, pp. 28–35, 2018.

[3] The European Road Transport Research Advisory Council (ERTRAC), "Automated driving roadmap," ERTRAC, Tech. Rep., 2017.

[4] I. Giannopoulos, "Modern technology on automobiles and how to turn them into safeguards of senior citizen drivers: A review of the literature and personal outlook," *International Journal of Advancements in Technology*, vol. 8, no. 3, pp. 1 – 4, 2017.

[5] M. Chapman, "Senior drivers confront new car technology," Chicago Tribune, Jun. 2016.

[6] The European Road Transport Research Advisory Council (ERTRAC), "Strategic research agenda: input to the 9th EU framework programme," ERTRAC, Tech. Rep., 2018.

[7] D. Milakis, M. Snelder, B. van Arem, B. van Wee, and G. H. de Almeida Correia, "Development and transport implications of automated vehicles in the netherlands: scenarios for 2030 and 2050," *European Journal of Transport and Infrastructure Research (EJTIR)*, vol. 17, no. 1, pp. 63–85, 2017.

[8] "Impacts and potential benefits of autonomous vehicles : from an international context to Grand Paris," The Paris Urbanism Agency (APUR), Tech. Rep., Oct. 2018.

[9] World Health Organization, "Global status report on road safety," 2018.

[10] M. Xie, L. Trassoudaine, J. Alizon, and J. Gallice, "Road obstacle detection and tracking by an active and intelligent sensing strategy," *Machine Vision and Applications*, vol. 7, no. 3, pp. 165–177, 1994.

[11] M. Williams, "The prometheus programme," in *IEE Colloquium on Towards Safer Road Transport-Engineering Solutions*, 1992, pp. 1 – 4.

[12] U. Ozguner, K. A. Redmill, and A. Broggi, "Team terramax and the darpa grand challenge: A general overview," in *IEEE Intelligent Vehicle Symposium*, 2004, pp. 232–237.

[13] M. Buehler, K. Iagnemma, and S. Singh, Eds., *The 2005 DARPA Grand Challenge: the great robot race*. Springer, 2007.

[14] C. Reinholtz, C. Reinholtz, T. Alberi, S. Frash, D. Anderson, G. Cothing, A. Bacha, J. Hurdus, C. Bauman, S. Kimmel, S. Cacciola, C. Sharkey, P. Currier, A. Taylor, A. Dalton, C. Terwelp, J. Farmer, D. V. Covern, R. Faruque, M. Webster, M. Fleming, and A. Wicks, "Darpa urban challenge technical paper," Virginia Tech, Tech. Rep., 2007.

[15] Q. Chen, Ü. Özgüner, and K. Redmill, "Ohio state university at the 2004 darpa grand challenge: Developing a completely autonomous vehicle," *IEEE Intelligent Systems*, pp. 8–11, 2004.

[16] T. Gindele, D. Jagszent, B. Pitzer, and R. Dillmann, "Design of the planner of team annieway's autonomous vehicle used in the darpa urban challenge 2007," in *IEEE Intelligent Vehicle Symposium*, 2008, pp. 1131 – 1136.

[17] S. Nordhoff, J. de Winter, R. Madigan, N. Merat, B. van Arem, and R. Happee, "User acceptance of automated shuttles in berlin-schöneberg: A questionnaire study," *Transportation Research Part F*, pp. 843 – 854, 2018.

[18] A. Alessandrini, A. Cattivera, C. Holguin, and D. Stam, *Road Vehicle Automation*. Springer, 2014, ch. CityMobil2: Challenges and Opportunities of Fully Automated Mobility, pp. 169–184.

[19] M. Glotz-Richter, *Implementing Automated Road Transport Systems in Urban Settings*, 2018, ch. 6.2: Reviewing CityMobil2 for the European Commission, pp. 306–310.

[20] D. Gonzalez, J. Perez, R. Lattarulo, V. Milanes, and F. Nashashibi, "Continuous curvature planning with obstacle avoidance capabilities in urban scenarios," *IEEE International Conference on Intelligent Transportation Systems (ITSC)*, pp. 1430–1435, 2018.

[21] D. Gonzalez, V. Milanes, J. Perez, and F. Nashashibi, "Speed profile generation based on quintic bezier curves for enhanced passenger comfort," *IEEE International Conference on Intelligent Transportation Systems (ITSC)*, 2016.

[22] R. Lattarulo, J. Perez, and M. Dendaluce, "A complete framework for developing and testing automated driving controllers," *IFAC PapersOnLine*, pp. 258–263, 2017.

[23] H. Mouhagir, R. Talj, V. Cherfaoui, F. Guillemard, and F. Aioun, "A markov decision process-based approach for trajectory planning with clothoid tentacles," *IEEE Intelligent Vehicles Symposium (IV)*, pp. 1254 – 1259, June 2016.

[24] J. Derrick, "General motors ceo mary barra: More change to come in the next 5-10 years than in the last 50 years," Bezinga, Oct. 2017.

[25] S. Taymaz, "The road ahead—how a 100-year old mobility service transforms into a world of automated driving," in *Automated Vehicles Symposium*, Springer, Ed., 2018, pp. 163 – 169.

[26] "Google, uber, and the evolution of transportation-as-a-service," Stratechery, Aug. 2016.

[27] A. Marshall, "After peak hype, self-driving cars enter the trough of disillusionment," Wired, Dec. 2017.

[28] E. Edmonds, "Americans feel unsafe sharing the road with fully self-driving car," American Automobile Association (AAA), Tech. Rep., 2017.

[29] ——, "More americans willing to ride in fully self-driving cars," American Automobile Association (AAA), Tech. Rep., 2018.

[30] B. Grush, "Automated vehicles – virtue or vice?" in *Conference of the Transportation Association of Canada Toronto*, 2016.

[31] "Taxonomy and definitions for terms related to driving automation systems for on-road motor vehicles," SAE International, Tech. Rep., 2018.

[32] M. Rizzi, A. Kullgren, and C. Tingvall, "Injury crash reduction of low - speed autonomous emergency braking (aeb) on passenger cars," in *IRCOBI Conference on Biomechanics of Impacts*, 2014, pp. 656 – 665.

[33] A. Ziebinski, R. Cupek, D. Grzechca, and L. Chruszczyk, "Review of advanced driver assistance systems (adas)," in *AIP Conference Proceedings*, 2017.

[34] M. Schinkel and K. Hunt, "Anti-lock braking control using a sliding mode like approach," in *Proceedings of the American Control Conference*, 2002, pp. 2386 – 2391.

[35] H. Mirzaeinejad and M. Mirzaei, "A novel method for non-linear control of wheel slip in anti-lock braking systems," *ELSEVIER Control Engineering Practice*, vol. 18, pp. 918 – 926, 2010.

[36] L. Junwei and W. Jian, "Research on the automotive ebd system based on fuzzy control," in *IEEE International Conference on Computer Engineering and Technology (ICCET)*, 2010, pp. 505 – 508.

[37] H. Z. Li, L. Li, L. He, M. X. Kang, J. Song, L. Y. Yu, and C. Wu, "PID plus fuzzy logic method for torque control in traction control system," *International Journal of Automotive Technology*, vol. 13, no. 3, pp. 441–450, 2012.

[38] U.S. Department of Transportation National Highway Traffic Safety Administration (NHTSA), "Statistical analysis of the effectiveness of electronic stability control (esc) systems - final report," Tech. Rep., 2007.

[39] T. Hirose, T. Taniguchi, T. Hatano, K. Takahashi, and N. Tanaka, "A study on the effect of brake assist systems (bas)," *SAE International Journal of Passenger Cars - Mechanical Systems*, vol. 1, no. 1, pp. 729–735, 2009.

[40] O. Buehler and J. Wegener, "Evolutionary functional testing of a vehicle brake assistant system," in *The Metaheuristics International Conference (MIC)*, 2005, pp. 157 – 162.

[41] C. Chauvel, Y. Page, B. Fildes, and J. Lahausse, "Automatic emergency braking for pedestrians effective target population and expected safety benefits," in *International technical conference on the enhanced safety of vehicles (ESV)*, 2013.

[42] D. S.D., A. R.W.G., M. J.R.R., and P. G., "The potential of autonomous emergency braking systems to mitigate passenger vehicle crashes," in *Australasian Road Safety Research, Policing and Education Conference*, 2012.

[43] A. Shaout and M. A. Jarrah, "Cruise control technology review," *ELSEVIER Computers and electrical engineering*, vol. 23, no. 4, pp. 259–271, 1997.

[44] J. Pauwelussen and P. J. Feenstra, "Driver behavior analysis during acc activation and deactivation in a real traffic environment," *IEEE Transactions on Intelligent Transportation Systems*, vol. 11, no. 2, pp. 329 – 338, 2010.

[45] M. Lu, K. Wevers, and R. V. D. Heijden, "Technical feasibility of advanced driver assistance systems (ADAS) for road traffic safety," *Transportation Planning and Technology*, vol. 28, no. 3, pp. 167 – 187, 2005.

[46] S. Shladover, J. Lappin, R. Denaro, and B. W. Smith, "Introduction: The transportation research board's 2013 workshop on road vehicle automation," *Springer Road Vehicle Automation*, 2014.

[47] T. Shelton, "Automobile utopias and traditional urban infrastructure: Visions of the coming conflict, 1925 - 1940," *Traditional Dwellings and Settlements Review*, pp. 63–76, 2011.

[48] F. Kröger, "Automated driving in its social, historical and cultural contexts," *Autonomous Driving*, pp. 41–68, 2016.

[49] J. Romeo, "What's on the inside? with 8 million autonomous vehicles expected to enter the world in the next five years, what will their interiors be like," *Plastics Engineering*, vol. 74, no. 8, pp. 22–27, 2018.

[50] G. Brusaglino, "Safe and effective mobility in europe-the contribution of the PROMETHEUS programme," *IEE Colloquium on Prometheus and Drive*, 1992.

[51] C. Mothe and B. Quélin, "Creating competencies through collaboration: the case of EUREKA R&D consortia," *European Management Journal*, vol. 18, no. 6, pp. 590–604, 2000.

[52] J. Hellaker, "Promethieus- strategy," *IEEE International Congress on Transportation Electronics*, 2002.

[53] A. Kemeny, "Prometheus- design technics," *IEEE International Congress on Transportation Electronics*, 2002.

[54] C. M. University, "No hands across america official press release."

[55] C. Thorpe, T. Jochem, and D. Pomerleau, "The 1997 automated highway free agent demonstration," *IEEE Conference on Intelligent Transportation Systems*, pp. 496–501, 2002.

[56] K. Hamada, Z. Hu, M. Fan, and H. Chen, "Surround view based parking lot detection and tracking," in *IEEE Intelligent Vehicles Symposium*, 2015, pp. 1106–1111.

[57] J. K. Suhr, H. G. Jung, K. Bae, and J. Kim, "Automatic free parking space detection by using motion stereo-based 3d reconstruction," *Machine Vision and Applications*, vol. 21, pp. 163 – 176, 2010.

[58] C. D. C. III, D. G. A. Jr., M. W. Torrie, and S. A. Gray, "Autonomous ground vehicle technologies applied to the DARPA grand challenge," in *ICCAS*, 2004.

[59] F. W. Rauskolb, K. Berger, C. Lipski, M. Magnor, K. Cornelsen, J. Effertz, T. Form, F. Graefe, S. Ohl, W. Schumacher, J.-M. Wille, P. Hecker, T. Nothdurft, M. Doering, K. Homeier, J. Morgenroth, L. Wolf, C. Basarke, C. Berger, T. Gulke, F. Klose, and B. Rumpe, "Caroline: An autonomously driving vehicle for urban environments," *Journal of Field robotics*, pp. 674 – 724, 2008.

[60] C. Crane, D. Armstrong, A. Arroyo, A. Baker, D. Dankel, G. Garcia, N. Johnson, J. Lee, S. Ridgeway, E. Schwartz, E. Thorn, S. Velat, , and J. H. Yoon, "Team gator nation's autonomous vehicle development for the 2007 darpa urban challenge," *Journal of aerospace computing, information and communication*, vol. 4, pp. 1059–1085, 2007.

[61] C. Urmson, J. Anhalt, D. Bagnell, C. Baker, R. Bittner, M. N. Clark, J. Dolan, D. Duggins, T. Galatali, C. Geyer, M. Gittleman, S. Harbaugh, M. Hebert, T. M. Howard, S. Kolski, A. Kelly, M. Likhachev, M. McNaughton, N. Miller, K. Peterson, B. Pilnick, R. Rajkumar, P. Rybski, B. Salesky, Y.-W. Seo, S. Singh, J. Snider, A. Stentz, W. Whittaker, Z. Wolkowicki, , J. Ziglar, H. Bae, T. Brown, D. Demitrish, B. Litkouhi, J. Nickolaou, V. Sadekar, W. Zhang, J. Struble, M. Taylor, M. Darms,

and D. Ferguson, "Autonomous driving in urban environments: Boss and the urban challenge," *Journal of Field Robotics*, pp. 425 – 466, 2008.

[62] M. Bertozzi, L. Bombini, A. Broggi, and P. Grisleri, "The viac challenge: Setup of an autonomous vehicle for a 13,000 km intercontinental unmanned drive," *IEEE International Conference on Robotics and Automation*, 2010.

[63] A. Broggi, "Latest challenges in autonomous vehicles: A practitioner's perspective: Technology leadership brief," *Sae journals*, 2012.

[64] A. Broggi, P. Cerri, M. Felisa, M. C. Laghi, L. Mazzei, and P. P. Porta, "The vislab intercontinental autonomous challenge: an extensive test for a platoon of intelligent vehicles," *Journal of Vehicle Autonomous Systems*, vol. 10, pp. 147–164, 2012.

[65] A. Broggi, P. Medici, P. Zani, A. Coati, and M. Panciroli, "Autonomous vehicles control in the vislab intercontinental autonomous challenge," *ELSEVIER Annual Reviews in Control*, 2011.

[66] M. Bertozzi, L. Bombini, A. Broggi, M. Buzzoni, E. Cardarelli, S. Cattani, P. Cerri, S. Debattisti, R. Fedriga, M. Felisa, and L. Gatti, "The vislab intercontinental autonomous challenge: 13,000 km, 3 months, no driver," *World Congress on ITS*, 2010.

[67] S. L. Poczter and L. M. Jankovic, "The google car: Driving toward a better future?" *Journal of Business Case Studies*, vol. 10, no. 1, pp. 7–14, 2014.

[68] E. R. Teoh and D. G. Kidd, "Rage against the machine? google's self-driving cars versus human drivers," *ELSEVIER Journal of Safety Research*, pp. 57 – 60, 2017.

[69] M. S. Carlson, M. Desai, J. L. Drury, H. Kwak, and H. A. Yanco, "Identifying factors that influence trust in automated cars and medical diagnosis systems," *The Intersection of Robust Intelligence and Trust in Autonomous Systems*, pp. 20–27, 2013.

[70] J. Funke, P. Theodosis, R. Hindiyeh, G. Stanek, K. Kritatakirana, C. Gerdes, D. Langer, M. Hernandez, and B. Muller-Bessler, "Up to the limits: Autonomous audi tts," *IEEE Intelligent Vehicles Symposium*, pp. 541 – 547, 2012.

[71] J. Ziegler, P. Bender, T. Dang, and C. Stiller, "Trajectory planning for BERTHA - a local, continuous method," *IEEE Intelligent Vehicles Symposium*, pp. 450 – 457, 2014.

[72] J. Ziegler, P. Bender, M. Schreiber, H. Lategahn, T. Strauss, C. Stiller, T. Dang, U. Franke, N. Appenrodt, C. G. Keller, E. Kaus, R. G. Herrtwich, C. Rabe, D. Pfeiffer, F. Lindner, F. Stein, F. Erbs, M. Enzweiler, C. Knoppel, J. Hipp, M. Haueis, M. Trepte, C. Brenk, A. Tamke, M. Ghanaat, M. Braun, A. Joos, H. Fritz, H. Mock, M. Hein, and E. Zeeb, "Making bertha drive - an autonomous journey on a historic route," *IEEE Intelligent Transportation Systems Magazine*, vol. 6, no. 2, pp. 8 – 20, 2014.

[73] S. Robarts, "Delphi's self-driving car completes us coast-to-coast trip," Apr. 2015.

[74] M. Dikmen and C. M. Burns, "Autonomous driving in the real world: Experiences with tesla autopilot and summon," *International Conference on Automotive User Interfaces and Interactive Vehicular Applications*, pp. 225 – 228, 2016.

[75] M. Dikmen and C. Burn, "Trust in autonomous vehicles the case of tesla autopilot and summon," *IEEE International Conference on Systems, Man, and Cybernetics (SMC)*, pp. 1093–1098, 2017.

[76] X. Krasniqi and E. Hajrizi, "Use of iot technology to drive the automotive industry from connected to full autonomous vehicles," *ELSEVIER IFAC-PapersOnLine*, pp. 269–274, 2016.

[77] P. Lin, "Tesla Autopilot crash: why we should worry about a single death," 2016.

[78] J. Golson, "Driver in fatal tesla autopilot crash had seven seconds to take action," The Verge, Tech. Rep., 2017.

[79] P. Kiger, "Imagining the driverless city," Oct. 2015.

[80] A. Brown, "Driverless taxis launch in two cities," *Mechanical Engineering;*, 2016.

[81] J. D. Walpert, "Carpooling liability?: Applying tort law principles to the joint emergence of self-driving automobiles and transportation network companies," *Fordham Law Review,*, vol. 85, pp. 1863–1897, 2017.

[82] G. Meyer and S. Beiker, *Road Vehicle Automation 5*. Springer, 2019.

[83] J. G. Gaspar, C. Schwarz, O. Kashef, R. Schmitt, and E. Shull, "Using driver state detection in automated vehicles," 2018.

[84] E. Uhlemann, "Continued dispute on preferred vehicle-to-vehicle technologies," *IEEE Vehicular Technology Magazine*, vol. 12, no. 3, pp. 17–20, 2017.

[85] Audi Group, "Audi a8 - audi ai traffic jam pilot," Jul. 2017.

[86] Press Realese BMW, "Bmw group, intel and mobileye team up to bring fully autonomous driving to streets by 2021," Jul. 2016.

[87] Korean Herald, "Hyundai motor steps up investments in ai drive," May 2016.

[88] M. N. Center, "Renault-nissan and microsoft partner to deliver the future of connected driving."

[89] Ford Company, "Ford invests in argo ai, a new artificial intelligence company, in drive for autonomous vehicle leadership," Ford, Tech. Rep., 2017.

[90] J. van Dijke and M. van Schijndel, "Citymobil, advanced transport for the urban environment: Update." in *Transportation Research Record: Journal of the Transportation Research Board*, 2012, pp. 29–36.

[91] G. Meyer, *Road Vehicle Automation 2*. Springer, 2015.

[92] F. Nashashibi, P. Resende, F. Charlot, C. Holguin, M. Parent, and L. Bouraoui, "A cooperative personal automated transport system," in *IEEE International Conference on Control, Automation, Robotics & Vision*, 2012.

[93] A. Benmimoun, M. Lowson, A. Marques, G. Giustiniani, and M. Parent, "Demonstration of advanced transport applications in citymobil project," *Transportation Research Record: Journal of the Transportation Research Board*, pp. 9–17, 2009.

[94] Implementing Automated Road Transport Systems in Urban Settings, *Evaluation of Automated Road Transport Systems in Cities*. Springer, 2018, ch. 3, pp. 81 – 207.

[95] K. Tammi and V. Hyvarinen, "Lateral and longitudinal control of bus platoon," *IEEE International Conference on Electrical Systems for Aircraft, Railway, Ship Propulsion and Road Vehicles and International Transportation Electrification Conference (ESARS-ITEC)*, 2018.

[96] C. F. Caruntu, A. Maxim, and R. C. Rafaila, "Multiple-lane vehicle platooning based on a multi-agent distributed model predictive control strategy," *International Conference on System Theory, Control and Computing (ICSTCC)*, pp. 759–764, 2018.

[97] A. Davila, E. del Pozo, E. Aramburu, and A. Freixas, "Environmental benefi ts of vehicle platooning," *SAE International*, 2013.

[98] T. Zhang, Y. Zou, X. Zhang, N. Guo, and W. Wang, "A cruise control method for connected vehicle systems considering side vehicles merging behavior," *IEEE Access*, 2017.

[99] J. Pérez, V. Milanes, J. Godoy, J. Villagrá, and E. Onieva, "Cooperative controllers for highways based on human experience," *ELSEVIER Expert Systems with Applications*, vol. 40, pp. 1024–1033, 2013.

[100] C. Englund, L. Chen, J. Ploeg, E. Semsar-Kazerooni, A. VoronoV, H. H. Bengtsson, and J. didoff, "The grand cooperative driving challenge 2016: Boosting the introduction of cooperative automated vehicles," *IEEE Wireless Communications*, pp. 146 – 152, 2016.

[101] M. Obst, A. Marjovi, M. Vasic, I. Navarro, A. Martinoli, A. Amditis, P. Pantazopoulos, I. Llatser, A. de La Fortelle, and X. Qian, *Challenges for Automated Cooperative Driving: The AutoNet2030 Approach.* Springer, 2016, ch. 26, pp. 561–570.

[102] M. Lu and R. Blokpoel, "A sophisticated intelligent urban road-transport network and cooperative systems infrastructure for highly automated vehicles," *World Congress on ITS*, 2017.

[103] P. O., V. J., S. Hoadley, R. Blokpoel, and H. T, "Incorporating stakeholder input in eu projects," *Smart Cities Symposium*, 2017.

[104] M. Rooker, P. Horstrand, A. S. Rodriguez, S. Lopez, R. Sarmiento, J. Lopez, R. A. Lattarulo, J. M. P. Rastelli, Z. Slavik, D. Pereira, M. Pusenius, and T. Leppälampi, "Towards improved validation of autonomous systems for smart farming," *Workshop on smart farming*, 2018.

[105] H. Beglerovic, S. Metzner, and M. Horn, "Challenges for the validation and testing of automated driving functions," *Springer Advanced Microsystems for Automotive Applications*, pp. 179–187, 2017.

[106] H. Beglerovic, A. Ravi, N. Wikström, H.-M. Koegeler, A. Leitner, and J. Holzinger, "Model-based safety validation of the automated driving function highway pilot," *International Munich Chassis Symposium*, 2017.

[107] H. Thompson, "Smart cyber-physical systems clustering and communication event synergies," 2016.

[108] J. F. Sencerin, "Autonomous driving french national plan new france for industry (nfi) plan," RENAULT, Tech. Rep., 2017.

[109] J. Perez, V. Milanes, and E. Onieva, "Cascade architecture for lateral control in autonomous vehicles," *IEEE transactions on intelligent transaportation systems*, pp. 73–82, 2011.

[110] F. Yakub and Y. Mori, "Comparative study of autonomous path-following vehicle control via model predictive control and linear quadratic control," *Journal of Automobile engineering*, 2015.

[111] V. Milanes, J. Villagra, J. Perez, and C. Gonzalez, "Low-speed longitudinal controllers for mass-produced cars: A comparative study," *IEEE Transactions on industrial electronics*, 2012.

[112] J. Suh, K. Yi, J. Jung, K. Lee, H. Chong, and B. Ko, "Design and evaluation of a model predictive vehicle control algorithm for automated driving using a vehicle traffic simulator," *ELSEVIER Control Engineering Practice*, vol. 51, pp. 92 – 107, 2016.

[113] N. Chen, M. Wang, T. Alkim, and B. van Arem, "A robust longitudinal control strategy of platoons under model uncertainties and time delays," *Hindawi Journal of Advanced Transportation*, 2018.

[114] J. Han, A. Sciarretta, L. L. Ojeda, G. D. Nunzio, and L. Thibault, "Safe- and eco-driving control for connected and automated electric vehicles using analytical state-constrained optimal solution," *IEEE Transactions on Intelligent Vehicles*, 2017.

[115] J. Kong, M. Pfeiffer, G. Schildbach, and F. Borrelli, "Kinematic and dynamic vehicle models for autonomous driving control design," *IEEE Intelligent Vehicles Symposium*, pp. 1094–1099, 2015.

[116] Y. Zheng, S. E. Li, K. L. andFrancesco Borrelli, and J. K. Hedrick, "Distributed model predictive control for heterogeneous vehicle platoons under unidirectional topologies," *IEEE Transactions on Control Systems technology*, 2016.

[117] X. Ji, X. He, C. Lv, Y. Liu, and J. Wu, "Adaptive-neural-network-based robust lateral motion control for autonomous vehicle at driving limits," *ELSEVIER Control Engineering Practice*, vol. 76, pp. 41–53, 2018.

[118] M. Li, H. Cao, X. Song, Y. Huang, J. Wang, and Z. Huang, "Shared control driver assistance system based on driving intention and situation assessment," *IEEE Transactions on industrial informatics*, vol. 14, pp. 4982–4994, 2018.

[119] C. Katrakazas, M. Quddus, W.-H. Chen, and L. Deka, "Real-time motion planning methods for autonomous on-road driving: State-of-the-art and future research directions," *ELSEVIER Transportation Research Part C*, vol. 60, pp. 416–442, 2015.

[120] V. Kunchev, L. Jain, V. Ivancevic, and A. Finn, "Path planning and obstacle avoidance for autonomous mobile robots: A review," *Springer Knowledge-Based Intelligent Information and Engineering Systems*, pp. 537–544, 2006.

[121] P. Marin-Plaza, A. Hussein, D. Martin, and A. de la Escalera, "Global and local path planning study in a ros-based research platform for autonomous vehicles," *Hindawi Journal of Advanced Transportation*, 2018.

[122] M. Elbanhawi and M. Simic, "Sampling-based robot motion planning: A review," *IEEE Access*, 2014.

[123] I. Noreen, A. Khan, and Z. Habib, "Optimal path planning using rrt* based approaches: A survey and future directions," *International Journal of Advanced Computer Science and Applications (IJACSA)*, vol. 7, no. 11, pp. 97–107, 2016.

[124] M. McNaughton, C. Urmson, J. M. Dolan, and J.-W. Lee, "Motion planning for autonomous driving with a conformal spatiotemporal lattice," *IEEE International Conference on Robotics and Automation*, 2011.

[125] B. Zhou, W. Schwarting, D. Rus, and J. Alonso-Mora, "Joint multi-policy behavior estimation and receding-horizon trajectory planning for automated urban driving," *IEEE International Conference on Robotics and Automation (ICRA)*, pp. 2388–2394, 2018.

[126] D. Yang, S. Zheng, C. Wen, P. J. Jin, and B. Ran, "A dynamic lane-changing trajectory planning model for automated vehicles," *Transportation Research Part C*, vol. 95, pp. 228–247, 2018.

[127] M. Mischinger, M. Rudigier, P. Wimmer, and A. Kerschbaumer, "Towards comfort-optimal trajectory planning and control," *International Journal of Vehicle Mechanics and Mobility*, 2018.

[128] B. Sakcak, L. Bascetta, G. Ferretti, and M. Prandini, "Using motion primitives to enforce vehicle motion constraints in sampling-based optimal planners," *IEEE International Symposium on Circuits and Systems (ISCAS)*, 2018.

[129] M. Graf, O. Speidel, J. Ziegler, and K. Dietmayer, "Trajectory planning for automated vehicles using driver models," *IEEE International Conference on Intelligent Transportation Systems*, 2018.

[130] M. G. Plessen, D. Bernardini, H. Esen, and A. Bemporad, "Spatial-based predictive control and geometric corridor planning for adaptive cruise control coupled with obstacle avoidanc," *IEEE Transactions on Control Systems Technology*, 2017.

[131] H. Guo, C. Shen, H. Zhang, H. Chen, and R. Jia, "Simultaneous trajectory planning and tracking using an mpc method for cyber-physical systems: A case study of obstacle avoidance for an intelligent vehicle," *IEEE Transactions on Industrial Informatics*, 2018.

[132] B. Yi, P. Bender, F. Bonarens, and C. Stiller, "Model predictive trajectory planning for automated driving," *IEEE Transactions on Intelligent Vehicles*, 2018.

[133] L. Svensson, L. Massony, N. Mohan, E. Wardz, A. P. Brenden, L. Feng, and M. Torngren, "Safe stop trajectory planning for highly automated vehicles: An optimal control problem formulation," *IEEE Intelligent Vehicles Symposium*, pp. 517–522, 2018.

[134] J. Kim, K. Jo, W. Lim, and M. Sunwoo, "A probabilistic optimization approach for motion planning of autonomous vehicles," *Journal of Automobile Engineering*, 2017.

[135] B. Li, N. Jia, P. Li, X. Ran, and Y. Li, "Incrementally constrained dynamic optimization: A computational framework for lane change motion planning of connected and automated vehicles," *Taylor and Francis Journal of Intelligent Transportation Systems Technology, Planning, and Operations*, 2019.

[136] W. Zhao, R. Liu, and D. Ngoduy, "A bilevel programming model for autonomous intersection control and trajectory planning," *Taylor and Francis Transportmetrica A: Transport Science*, 2018.

[137] L. Sun, C. Peng, W. Zhan, and M. Tomizuka, "A fast integrated planning and control framework for autonomous driving via imitation learning," *ASME Dynamic Systems and Control Conference (DSCC)*, 2018.

[138] D. J. Fagnant and K. Kockelman, "Preparing a nation for autonomous vehicles: opportunities, barriers and policy recommendations," *ELSEVIER Transportation Research Part A: Policy and Practice 77*, pp. 167 – 181, July 2015.

[139] G. Meyer and S. Deix, "Research and innovation for automated driving in germany and europe," *Springer Road Vehicle Automation*, pp. 71 – 81, 2014.

[140] E. Adell, A. Várhelyi, and M. dalla Fontana, "The effects of a driver assistance system for safe speed and safe distance – a real-life field study," *ELSEVIER Transportation Research Part C 19*, pp. 145 – 155, 2011.

[141] J. Ni and J. Hu, "Dynamics control of autonomous vehicle at driving limits and experiment on an autonomous formula racing car," *ELSEVIER Mechanical Systems and Signal Processing 90*, pp. 154 – 174, December 2016.

[142] M. Zhu, H. Chen, and G. Xiong, "A model predictive speed tracking control approach for autonomous ground vehicles," *ELSEVIER Mechanical Systems and Signal Processing 87*, pp. 138 – 152, March 2017.

[143] R. Domínguez, E. Onieva, J. Alonso, J. Villagra, and C. González, "LIDAR based perception solution for autonomous vehicles," *IEEE 11th International Conference on Intelligent Systems Design and Applications (ISDA)*, pp. 790 – 795, November 2011.

[144] J.-P. Jodoin, G.-A. Bilodeau, and N. Saunier, "Urban tracker: Multiple object tracking in urban mixed traffic," *IEEE Winter Conference on Applications of Computer Vision (WACV)*, pp. 885 – 892, June 2014.

[145] L. Li, D. Wen, and D. Yao, "A survey of traffic control with vehicular communications," *IEEE Transactions on Intelligent Transportation Systems*, pp. 425 – 432, August 2013.

[146] T. Gu1, J. Snider, J. M. Dolan, and J.-w. Lee, "Focused trajectory planning for autonomous on-road driving," *IEEE Intelligent Vehicles Symposium (IV)*, pp. 547 – 552, October 2013.

[147] N. Wan, A. Vahidi, and A. Luckow, "Optimal speed advisory for connected vehicles in arterial roads and the impact on mixed traffic," *ELSEVIER Transportation Research Part C: Emerging Technologies 69*, pp. 548 – 563, August 2016.

[148] T. Shim, G. Adireddy, and H. Yuan, "Autonomous vehicle collision avoidance system using path planning and model-predictive-control-based active front steering and wheel torque control," *SAGE Proceedings of the Institution of Mechanical Engineers, Part D: Journal of Automobile Engineering*, pp. 767 – 778, January 2012.

[149] W. Cao, M. Mukai, T. Kawabe, H. Nishira, and N. Fujiki, "Cooperative vehicle path generation during merging using model predictive control with real-time optimization," *ELSEVIER Control Engineering Practice 34*, pp. 98 – 105, January 2015.

[150] T. Nothdurft, P. Hecker, S. Ohl, F. Saust, M. Maurer, A. Reschka, and J. R. Bohmer, "Stadtpilot: First fully autonomous test drives in urban traffic," *IEEE Conference on Intelligent Transportation Systems*, 2011.

[151] K. Jo, J. Kim, D. Kim, C. Jang, and M. Sunwoo, "Development of autonomous car - part i: Distributed system architecture and development process," *IEEE Transactions on Industrial Electronics*, 2014.

[152] A. Broggi, P. Cerri, S. Debattisti, M. C. Laghi, P. Medici, M. Panciroli, and A. Prioletti, "Proud - public road urban driverless test: architecture and results," *IEEE Intelligent Vehicles Symposium*, 2014.

[153] S. Behere and M. Torngren, "A functional architecture for autonomous driving," *Proceedings of the First International Workshop on Automotive Software Architecture* , 2015.

[154] Ö. S. Tas, S. Hörmann, B. Schäufele, and F. Kuhnt, "Automated vehicle system architecture with performance assessment," *IEEE International Conference on Intelligent Transportation Systems*, 2018.

[155] K. Berntorp, T. Hoang, R. Quirynen, , and S. D. Cairano, "Control architecture design for autonomous vehicles," *Conference on Control Technology and Applications (CCTA)*, 2018.

[156] Ö. S. Tas, S. Hörmann, B. Schäufele, and F. Kuhnt, "Automated vehicle system architecture with performance assessment," *IEEE International Conference on Intelligent Transportation Systems*, 2018.

[157] T. Jones, S. Lennox, J. Sgueglia, J. Demerly, N. A. Zervoglos, and H.-H. Yang, "Autonomous vehicle: modular architecture," Patent US20 180 086 336A1, 2018.

[158] J. Harding, G. Powell, R. Yoon, J. Fikentscher, C. Doyle, D. Sade, M. Lukuc, J. Simons, and J. Wang, "Vehicle-to-Vehicle Communications: Readiness of V2v Technology for Application," Aug. 2014. [Online]. Available: https://trid.trb.org/view.aspx?id=1323282

[159] M. Bagheri, M. Siekkinen, and J. K. Nurminen, "Cellular-based vehicle to pedestrian (V2p) adaptive communication for collision avoidance," in *2014 International Conference on Connected Vehicles and Expo (ICCVE)*, Nov. 2014, pp. 450–456.

[160] V. Milanes, J. Villagra, J. Godoy, J. Simo, J. Perez, and E. Onieva, "An Intelligent V2i-Based Traffic Management System," *IEEE Transactions on Intelligent Transportation Systems*, vol. 13, no. 1, pp. 49–58, Mar. 2012.

[161] R. Lattarulo, J. A. Matute, J. Perez, and V. G. Garay, "Arquitectura dual-modular para desarrollos y validación de módulos de decisión y control en vehículos automatizados," *Revista Iberoamericana de Automatica e Informatica industrial*, 2019.

[162] D. Hess, R. Lattarulo, J. Perez, J. Schindler, T. Hesse, and F. Koster, "Fast maneuver planning for cooperative automated vehicles," *IEEE International Conference on Intelligent Transportation Systems (ITSC)*, 2018.

[163] A. Urutegui, R. Lattarulo, and G. Fernandez-Lopez, "Coordinated control for vehicles coopearative maneuvers using distributed model predictive control," *Memorias de Congresos UTP*, 2018.

[164] R. Lattarulo, D. Heß, and J. Perez, "A linear model predictive planning approach for overtaking manoeuvres under possible collision circumstances," *IEEE Intelligent Vehicles Symposium (IV)*, 2018.

[165] R. Lattarulo, E. MArti, M. Marcano, J. Matute, and J. Perez, "A speed planner approach based on bezier curves using vehicle dynamic constrains and passengers comfort," *IEEE International Symposium on Circuits and Systems (ISCAS)*, 2018.

[166] M. Marcano, J. A. Matute, R. Lattarulo, E. Marti, and J. Perez, "Low speed longitudinal control algorithms for automated vehicles in simulation and real platforms," *Complexity*, 2018.

[167] R. Lattarulo, L. Gonzalez, E. Marti, J. Matute, M. Marcano, and J. Perez, "Urban motion planning framework based on n-bézier curves considering comfort and safety," *Journal of Advanced Transportation*, 2018.

[168] G. Juez, E. Amparan, R. Lattarulo, A. Ruiz, J. Perez, and H. Espinoza, "Early safety assessment of automotive systems using sabotage simulation-based fault injection framework," *International Conference on Computer Safety, Reliability, and Security*, 2017.

[169] G. Juez, E. Amparan, R. Lattarulo, J. Perez, A. Ruiz, and H. Espinoza, "Safety assessment of automated vehicle functions by simulation-based fault injection," *IEEE International Conference on Vehicular Electronics and Safety (ICVES)*, 2017.

[170] R. Lattarulo, M. Marcano, and J. Perez, "Overtaking maneuver for automated driving using virtual environments," *International Conference on Computer Aided Systems Theory*, 2017.

[171] J.-w. Choi, R. Curry, and G. Elkaim, "Path planning based on Bézier curve for autonomous ground vehicles," *IEEE Advances in Electrical and*

Electronics Engineering - IAENG Special Edition of the World Congress on Engineering and Computer Science 2008, WCECS 08, pp. 158 – 166, October 2008.

[172] L. Han, H. Yashiro, H. Tehrani, Q. Huy Do, and S. Mita, "Bézier curve based path planning for autonomous vehicle in urban environment," *IEEE Intelligent Vehicles Symposium 2010*, pp. 1036 – 1042, June 2010.

[173] S. Glaser, B. Vanholme, S. Mammar, D. Gruyer, and L. Nouveliere, "Manoeuvre-based trajectory planning for highly autonomous vehicles on real road with traffic," *IEEE Transactions on Intelligent Transportation Systems*, pp. 589 – 606, 2010.

[174] H. Delingette, M. Herbert, and K. Ikeuchi, "Trajectory generation with curvature constraint based on energy minimization," *IEEE International Workshop on Intelligent Robots and Systems*, pp. 206 – 211, 1991.

[175] L. Labakhua, U. Nunes, R. Rodrigues, and F. S. Leite, "Smooth trajectory planning for fully automated passengers vehicles: Spline and clothoid based methods and its simulation," *Informatics in Control Automation and Robotics*, pp. 169–182, 2008.

[176] J. Perez, R. Lattarulo, and F. Nashashibi, "Dynamic trajectory generation using continuous-curvature algorithms for door to door assistance vehicles," *IEEE Intelligent Vehicles Symposium*, 2014.

[177] J. Nilsson, J. Silvlin, M. Brannstrom, E. Coelingh, and J. Fredriksson, "If, when, and how to perform lane change maneuvers on highways," *IEEE Intelligent Transportation Systems Magazine*, 2016.

[178] National Highway Traffic Safety Administration, "Analysis of lane-change crashes and near-crashes," 2009.

[179] Q. H. Do, S. Mita, H. Tehrani, M. Egawa, and K. Muto, "Human drivers based active-passive model for automated lane change," *IEEE Intelligent Transportation Systems Magazine*, 2017.

[180] D. Bevly, X. Cao, M. Gordon, G. Ozbilgin, D. Kari, B. Nelson, J. Woodruff, M. Barth, C. Murray, A. Kurt, K. Redmill, and U. Ozguner, "Lane change and merge maneuvers for connected and automated vehicles: A survey," *IEEE Transactions on Intelligent Vehicles*, 2016.

[181] S. Kouro, P. Cortes, R. Vargas, U. Ammann, and J. Rodríguez, "Model predictive control - a simple and powerful method to control power converters," *IEEE Transactions On Industrial Electronics*, 2009.

[182] Y. Wang and S. Boyd, "Fast model predictive control using online optimization," *IEEE Transactions on Control Systems Technology*, 2010.

[183] J. Funke, M. Brown, S. M. Erlien, and J. C. Gerdes, "Collision avoidance and stabilization for autonomous vehicles in emergency scenarios," *IEEE Transactions on Control Systems Technology*, 2016.

[184] R. C. Rafaila and G. Livint, "Nonlinear model predictive control of autonomous vehicle steering," *International Conference on System Theory, Control and Computing (ICSTCC)*, 2015.

[185] V. L. Bageshwar, W. L. Garrard, and R. Rajamani, "Model predictive control of transitional maneuvers for adaptive cruise control vehicles," *IEEE Transactions on Vehicular Technology*, 2004.

[186] G. V. Raffo, G. K. Gomes, J. E. Normey-Rico, C. R. Kelber, and L. B. Becker, "A predictive controller for autonomous vehicle path tracking," *IEEE Transactions on Intelligent Transportation Systems*, 2009.

[187] S. Mata, A. Zubizarreta, and C. Pinto, "Robust tube-based model predictive control for lateral path tracking," *IEEE Transactions on Intelligent Vehicles*, 2019.

[188] M. A. S. Kamal, M. Mukai, J. Murata, and T. Kawabe, "Model predictive control of vehicles on urban roads for improved fuel economy," *IEEE Transactions on Control Systems Technology*, 2013.

[189] S. D. Cairano, H. E. Tseng, D. Bernardini, and A. Bemporad, "Vehicle yaw stability control by coordinated active front steering and differential braking in the tire sideslip angles domain," *IEEE Transactions on Control Systems Technology*, 2012.

[190] S. J. Anderson, S. C. Peters, T. E. Pilutti, and K. Iagnemma, "An optimal-control-based framework for trajectory planning, threat assessment, and semi-autonomous control of passenger vehicles in hazard avoidance scenarios," *International Journal Vehicle Autonomous Systems*, 2010.

[191] G. Schildbach and F. Borrelli, "Scenario model predictive control for lane change assistance on highways," *IEEE Intelligent Vehicles Symposium (IV)*, 2015.

[192] C. Liu, S. Lee, S. Varnhagen, and H. E. Tseng, "Path planning for autonomous vehicles using model predictive control," *IEEE Intelligent Vehicles Symposium (IV)*, 2017.

[193] J. Villagra, V. Milanes, J. Perez, and J. Godoy, "Smooth path and speed planning for an automated public transport vehicle," *Robotics and Autonomous Systems*, pp. 252–265, 2012.

[194] V. Milanes, J. Perez, E. Onieva, and C. Gonzalez, "Controller for urban intersections based on wireless communications and fuzzy logic," *IEEE Transactions on Intelligent Transportation Systems*, vol. 11, no. 1, pp. 243–248, 2009.

[195] S. M. Erlien, S. Fujita, and J. C. Gerdes, "Shared steering control using safe envelopes for obstacle avoidance and vehicle stability," *IEEE Transactions on Intelligent Transaportation Systems*, 2015.

[196] *ACADO Toolkit User's Manual*, Optimization in Engineering Center (OPTEC), 2014.

[197] D. Ariens, *ACADO for Matlab User's Manual*, Optimization in Engineering Center (OPTEC), 2010.

[198] B. Houska, H. J. Ferreau, and M. Diehl, "Acado toolkit—an open-source framework for automatic control and dynamic optimization," *OPTIMAL CONTROL APPLICATIONS AND METHODS*, pp. 298–312, 2011.

[199] R. Lattarulo, D. Hess, J. A. Matute, and J. Perez, "Towards conformant models of automated electric vehicles," *IEEE International Conference on Vehicular Electronics and Safety (ICVES)*, pp. 227–232, 2018.

[200] J. Cuadrado, D. Vilela, I. Iglesias, A. Martin, and A. Peña, "A multibody model to assess the effect of automotive motor in-wheel configuration on vehicle stability and comfort," *ECCOMAS Multibody Dynamics*, 2013.

[201] F. Wang, M. Yang, and R. Yang, "Conflict-probability-estimation-based overtaking for intelligent vehicles," *IEEE Transactions on Intelligent Transportation Systems*, vol. 10, no. 2, pp. 366 – 370, 2009.

[202] E. I. Vlahogianni, "Modeling duration of overtaking in two lane highways," *Transportation Research Part F*, vol. 20, pp. 135–146, 2013.

[203] T. Mocsari, "Analysis of the overtaking behaviour of motor vehicle drivers," *Transportation Science, Logistics and Agricultural Engineering*, 2009.

[204] S. J. Park, M. Subramaniyam, S. E. Kim, S. Hong, J. H. Lee, and C. M. Jo, "Older driver's physiological response under risky driving conditions-overtaking, unprotected left turn," *Advances in Applied Digital Human Modeling and Simulation*, pp. 107–114, 2016.

[205] V. Milanes, D. F. Llorca, J. Villagra, J. Perez, C. Fernandez, I. Parra, C. Gonzalez, and M. A. Sotelo, "Intelligent automatic overtaking system using vision for vehicle detection," *Expert Systems with Applications*, vol. 39, pp. 3362–3373, 2012.

[206] T. Shamir, "How should an autonomous vehicle overtake a slower moving vehicle: design and analysis of an optimal trajectory," *IEEE Transactions on Automatic Control*, 2004.

[207] V. Sezer, "Intelligent decision making for overtaking maneuver using mixed observable markov decision process," *Journal of Intelligent Transportation Systems*, 2017.

[208] Y. Kuwata, G. A. Fiore, J. Teo, E. Frazzoli, and J. P. How, "Motion planning for urban driving using rrt," *IEEE/RSJ International Conference on Intelligent Robots and Systems*, pp. 1681–1686, 2008.

[209] H.-H. Chiang, Y.-L. Chen, B.-F. Wu, and T.-T. Lee, "Embedded driver-assistance system using multiple sensors for safe overtaking maneuver," *IEEE Systems Journal*, vol. 8, no. 3, pp. 681–698, 2014.

[210] Z. Huang, D. Chu, C. Wu, and Y. He, "Path planning and cooperative control for automated vehicle platoon using hybrid automata," *IEEE Transactions on Intelligent Transportation Systems*, pp. 959 – 974, 2018.

[211] C. Menendez-Romero, M. Sezer, F. Winkler, C. Dornhege, and W. Burgard, "Courtesy behavior for highly automated vehicles on highway interchanges," *IEEE Intelligent Vehicles Symposium (IV)*, pp. 943–948, 2018.

[212] Q. Guoa, L. Li, and X. J. Ban, "Urban traffic signal control with connected and automated vehicles: A survey," *Transportation Research Part C: Emerging Technologies*, 2019.

[213] W. Zhao, D. Ngoduy, S. Shepherd, R. Liu, and M. Papageorgiou, "A platoon based cooperative eco-driving model for mixed automated and human-driven vehicles at a signalised intersection," *Transportation Research Part C: Emerging Technologies*, vol. 95, pp. 802–821, 2018.

[214] S. Gupta, M. Vasardani, and S. Winter, "Negotiation between vehicles and pedestrians for the right of way at intersections," *IEEE Transactions on Intelligent Transportation Systems*, 2018.

[215] A. M. Pereira, H. Anany, O. pribyl1, and J. Prikryl, "Automated vehicles in smart urban environment: A review," *IEEE Smart City Symposium Prague (SCSP)*, 2017.

[216] A. Mirhelia, M. Tajallib, L. Hajibabaia, and A. Hajbabaie, "A consensus-based distributed trajectory control in a signal-free intersection," *Transportation Research Part C*, vol. 100, pp. 161–176, 2019.

[217] O. Sawade, M. Schulze, and I. Radusch, "Robust communication for cooperative driving maneuvers," *IEEE Intelligent Transportation Systems Magazine*, vol. 10, no. 3, 2018.

[218] ETSI EN 302 637-3 V1.2.2, "Intelligent transport systems (its); vehicular communications; basic set of applications; part 3: Specifications of decentralized environmental notification basic service," 2014.

[219] J. Ploeg, E. Semsar-Kazerooni, A. I. M. Medina, J. F. C. M. de Jongh, J. van de Sluis, A. Voronov, C. Englund, R. J. Bril, H. Salunkhe, A. Arrue, A. Ruano, L. Garcia-Sol, E. van Nunen, and N. van de Wouw, "Cooperative automated maneuvering at the 2016 grand cooperative driving challenge," *IEEE Transactions on Intelligent Transportation Systems*, vol. 19, no. 4, pp. 1213 – 1226, 2018.

[220] B. Lehmann, H.-J. Gunther, and L. Wolf, "A generic approach towards maneuver coordination for automated vehicles," *IEEE International Conference on Intelligent Transportation Systems (ITSC)*, pp. 3333–3339, 2018.

[221] D. Hess, C. Lopper, and T. Hesse, "Safe cooperation of automated vehicles," *AAET Automatisiertes & Vernetztes Fahren, ITS automotive nord*, pp. 309–334, 2017.

[222] The European Road Transport Research Advisory Council (ERTRAC), "Connected automated driving roadmap," ERTRAC, Tech. Rep., 2019.